IX Annexes

Annexe 1. Proteome Screens for Cys Residues Oxidation: The Redoxome; Chiappetta G, Ndiaye S, Igbaria A, Kumar C, Vinh J, Toledano MB. Methods Enzymol. 2010; 473:199-216. Review. PMID: 20513479

CHAPTER TEN

Proteome Screens for Cys Residues Oxidation: The Redoxome

Giovanni Chiappetta,* Sega Ndiaye,† Aeid Igbaria,* Chitranshu Kumar,* Joelle Vinh,† *and* Michel B. Toledano*

Contents

Abstract

The oxidation of the cysteine (Cys) residue to sulfenic (–S–OH), disulfide (–S–S–), or *S*-nitroso (S–NO) forms are thought to be a posttranslational modifications that regulate protein function. However, despite a few solid examples of its occurrence, thiol-redox regulation of protein function is still debated and often seen as an exotic phenomenon. A systematic and exhaustive characterization of all oxidized Cys residues, an experimental approach called redox proteomics or redoxome analysis, should help establish the physiological scope of Cys residue oxidation and give clues to its mechanisms. Redox proteomics still remains a technical challenge, mainly because of the labile nature of thiol-redox reactions and the lack of tools to directly detect the modified residues. Here we consider recent technical advances in redox proteomics, focusing on a gel-based fluorescent method and on the shotgun OxICAT technique.

* Laboratoire Stress Oxydants et Cancer, DSV, IBITECS, CEA-Saclay, Gif-sur-Yvette, France
† Biological Mass Spectrometry and Proteomics, USR CNRS/ESPCI ParisTech, Ecole Supérieure de Physique et de Chimie Industrielles, Paris Cedex, France

Methods in Enzymology, Volume 473
ISSN 0076-6879, DOI: 10.1016/S0076-6879(10)73010-X

1. Introduction

Until recently, cysteine (Cys) residue oxidation was thought to be confined to the endoplasmic-reticulum (ER), in which catalyzed disulfide bond formation contributes to the folding of proteins in their way to secretion (Ito and Inaba, 2008; Sevier and Kaiser, 2008), and to a few cytoplasmic enzymes that carry an oxidation–reduction step in their catalytic cycle, such as ribonucleotide reductase or the thiol- and selenothiol-based peroxiredoxins and glutathione peroxidases (Fourquet *et al.*, 2008; Toledano *et al.*, 2007). The paradigm concept of the ER as an oxidizing environment and the cytoplasm, and remaining compartments, as reducing ones has shifted as a result of an increasing number of observations indicating the occurrence of Cys residue oxidation as a posttranslational modification regulating the function of cytoplasmic and nuclear proteins (D'Autreaux and Toledano, 2007; Janssen-Heininger *et al.*, 2008; Linke and Jakob, 2003; Rhee *et al.*, 2005; Toledano *et al.*, 2004). Cys residue oxidation to the sulfenic (–S–OH), disulfide (–S–S–), or *S*-nitro (*S*-nitrosylation, S–NO) forms have been identified in several proteins, and are proposed to drive cell signaling by H_2O_2 and nitric oxide (NO) (Hess *et al.*, 2005). Further, import into the mitochondrial intermembrane space (IMS) of a protein subclass was recently shown to involve catalyzed disulfide formation that mediates folding of the polypeptide, thereby preventing its back-translocation to the cytoplasm (Mesecke *et al.*, 2005). Cys residue oxidation in the ER and IMS is mechanistically well understood, as being a catalyzed event for which the enzyme is identified. In contrast, the occurrence of Cys residue oxidation in the cytoplasm is not well understood, except for a few cases for which an oxidation mechanism has been described (D'Autreaux and Toledano, 2007). A systematic and exhaustive characterization of all oxidized Cys residues, an experimental approach called redox proteomics or redoxome analysis, should help establish the inventory of all thiol-redox-based phenomena and their physiological scope. In addition, inventory of the targets of the thiol reductases thioredoxins and glutaredoxins might be established through redoxome analyses of cells in which either of these activities has been shut down. Here we consider the main experimental methods that have been devised to characterize Cys residue oxidation at the proteome-wide level. We then focus on a two-dimensional electrophoresis gel (2DE)-based fluorescent method and on the novel shotgun proteomics OxICAT method developed by Jakob and colleagues (Leichert *et al.*, 2008), two approaches having complementary attributes (Fu *et al.*, 2008). These methods have already provided important advances in understanding thiol-redox metabolism. Nevertheless, redox proteomics still remains a technological challenge and needs further improvements.

2. General Considerations

2.1. Limits in the access to Cys-residues redox modifications

Proteomic analysis is a powerful tool to depict the posttranslational modifications of the proteome, but is still limited with regard to the characterization of the redox state of cysteine (Cys) residues. One major limit is the chemical labile nature of Cys residues redox modifications. Upon cell disruption, air-mediated Cys oxidation can occur and reciprocally disulfides can be reduced by cellular reductases, or they can reshuffle, thereby causing loss of information. Acidic quenching of thiol groups, which consists of breaking cells in the presence of trichloroacetic acid (TCA), circumvents this problem, also precipitating soluble proteins (Delaunay *et al.*, 2000; Le Moan *et al.*, 2009). Acidic quenching relies on the property of the thiol group to engage in redox reactions only when in the thiolate (deprotonated) form ($-S^-$), which occurs when the pH of the solution > p*K*a value of the Cys residue. Free cysteine has a p*K*a of 8.3, and Cys residues have p*K*a values from 4 to 10 depending on their amino acid environment. Thus, at pH < 1, all Cys residues are protonated and cannot undergo redox modifications. Alternatively, cell-permeable Cys-specific reagents, such as the alkylating agents iodoacetamide (IAM) or *N*-ethylmaleimide (NEM), can also trap Cys residues in their *in vivo* redox state and therefore can substitute for the TCA-based acidic quenching in specific protocols.

Lack of antibodies capable of recognizing oxidized Cys residues prevents the "*divide et impera*" strategy of immunoenrichment protocols or selective detection of proteins separated by 2D gels (Eaton, 2006).

Mass spectrometry (MS) detection of oxidized Cys residues has also limitations. Reducing agents, such as dithiothreitol (DTT) or tris(2-carboxyethyl) phosphine (TCEP), which are routinely used for improving protein solubility during cell extraction or for increasing the efficiency of polypeptide-enzymatic hydrolysis for MS-sample preparation, must be avoided or used with caution. Further, disulfide-linked peptides are more resistant to fragmentation under low-energy collision-induced-dissociation (CID) (Gorman *et al.*, 2002), and may undergo in-source reduction during UV MALDI experiments (337 nm) (Patterson and Katta, 1994).

2.2. Acid quenching and Cys differential labeling

TCA-based acidic quenching is common to and the first step of all methods described here. Upon solubilizing TCA-precipitated cell extracts by pH increase >6.8, reduced versus oxidized cysteine residues are differentially labeled—sequentially, before and after reduction with DTT—with Cys-specific reagents. Most of these reagents are derived from IAM or

NEM. Of note, one can increase the stringency of screens by targeting the Cys residue with low p*Ka*, which make up a majority of redox-regulated residues. This can be achieved using low pH conditions during the oxidized-residues alkylation step (Boivin *et al.*, 2008). The Cys-redox forms accessible to analysis are essentially disulfide bonds, whether intra- or intermolecular, including *S*-glutathionylation. The sulfinic and sulfonic acid forms are not reducible, but can conceivably be accessed when comparing two conditions, with one carrying a large proportion of the Cys residue in these higher irreversibly oxidized forms. Cysteine residues in the sulfenic acid form are difficult to identify because of their unstable chemical nature, although this has been achieved by exclusive reduction of the sulfenic acid by sodium arsenite (Saurin *et al.*, 2004), or by its reaction with specific chemicals such as dimedone (Poole *et al.*, 2005).

3. Overview of the Different Methods

3.1. 2DE-based methods

Most 2DE separation-based methods use NEM or IAM coupled to a functional group that has analytical usefulness and/or can be visualized on the gel.

3.1.1. Radioactive ^{14}C-based labeling

Radioactive ^{14}C-IAM and ^{14}C-NEM have been used to selectively detect and quantify oxidized proteins on 2D gels (Leichert and Jakob, 2004; Le Moan *et al.*, 2006). Upon blocking reduced Cys residue with cold IAM or NEM, oxidized residues are reduced and labeled with the ^{14}C-labeled corresponding reagent. Proteins containing oxidized protein-thiols are then visualized by autoradiography or by storage phosphor technology after 2DE separation. Radioactive signals can be normalized to the amount of protein estimated by Coomassie staining (Leichert and Jakob, 2004), or to the signals of total Cys residues obtained by labeling all Cys residues after extract reduction (Le Moan *et al.*, 2006). This procedure has the advantage of not generating differences in protein 2DE migration since the same reagent is used for both reduced and oxidized Cys residues. Moreover, these reagents are commonly used for proteomic analysis, and are compatible with all analytical steps. The main limitation of this procedure is the signal-to-noise ratio, which is often very high and the need of manipulating radioactive compounds.

3.1.2. Single fluorescence-based labeling

The IAM-derivatives 5-iodoacetamidofluorescein (Baty *et al.*, 2002) and BODIPY FL C1-IA (Hochgrafe *et al.*, 2005), and monobromobimane (Yano, 2003), a Cys-specific reagent that fluoresces upon UV irradiation, have been used to

reveal the extent of Cys residue oxidation by 2D gels. Reduced Cys residues were blocked by alkylation with NEM or IAM, and oxidized residues were labeled with the fluorescent Cys-reagent. Labeled proteins were visualized on 2D gels using an infrared fluorescence imaging system. Estimates of spots intensity, normalized to the protein amount in one protocol (Hochgrafe *et al.*, 2005), were taken as indexes of protein-thiol oxidation.

3.1.3. The DIGE approach

An improvement of 2DE-based fluorescence analysis of the redoxome has been obtained by applying the differential in gel electrophoresis (DIGE) technique. This strategy uses a set of fluorophores of similar molecular weights and chemical structures that differ by their spectral features. Redox-DIGE has been performed using the NEM or IAM derivatives of Cyanine (Cy3, Cy5) (Bruschi *et al.*, 2009; Fu *et al.*, 2008; Hurd *et al.*, 2007) and DY-dyes (Riederer and Riederer, 2007). Upon blocking reduced thiols by alkylation, the oxidized thiols of two different cell extracts are labeled with two different fluorophores. Labeled cell extracts are then mixed and analyzed on the same 2DE. Differences in Cys residues oxidation between samples are quantified by the intensity of each fluorophore at each spot. Acquisition of fluorescence intensities is performed by the dual-channel imaging technique with a laser scan capable of recording different wavelengths (Bernhardt *et al.*, 1999). Such multiplexed analysis overcomes the lack of reproducibility of the 2DE separation procedure when comparing two conditions and limits the number of gels that have to be done. However, the major limitation of this procedure is that fluorescence intensity cannot be normalized to the protein amount when using two dyes. Coomassie staining cannot be adapted here for protein quantification because of the very low amounts of cell extracts used in the procedure, and staining by the Sypro or Flamingo dyes (Bio-Rad) can modify 2DE profiles (Dietz *et al.*, 2009). Due to this limitation, redox-DIGE has so far compared only cell extracts or subfractions (mitochondria) of it treated or not by H_2O_2. Hence, redox-DIGE cannot be used to compare different cell extracts, because changes in protein expression profiles will invalidate quantitative estimates.

3.1.4. Two-fluorescent dyes differential labeling

To circumvent the limitation of redox-DIGE in cell extracts comparisons, Le Moan *et al.* (2009) proposed a new gel-based approach. This procedure consists in differentially labeling both reduced and oxidized thiols (Fig. 10.1A) using two 2DE-compatible fluorescent dyes absorbing and emitting at different wavelengths of the infrared region (Dy680 and Dy780, Dynomics). After 2DE separation, the ratio of the intensity of each fluorophore at each spot reflects the Cys residue(s) redox state of the corresponding protein. As the value obtained is a ratio, it is independent of the protein amount, allowing comparison of cell extracts independently separated by 2DE. Although the multiplexed feature of

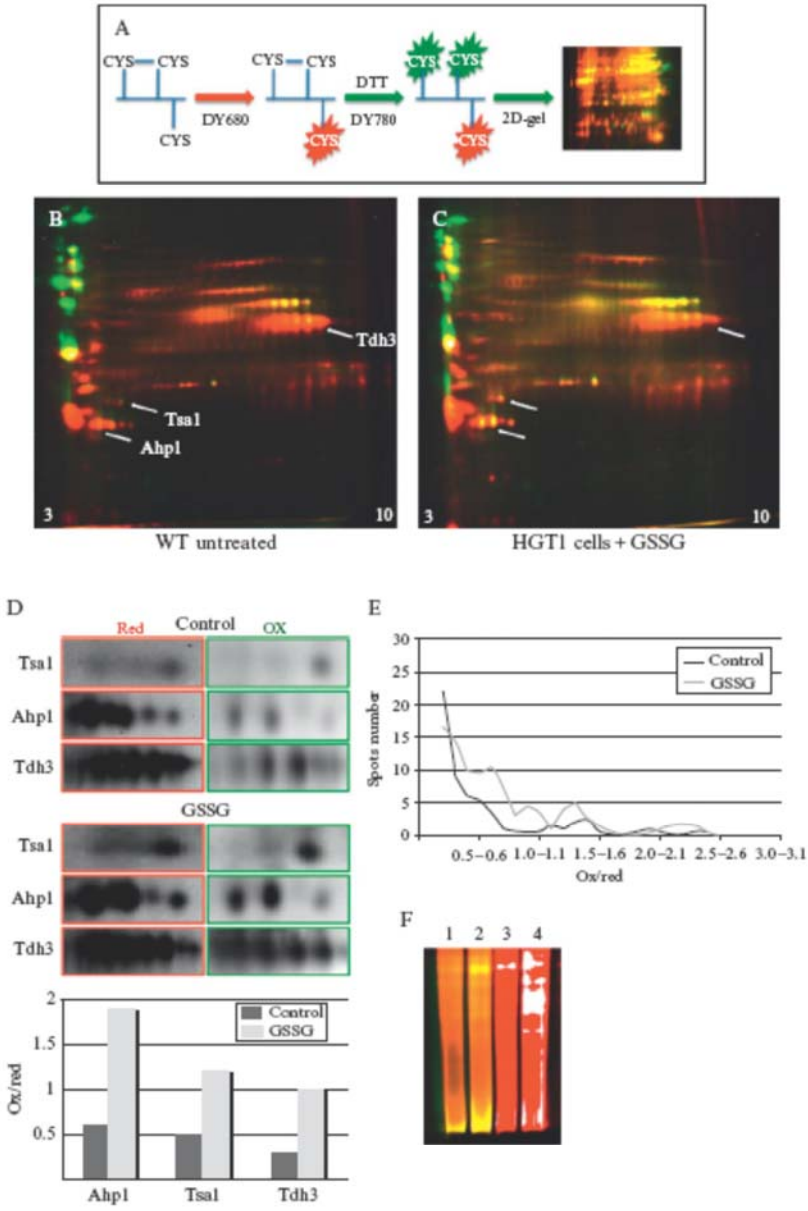

Figure 10.1 Use of the 2DE-based two-fluorescent dyes approach in *S. cerevisiae*. (A) Schematics of the procedure. Extracts of wild-type (WT) and of (B) HGT1 cells exposed to 50 μM GSSG during 30 min (C) were submitted to the two-fluorescent dyes

redox-DIGE is lost here, this approach provides a powerful means of comparing snapshots of the redoxome of cells grown under different conditions or having gene mutations. The two-fluorescent dyes differential labeling approach will be thoroughly detailed below.

3.1.5. The biotin-HPDP-based procedure decreases cell extracts complexities

As mentioned above, one limit of redox proteomics is the lack of proper tools for decreasing samples complexities. The thiol-reagent *N*-(6-(biotininamido) hexyl)-3′-(2′-pyridylthio)propionamide (biotin-HPDP) contains a biotin moiety and attaches to free thiols by means of a disulfide linkage. It can therefore be used to specifically enrich for the oxidized protein-thiol fraction of the proteome (Jaffrey and Snyder, 2001; Le Moan *et al.*, 2006). Upon blocking free thiols by NEM- or IAM-alkylation, oxidized Cys residues are reacted with biotin-HPDP. Labeled proteins are then adsorbed to a streptavidin column by virtue of their biotin moiety, eluted by reduction with DTT—which leave the biotin-HPDP label attached to the column—and separated by 2DE. 2DE of extracts from different cell cultures can be compared giving a rough estimate of differences in Cys residue oxidation, and spots can also be excised from gels for MS identification. Using this approach, about 60 oxidized protein-thiols were identified in yeast (Le Moan *et al.*, 2006). This labeling procedure can also serve as a labeling step for shotgun proteomic analysis (Wan *et al.*, 2007), and polypeptides could even be digested before affinity-purification, thus enriching for Cys-containing peptides.

3.2. Shotgun proteomic: The MS-based ICAT technology

The 2DE-based methods described above have many limits with regard to reproducibility, time-consumption of 2DE procedures, and the need of skilful operators. They also carry major drawbacks: the extent of oxidation

differential labeling protocol and separated by 2DE. Arrows indicate the spots of the peroxiredoxins Tsa1, Ahp1 and of glyceraldehyde-3-phosphate dehydrogenase (Tdh3). (D) The regions of the 2DE of panels B and C containing Tsa1, Ahp1, and Tdh3 were overblown, and the images corresponding to the DY780 (reduced Cys residues) and DY680 (Oxidized Cys residues) fluorescences are shown separately. Spot quantification of the oxidized to reduced Cys residues (Ox/Red) is represented below, as indicated. (E) Graphic representation of the Ox/Red ratios of the 150 larger spots of the 2DE of B and C, as indicated. (F) Reduced Cys residues saturation control analyzed by one-dimensional SDS–PAGE. Lanes 1 and 2 correspond to the experimental differentially labeled samples used in the 2DE of B and C, respectively. Here, both fluorescence colors can be seen as in the 2DE. Lanes 3 and 4 represent the saturation control of the same samples, respectively. Here, the reduced Cys residues labeled samples were submitted to the second dye without prior reduction of oxidized Cys residues. Reduced Cys residue saturation is optimal, as no green fluorescence is seen.

can only be roughly estimated and always corresponds to an average contribution of the Cys residues present in a polypeptide. Further, when applicable, protein identification must be performed by one spot at a time and the oxidized Cys residue cannot be identified. Another important limitation is that only the most abundant proteins are usually visualized on 2DE, denying all attempts of exhaustiveness.

Isotope coded affinity tag (ICAT) is a shotgun proteomic strategy based on the use of isotopic Cys-specific reagents that has been initially introduced for protein expression profiles measurements (Gygi *et al.*, 1999). ICAT has been adapted to redox proteomics coined OxICAT (Leichert *et al.*, 2008). OxICAT addresses all drawbacks of conventional 2DE-based procedures, potentially allowing exhaustive identification of all oxidized Cys residues in one single analysis, the precise identification of the oxidized Cys residues within polypeptides, and the rigorous estimate of the extent of oxidation at the level of each Cys residue. It therefore not only constitutes a screening procedure for identifying oxidized protein-thiols, but can also be used for comparative analysis between different cell cultures. The ICAT reagent consists of the IAM-moiety, a cleavable biotin tag, and a nine-carbon linker, which exists in an isotopically light ^{12}C- and heavy ^{13}C-form (Gygi *et al.*, 1999). After acidic quenching, oxidized versus reduced Cys residues are differentially labeled with the heavy and light ICAT reagents. Extracts are then submitted to enzymatic digestion and the ICAT-labeled peptides purified by streptavidin–biotin affinity chromatography. Purified peptides, and hence their oxidized Cys residues, are identified by LC–MS/MS, which also establishes the ratio of oxidized to reduced (heavy to light) Cys residues according to MS signal relative intensities. As the extent of oxidation is given as an Ox/Red ratio, absolute proteins amounts are not considered, therefore allowing cell extracts comparisons. Some limitations of OxICAT should be however underlined. When quantification relies on simple MS measurements, no discrimination is possible between different Cys residues within a given peptide. Furthermore, the yield of purification of some Cys-containing peptides can be low and therefore not detected by MS. The OxICAT method will be thoroughly detailed below.

4. Results and Discussion

4.1. Methods

4.1.1. Chemicals

TCA (Fluka), Urea (PlusOne, GE) CHAPS (PlusOne, GE), nondetergent sulfobetain 256 (NDSB) (Calbiochem), tris(hydroxymethyl)-aminomethane (Tris) (Fluka), IAM, Amberlite IRN-150L (PlusOne, GE), glass beads (Sigma-Aldrich), DY-680 and DY-780 dyes (Dynomics), 1,4-dithio-DL-

threitol (DTT) (Invitrogen), IPG buffer 3–10 (GE), microBCA kit (Pierce-Thermo), 18 cm immobiline dry gel-strip pH 3–10 nonlinear, (GE) glycerol (PlusOne, GE), sodium dodecyl sulfate (SDS) (Sigma-Aldrich), TCEP (Sigma-Aldrich), L-1-tosylamido-2-phenylethyl chloromethyl ketone (TPCK) treated trypsin (Sigma-Aldrich), α-cyano-4-hydroxycinnamic acid (CHCA) (Sigma-Aldrich), and ICAT kit (Applied Biosystems, ABI). Chemicals for casting SDS–PAGE gels are purchased from Bio-Rad. Highest purity solvents are purchased from Sigma-Aldrich.

4.1.2. Cell lysis procedures

For the OxICAT procedure, we used the human uterine cervix carcinoma cell line HeLa. Five hundred microliters of a TCA water solution (20%, w/v) was added to the pellet of centrifuged cells (5.0×10^6 cells). The sample was incubated on ice for 15 min, and then centrifuged (13 000×*g*, 4 °C for 15 min). For the fluorescence labeling procedure, 400 μl of the TCA solution (20%, w/v) was added to the pellet of *Saccharomyces cerevisiae* cells grown to the exponential-phase (1.0×10^7 cells), together with 200 μl of glass beads. The sample was iteratively agitated on a vortex for 1 min and left on ice for 1 min, and then centrifuged (13,000×*g*, 4 °C for 15 min). For both human and yeast cell samples, the TCA-precipitated pellet was washed three times with prechilled acetone.

4.1.3. Two-fluorescent dyes differential labeling

The labeling solution [urea (8 *M*), CHAPS (4% w/v), NDSB (1% w/v), Tris–HCl (25 m*M* pH 7.5), IAM (200 m*M*), DY-680 or DY-780 (0.1 m*M*)] was prepared extemporaneously. Urea (5.0 g) was dissolved in MilliQ water (6.0 ml) (final volume 10 ml) by agitation, at room temperature. The urea solution was treated with Amberlite (0.1 g) for 10 min under agitation at room temperature, and then filtered on a 0.45-μm filter. CHAPS (400 mg) and NDSB (100 mg) were then added to the urea solution. IAM and DTT stock solutions (1 *M* each) were prepared by adding 184.9 mg/ml IAM or 154.2 mg/ml DTT to 1 ml of the urea/CHAPS/NDSB solution. The labeling solution was made by adding 465 μl of the urea/CHAPS/NDSB solution, 120 μl of the 1 *M* IAM stock solution, 10 μl of Tris–HCl (1.5 *M*, pH 7.5), 5 μl of DY-680 (10 μg/μl in dimethylformamide).

4.1.3.1. Labeling reduced thiols TCA-precipitated cell extracts were solubilized in labeling solution (600 μl), and the pH of the sample checked and adjusted by adding a few microliters Tris–HCl solution (1.5 *M*, pH 7.5) (residual TCA often remains). The dye was then added and the labeling reaction carried out at 30 °C for 1 h on a stirring device (900 rpm) in the dark. Ten microliters of the labeled sample was taken for reduced-thiol alkylation saturation control. The reduced-thiols labeled sample was then

centrifuged (13,000×*g*, 4 °C for 5 min) and the supernatant recovered. The excess dye was removed by precipitation with 600 µl of the TCA solution (20%).

4.1.3.2. Labeling oxidized thiols Disulfide bonds were reduced by solubilizing the TCA-precipitated pellet in 600 µl of reducing solution [578 µl of the urea/CHAPS/NDSB solution, 12 µl of the 1 *M* DTT stock solution (20 m*M* final), 10 µl of Tris–HCl (1.5 *M* pH 7.5)]. The reaction was carried out at 37 °C for 30 min on a stirring device (900 rpm). The excess DTT was removed by TCA precipitation. To label oxidized thiols, the TCA-precipitated sample was solubilized in 600 µl of the labeling solution that contained dye DY-780 instead of DY-680. The sample pH was also checked here. The reaction was carried for 15 min at 4 °C under stirring, and the excess dye removed by TCA precipitation.

4.1.3.3. Control of reduced-thiol alkylation saturation To the 10 µl aliquot of the reduced sample kept for this purpose, 110 µl of labeling buffer and 1 µl of DY-780 were added. The reaction was carried out at 4 °C for 15 min. The sample was then TCA-precipitated. The TCA pellet solubilized in Laemli buffer was separated by SDS–PAGE.

4.1.3.4. Cell extracts quantities The number of cells used for each condition analyzed should be set up to obtain at least 100 µg of yeast cell extract at the end of the labeling procedure, to allow triplicate 2DE analyses.

4.1.4. 2DE analysis

The TCA pellet of labeled extracts was solubilized in 100 µl of freshly prepared loading buffer [urea (8 *M*), CHAPS (2%, w/v), NDSB (1%, w/v), IPG Buffer 3–10 (0.5%, v/v)]. Protein concentration was measured by bicinchoninic acid-based colorimetric detection (micro BCA Kit, Pierce). Twenty micrograms of extracts were used for analytical gels, and 600 µg of unlabeled extract for preparative gels. Samples were diluted in 350 µl loading buffer and loaded on an 18 cm Immobiline DryStrip, pH 3–10, nonlinear. Gel-strips were rehydrated with the Ettan IPGphor device for 12 h at 30 V, and submitted to isoelectric focusing (1 h 150 V constant, 2 h 500 V constant, 2 h 1000 V constant, 5 h 8000 V constant reaching ~43 kVh at the end of the run). The strips were first equilibrated for 15 min in 15 ml of the equilibration solution [urea (6 *M*), Tris–HCl (75 m*M* pH 8.8), glycerol (29.3%), SDS (2%, w/v), traces bromophenol blue] that contained DTT (10 mg/ml), then for 15 min in 15 ml of the equilibration solution containing IAM (25 mg/ml) in the dark. The second dimension was performed using the Ettan DALT six device, by overnight migration at 1.5 W/gel. Images of the analytical gels were recorded with the Odyssey scanner (LI-COR biosciences) at a resolution of 169 µm and

medium quality laser intensities. Image analyses used the Delta2D Decodon software. Preparative gels were stained with Coomassie brilliant blue or with Sypro following manufacturers' protocols. Gel spots were manually excised and submitted to *in situ* trypsin digestion followed by MALDI-MS/MS analysis.

4.1.5. The OxICAT procedure

OxICAT experiments were performed according to the procedure of Leichert *et al.* (2008). Briefly, 10^6 HeLa cells were used per sample. TCA-precipitated extracts' pellets were suspended in 80 μl of denaturing buffer [urea (6 *M*), SDS (0.5%, w/v), EDTA (10 m*M*), Tris–HCl (200 m*M*, pH 8.5)] to which was added one standard vial of light ICAT reagent dissolved in 20 μl of ACN. Free thiols were ICAT-labeled in the dark for 1 h at 37 °C on a stirring device (900 rpm). The reaction was stopped by TCA precipitation also removing excess reagents. The TCA-precipitated pellet was dissolved in 80 μl of denaturing buffer and 2 μl TCEP (50 m*M* stock solution) to which was added one standard vial of heavy ICAT reagent dissolved in 20 μl of ACN. Oxidized thiols were ICAT-labeled in the dark for 1 h at 37 °C on a stirring device (900 rpm). The reaction was stopped as above. Proteins were digested overnight at 37 °C by adding directly to the TCA-precipitated pellet 80 μl of digestion buffer [SDS (0.1%, w/v), Tris–HCl (pH 8.5, 50 m*M*)], 20 μl of ACN, and 100 μl of TPCK-treated trypsin solution (0.1 μg/μl). Peptide purification by SCX and avidin cartridges and biotin cleavage were performed according to the manufacturer's instructions.

4.1.6. MS analyses

Peptide mixtures obtained from *in situ* protein digestion were analyzed by MALDI-MS/MS using a 4800 MALDI-TOF/TOF (Applied Biosystems, ABI) mass spectrometer. Desalting of the samples (C18 Zip-Tip, Millipore) was performed if necessary. Proteolytic peptides solution (0.5 μl) and 1 μl of 5 μg/μl CHCA solution [ACN/water (7:3, v/v), TFA (0.1%, v/v)] were spotted onto a stainless steel MALDI plate. The samples were first analyzed in MS mode (constant laser intensity at 2100 (arbitrary units), just above the desorption threshold, 1200 shots averaged). The 15 most intense peaks (threshold of signal/noise ratio: 100) were selected as precursors for further MS/MS analyses (laser intensity at 3500, 2400 shots averaged, acceleration voltage 2 kV, CID mode OFF, and metastable suppressor mode ON).

4.1.7. LC/MALDI-MS/MS analyses

Nano-LC–MALDI-MS/MS experiments were performed on a 4800 TOF/TOF mass spectrometer (Applied Biosystems) coupled to an Ultimate3000 system (Dionex). Proteolytic peptide samples were loaded and desalted on a reversed-phase cartridge (C18 PepMap 100 Dionex, 15×1 mm, 5 μm) at

20 μl/min with solvent A (ACN/water 2:98, v/v, formic acid 0.1%, v/v), for 5 min before to be eluted on a reversed-phase column (C18 PepMap 100 Dionex, 150 mm×75 μm), at 220 nl/min with a linear gradient of solvent B (ACN/water 90:10, v/v, formic acid 0.1%, v/v) from 0% to 50% in 35 min. The eluate was continuously mixed online with a solution of CHCA [5 mg/ml in ACN/water (7:3, v/v), TFA (0.1%, v/v), 436 nl/min] with postcolumn a T junction. Two hundred and fourty spots were collected (one fraction/10 s) on a stainless steel MALDI plate and analyzed in MS and MS/MS modes. A first MS analysis of the spots generated a list of precursors that were further fragmented in the second MS/MS analysis. The protocol for MS acquisition was the same as above except that seven precursors instead of 15 were selected *per* spot for MS/MS analysis.

4.1.8. Protein identification

GPS software (Applied Biosystems) extracted peak lists from MS and MS/MS data for database search (*S/N* threshold: 50 for MS data and 30 for MS/MS data). The peak lists were submitted to MASCOT search engine (taxonomy *human* or *S. cerevisiae* according to the sample, Swiss Prot database, mass tolerance accuracy 50 ppm for MS and 0.3 Da for MS/MS, instrument type MALDI-TOF/TOF).

4.2. Results

4.2.1. The 2DE-based two-fluorescent dyes differential labeling approach

To circumvent the limit of redox-DIGE (see above), Le Moan *et al.* (2009) introduced a new gel-based approach consisting in differentially labeling both reduced and oxidized Cys resides with two-fluorescent Cys-specific reagents (Dy680 and Dy780, Dynomics) (Fig. 10.1A). We used this technique in *S. cerevisiae* to evaluate the effect of extremely high intracellular levels of glutathione (GSH) disulfide (GSSG) on the redox state of cytoplasmic protein-thiols. Such high GSSG levels are expected to cause widespread Cys residue oxidation. HGT1 is a glutathione-specific transporter (Srikanth *et al.*, 2005), and cells that overexpress it accumulate up to 100 m*M* GSH or GSSG, when grown in the presence of either of these compounds, respectively (Kumar *et al.*, unpublished data). We prepared extracts from exponentially growing wild-type (WT) cells and *HGT1*-expressing cells exposed to GSSG (50 μ*M*) for 15 min, which are known to contain GSSG at concentrations of about 0.1–0.3 and 40 m*M*, respectively.

Differentially labeled and 2DE-separated proteins were detected as spots colored between the red and green tones (Fig. 10.1B and C). GSSG exposure caused some increase in the green over the red component for some spots, indicating increased oxidation of the corresponding proteins. We quantified

the green/red fluorescence ratio for three select proteins, the peroxiredoxins Tsa1 and Ahp1 and glyceraldehyde-3-phosphate dehydrogenase (Tdh3), which are all known to oxidize *in vivo* at Cys residues (Fig. 10.1D). All three were significantly more oxidized after GSSG treatment. We also quantified the green/red fluorescence intensities of the 150 more visible spots, enabling graphic representation and easy comparison of the redoxome of the two yeast samples (Fig. 10.1E). The increased oxidation caused by GSSG was not as important as expected, which might indicate that the GSSG/GSH couple has only a moderate effect on cytoplasmic thiol-redox control, in keeping with published results (Le Moan *et al.*, 2006).

Efficiency of protein extraction and the amount of Cys residues are highly dependent on the nature of the sample, which requires optimizing the procedure for each cell extract. It is also highly recommended that the reduced Cys residue saturation after the first labeling step be taken into account in order to avoid cross-reactions with the second dye. We indeed found that saturation could not be reached with fluorescent reagents, which led us to use the dye as a tracer by performing the first labeling step in the presence of a high concentration of IAM. Accordingly, saturation conditions have to be set up for each extracts by testing different concentrations of IAM, as shown in Fig. 10.1F. Proteins isoelectric focalization also requires optimization. Usually, 15–25 μg of cell extracts are sufficient for one 2DE. Sample dilution in loading buffer should avoid undesired high conductivity, but its occurrence, which limits the voltage that can be applied to the gel-strip, can be corrected by sample purification with the GE 2D Clean-up kit and/or by decreasing the concentration of IPG buffer.

In summary, 2DE-based two-fluorescent dyes differential labeling provides snapshots of the redoxome for easy and relatively fast comparisons of cellular conditions.

4.2.2. The shotgun OxICAT procedure

As already mentioned, the OxICAT procedure (Leichert *et al.*, 2008) identifies oxidized Cys residues within polypeptides, and rigorously quantifies their redox state as a ratio, thus allowing comparison of cell conditions. Further, as a high-throughput method, it theoretically considers all cellular Cys residues, most of which are inaccessible by the 2DE-based methods described above. We submitted untreated HeLa cells to the OxICAT procedure, and focused on the Parkinson disease (PD) protein 7 (DJ-1) within the MS data obtained. DJ-1 is a redox-responsive protein with neuroprotective functions, for which mutations have been linked to hereditary forms of PD (Kahle *et al.*, 2009). DJ-1 is also a biomarker for cancer and neurodegenerative diseases, particularly when in its oxidized form. Of its three Cys residues, DJ-1 Cys106 was shown to be oxidized to sulfinic, by crystallographic studies (Canet-Aviles *et al.*, 2004) and sulfonic by mass spectrometry analysis (Kinumi *et al.*, 2004). All Cys-containing proteolytic

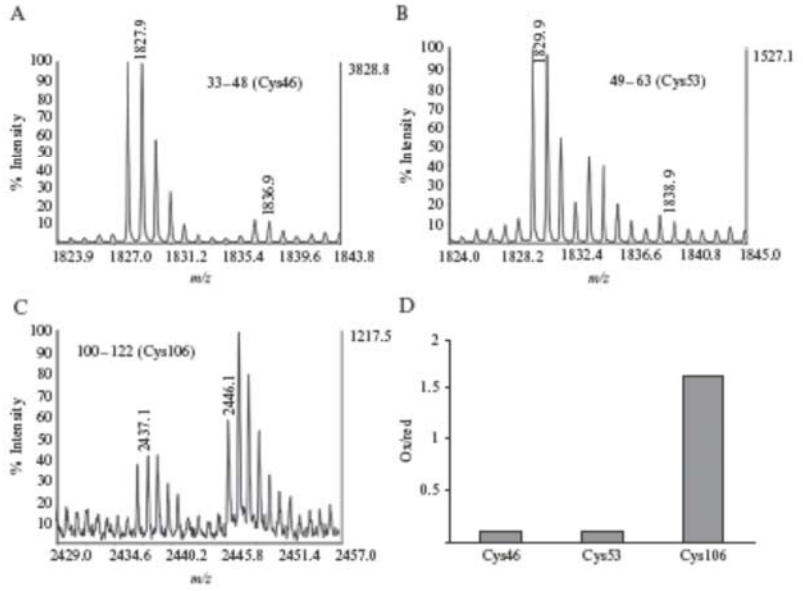

Figure 10.2 The redox state of the DJ-1 three Cys residues (Cys46, Cys53, Cys106) as established by OxICAT. (A, B, and C) MALDI-MS spectra of the Cys residues-containing peptides, as indicated. (D) Quantification of the heavy to light (Ox/Red) ratio of the three Cys residues as indicated.

peptides of DJ-1 were detected by MS analysis. Heavy-to-light ICAT ratio measurements showed that redox-sensitive Cys106 residue was indeed selectively and significantly oxidized (Fig. 10.2). The oxidized form of Cys106 identified here is either a disulfide, possibly formed with GSH or with another protein, but less likely a sulfenic acid, due to its instability. However, due to their nonreversibility, the Cys106 higher oxides identified by others, at least *in vivo*, are not accessible to the ICAT reagents.

The OxICAT strategy also requires optimizing reduced Cys residues ICAT reagent saturation as a crucial step, as suggested by Leichert *et al.* (2008). As a high-throughput method, OxICAT allows recording a huge amount of MS and MS/MS spectra, which have then to be processed. However, not all the information obtained is relevant, creating interferences with the LC–MS/MS detection of interesting peptides. Therefore, designing software tools helping establish peptides "inclusion lists" are important to consider according to one's own needs. LC–MALDI-MS/MS analysis is best suited for the OxICAT strategy, as LC-fractionated peptides are spotted onto the MALDI plate, subsequently allowing specific offline acquisitions using "inclusion lists," which can be performed iteratively without the need of preparing new samples and thus consuming the expensive ICAT reagents.

4.2.3. Complementarities of 2DE-based fluorescence and OxICAT methods

We confronted results obtained with HeLa cell extracts analyzed by the 2DE-based two-fluorescence labeling and OxICAT methods (Fig. 10.3). Vimentin, a protein of the intermediate filament family containing a single Cys residue (Cys328), and GRP78, a chaperone protein of the ER containing two Cys residues (Cys41 and Cys420), were both visible on the 2DE gel but were missing from the initial LC–MALDI-MS/MS analysis. We thus acquired additional MS/MS spectra from the same LC MALDI spots using an "inclusion list" specifying the theoretical masses of ICAT-labeled peptides corresponding to these proteins. We thereby identified MS spectra for the vimentin peptide 322-342 (Cys328) that indicated that this residue was fully reduced (Fig. 10.3A), in total concordance with the fluorescence data that also showed this residue fully reduced (Fig. 10.3C and D). We also identified MS spectra for GRP78 peptide 25–46 (Cys41) (Fig. 10.3B), but

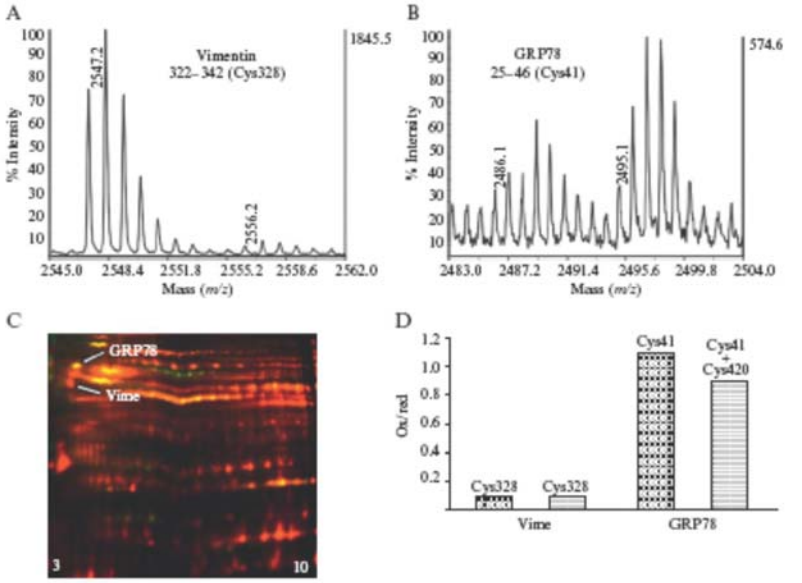

Figure 10.3 Confronting the results of the 2DE-based fluorescence and ICAT strategies. (A and B) HeLa cell extracts were submitted to OxICAT. Mass spectra of the vimentin peptide containing Cys328 (A) and the GRP78 peptide containing Cys41 (B) are represented, as indicated. (C) HeLa cell extracts were submitted to the 2DE-based fluorescence labeling procedure. The arrows indicate spots corresponding to vimentin and GRP78. (D) Oxidized to reduced ratios of vimentin GRP78 Cys residues established through the ICAT (spotted bars) and the 2DE-based fluorescence (stripped bars), as indicated.

not for the second GRP78 Cys-containing peptide (Cys420), which fell out of the experimental acquisition range, because of its large size ($m/z = 5069.6$). However, confronting the fluorescence data, which indicated that GRP78 is half-oxidized (Ox/Red ratio close to one) (Fig. 10.3C and D), and MS data, which indicated that GRP78 Cys41 is also half-oxidized (Fig. 10.3D), suggests that Cys420 is probably also oxidized, possibly to an intramolecular disulfide with Cys41. Indeed, Cys420 should also be half-oxidized to account for the half-oxidized state of GRP78 seen by fluorescence, a value reflecting the average redox state of both GRP78 Cys residues. This finding should be verified and the linearity between the fluorescence- and OxICAT-data validated by considering a larger number of proteins.

5. Conclusions

Redox proteomics is complex and remains an experimental challenge. OxICAT appears to be the most robust and reliable technique to identify and quantitatively assess the redox state of Cys residues. Further, its exhaustive nature will allow identification of proteins that are ignored by the other methods. Among the 2DE-based methods, the two-fluorescence differential labeling procedure appears to us the best method to obtain snapshots of the redoxome. This method should complement the OxICAT method when used as a screening procedure to select for the most informative cell conditions (growth, mutations, exogenous treatments, etc.), and also to select for interesting proteins that are then identified in the OxICAT MS data, as shown here. A systematic identification of the redoxome of mammalian cells should provide clues to understand Cys residues redox metabolism.

ACKNOWLEDGMENTS

We acknowledge the "DIM SEnT Région Ile-de-France" postdoctoral fellowship to GC. MBT is the recipient of a fund program "Equipe Labellisée Ligue 2009," from La Ligue Contre le Cancer (LCC).

REFERENCES

Baty, J. W., *et al.* (2002). Detection of oxidant sensitive thiol proteins by fluorescence labeling and two-electrophoresis. *Proteomics* **2,** 1261–1266.

Bernhardt, J., *et al.* (1999). Dual channel imaging of two-dimensional electropherograms in *Bacillus subtilis*. *Electrophoresis* **20,** 2225–2240.

Boivin, B., *et al.* (2008). A modified cysteinyl-labeling assay reveals reversible oxidation of protein tyrosine phosphatases in angiomyolipoma cells. *Proc. Natl. Acad. Sci. USA* **105,** 9959–9964.

Bruschi, M., *et al.* (2009). New iodo-acetamido cyanines for labeling cysteine thiol residues. A strategy for evaluating plasma proteins and their oxido-redox status. *Proteomics* **9,** 460–469.

Canet-Aviles, R. M., *et al.* (2004). The Parkinson's disease protein DJ-1 is neuroprotective due to cysteine-sulfinic acid-driven mitochondrial localization. *Proc. Natl. Acad. Sci. USA* **101,** 9103–9108.

D'Autreaux, B., and Toledano, M. B. (2007). ROS as signalling molecules: Mechanisms that generate specificity in ROS homeostasis. *Nat. Rev. Mol. Cell Biol.* **8,** 813–824.

Delaunay, A., *et al.* (2000). H2O2 sensing through oxidation of the Yap1 transcription factor. *EMBO J.* **19,** 5157–5166.

Dietz, L., *et al.* (2009). Quantitative DY-maleimide-based proteomic 2-DE-labeling strategies using human skin proteins. *Proteomics* **9,** 4298–4308.

Eaton, P. (2006). Protein thiol oxidation in health and disease: Techniques for measuring disulfides and related modifications in complex protein mixtures. *Free Radic. Biol. Med.* **40,** 1889–1899.

Fourquet, S., *et al.* (2008). The dual functions of thiol-based peroxidases in H_2O_2 scavenging and signaling. *Antioxid. Redox Signal.* **10,** 1565–1576.

Fu, C., *et al.* (2008). Quantitative analysis of redox-sensitive proteome with DIGE and ICAT. *J. Proteome Res.* **7,** 3789–3802.

Gorman, J. J., *et al.* (2002). Protein disulfide bond determination by mass spectrometry. *Mass Spectrom. Rev.* **21,** 183–216.

Gygi, S. P., *et al.* (1999). Protein analysis by mass spectrometry and sequence database searching: Tools for cancer research in the post-genomic era. *Electrophoresis* **20,** 310–319.

Hess, D. T., *et al.* (2005). Protein S-nitrosylation: Purview and parameters. *Nat. Rev. Mol. Cell Biol.* **6,** 150–166.

Hochgrafe, F., *et al.* (2005). Fluorescence thiol modification assay: Oxidatively modified proteins in *Bacillus subtilis*. *Mol. Microbiol.* **58,** 409–425.

Hurd, T. R., *et al.* (2007). Detection of reactive oxygen species-sensitive thiol proteins by redox difference gel electrophoresis: Implications for mitochondrial redox signaling. *J. Biol. Chem.* **282,** 22040–22051.

Ito, K., and Inaba, K. (2008). The disulfide bond formation (Dsb) system. *Curr. Opin. Struct. Biol.* **18,** 450–458.

Jaffrey, S. R., and Snyder, S. H. (2001). The biotin switch method for the detection of S-nitrosylated proteins. *Sci. STKE.* **86,** pl1.

Janssen-Heininger, Y. M., *et al.* (2008). Redox-based regulation of signal transduction: Principles, pitfalls, and promises. *Free Radic. Biol. Med.* **45,** 1–17.

Kahle, P. J., *et al.* (2009). DJ-1 and prevention of oxidative stress in Parkinson's disease and other age-related disorders. *Free Radic. Biol. Med.* **47,** 1354–1361.

Kinumi, T., *et al.* (2004). Cysteine-106 of DJ-1 is the most sensitive cysteine residue to hydrogen peroxide-mediated oxidation in vivo in human umbilical vein endothelial cells. *Biochem. Biophys. Res. Commun.* **317,** 722–728.

Le Moan, N., *et al.* (2006). The *Saccharomyces cerevisiae* proteome of oxidized protein thiols: Contrasted functions for the thioredoxin and glutathione pathways. *J. Biol. Chem.* **281,** 10420–10430.

Le Moan, N., *et al.* (2009). Protein-thiol oxidation, from single proteins to proteome-wide analyses. *Methods Mol. Biol.* **476,** 175–192.

Leichert, L. I., *et al.* (2008). Quantifying changes in the thiol redox proteome upon oxidative stress in vivo. *Proc. Natl. Acad. Sci. USA* **105,** 8197–8202.

Leichert, L. I., and Jakob, U. (2004). Protein thiol modifications visualized in vivo. *PLoS Biol.* **2,** e333.

Linke, K., and Jakob, U. (2003). Not every disulfide lasts forever: Disulfide bond formation as a redox switch. *Antioxid. Redox Signal.* **5,** 425–434.

Mesecke, N., *et al.* (2005). A disulfide relay system in the intermembrane space of mitochondria that mediates protein import. *Cell* **121,** 1059–1069.

Patterson, S. D., and Katta, V. (1994). Prompt fragmentation of disulfide-linked peptides during matrix-assisted laser desorption ionization mass spectrometry. *Anal. Chem.* **66,** 3727–3732.

Poole, L. B., *et al.* (2005). Synthesis of chemical probes to map sulfenic acid modifications on proteins. *Bioconjug. Chem.* **16,** 1624–1628.

Rhee, S. G., *et al.* (2005). Intracellular messenger function of hydrogen peroxide and its regulation by peroxiredoxins. *Curr. Opin. Cell Biol.* **17,** 183–189.

Riederer, I. M., and Riederer, B. M. (2007). Differential protein labeling with thiol-reactive infrared DY-680 and DY-780 maleimides and analysis by two-dimensional gel electrophoresis. *Proteomics* **7,** 1753–1756.

Saurin, A. T., *et al.* (2004). Widespread sulfenic acid formation in tissues in response to hydrogen peroxide. *Proc. Natl. Acad. Sci. USA* **101,** 17982–17987.

Sevier, C. S., and Kaiser, C. A. (2008). Ero1 and redox homeostasis in the endoplasmic reticulum. *Biochim. Biophys. Acta* **1783,** 549–556.

Srikanth, C. V., *et al.* (2005). Multiple cis-regulatory elements and the yeast sulphur regulatory network are required for the regulation of the yeast glutathione transporter, Hgt1p. *Curr. Genet.* **47,** 345–358.

Toledano, M. B., *et al.* (2004). Microbial H_2O_2 sensors as archetypical redox signaling modules. *Trends Biochem. Sci.* **29,** 351–357.

Toledano, M. B., *et al.* (2007). The system biology of thiol redox system in *Escherichia coli* and yeast: Differential functions in oxidative stress, iron metabolism and DNA synthesis. *FEBS Lett.* **581,** 3598–3607.

Wan, J., *et al.* (2007). Palmitoylated proteins: Purification and identification. *Nat. Protoc.* **2,** 1573–1584.

Yano, H. (2003). Fluorescent labeling of disulfide proteins on 2D gel for screening allergens: A preliminary study. *Anal. Chem.* **75,** 4682–4685.

Annexe 2. Dansyl-peptides matrix-assisted laser desorption/ionization mass spectrometric (MALDI-MS) and tandem mass spectrometric (MS/MS) features improve the liquid chromatography/MALDI-MS/MS analysis of the proteome. Chiappetta G, Ndiaye S, Demey E, Haddad I, Marino G, Amoresano A, Vinh J. Rapid Commun Mass Spectrom. 2010 Oct 30; 24(20):3021-32. PMID: 20872635

RAPID COMMUNICATIONS IN MASS SPECTROMETRY
Rapid Commun. Mass Spectrom. 2010; 24: 3021–3032
Published online in Wiley Online Library (wileyonlinelibrary.com) DOI: 10.1002/rcm.4734

RCM

Dansyl-peptides matrix-assisted laser desorption/ionization mass spectrometric (MALDI-MS) and tandem mass spectrometric (MS/MS) features improve the liquid chromatography/MALDI-MS/MS analysis of the proteome

Giovanni Chiappetta[1,2*], Sega NDiaye[1], Emmanuelle Demey[1], Iman Haddad[1], Gennaro Marino[2], Angela Amoresano[2] and Joëlle Vinh[1]

[1]USR 3149 CNRS/ESPCI ParisTech, Ecole Supérieure de Physique et de Chimie Industrielles de Paris, Paris, France
[2]Department of Organic Chemistry and Biochemistry, Federico II University of Naples, Naples, Italy

Received 26 April 2010; Revised 4 August 2010; Accepted 5 August 2010

Peptide tagging is a useful tool to improve matrix-assisted laser desorption/ionization tandem mass spectrometric (MALDI-MS/MS) analysis. We present a new application of the use of the dansyl chloride (DNS-Cl). DNS-Cl is a specific primary amine reagent widely used in protein biochemistry. It adds a fluorescent dimethylaminonaphthalene moiety to the molecule. The evaluation of MALDI-MS and MS/MS analyses of dansylated peptides shows that dansylation raises the ionization efficiency of the most hydrophilic species compared with the most hydrophobic ones. Consequently, higher Mascot scores and protein sequence coverage are obtained by combining MS and MS/MS data of native and tagged samples. The N-terminal DNS-Cl sulfonation improves the peptide fragmentation and promotes the generation of b-fragments allowing better peptide sequencing. In addition, we set up a labeling protocol based on the microwave chemistry. Peptide dansylation proved to be a rapid and cheap method to improve the performance of liquid chromatography (LC)/MALDI-MS/MS analysis at the proteomic scale in terms of peptide detection and sequence coverage. Copyright © 2010 John Wiley & Sons, Ltd.

Currently, the use of matrix-assisted laser desorption/ionization tandem time-of-flight (MALDI-TOF/TOF) instruments leads to the recording of a large number of MS/MS spectra in automatic and high-throughput mode, performed either by post-source decay (PSD) or by collision-induced dissociation (CID) experiments. As a consequence, robust liquid chromatography/matrix-assisted laser desorption/ionization tandem mass spectrometric (LC/MALDI-MS/MS) analyses can be implemented to provide complementary data to the more widespread LC/electrospray ionization (ESI)-MS/MS approach.[1]

Despite the fact that the MALDI ionization mechanism is not yet completely understood, it is widely acknowledged that the ionization efficiency is highly peptide dependent. In particular, the presence of basic and/or hydrophobic groups[2] enhances the yields of the ionization process. In addition, it has been postulated that UV-adsorbing groups such as aromatic moieties can favor desorption/ionization, because they promote the transfer of laser energy to the analyte.[2,3]

Different chemical derivatizations have been performed to add chemical moieties on to the peptides that could act as 'MALDI active' groups. It has been reported that C-terminal lysine gives a lower ionization efficiency of the peptides than C-terminal arginine because of the lower gas-phase basicity of the ε-amine group.[2,4,5] For this reason, the conditions for lysine conversion into homoarginine by guanidination with *O*-methylisourea were set up. This modification increases the relative intensity of labeled peptides and improves the recovery of previously undetected peptides.[6,7] Unfortunately, it was further demonstrated in PSD experiments that the permanent cationic tag sequestrates the 'mobile proton' and weakens the fragmentation yields, resulting in poor MS/MS spectra of modified peptides.[8]

In contrast, the introduction of a strong acid moiety at the N-terminal position (such as sulfonic or phosphonic acid) decreases the MS signal intensity because of the addition of a negative charge.[9,10] However, for a singly charged peptide the presence of a second mobile proton enhances the PSD fragmentation.[3,9,11] A combination of the two labeling

*Correspondence to: G. Chiappetta, Biological Mass Spectrometry and Proteomics, USR 3149 CNRS/ESPCI-ParisTech, Ecole Supérieure de Physique et de Chimie Industrielles, 10 rue Vauquelin, 75231 Paris cedex 05, France.
E-mail: giovanni.chiappetta@unina.it

procedures was performed with coumarin aromatic derivatives:[8] enhancing both the peptide ionization efficiency and the PSD fragmentation.. Other UV-adsorbing groups have been evaluated underlining the importance of the energy transfer assistance in the MALDI techniques.[12,13]

Dansyl chloride (DNS-Cl) is a fluorescent reagent which is widely used in biochemistry to modify the primary amine group of proteins and peptides for N-terminal sequencing[14] and in selective proteomics to perform advanced MS analyses.[15–17] The synthesis of the ^{13}C heavy labeled form of DNS-Cl allowed also relative quantitation in metabolomics to be performed.[18]

The MALDI features of dansylated peptides in TOF-MS analysis were first evaluated by Park *et al.*[19] Besides the improvement of signal-to-noise (S/N) ratios, the authors found that the typical protein MALDI-MS fingerprint changed because previously undetected peptides were revealed with higher signal intensities. However, some peptides were not any longer detected after dansylation. The combination of the peptide mass fingerprint (PMF) of the native and tagged complementary peptides mixtures can be used for the database analysis to improve identification and protein coverage. Dansylation labeling may also improve the MALDI ionization and fragmentation of glycosylated peptides whose analysis is often problematic.[20]

In this study the features of peptide dansylation are studied for LC/MALDI-MS/MS analysis. The PSD-like fragmentation characteristics of dansylated peptides are evaluated to understand the effects of the modification using a tryptic digest of bovine serum albumin (BSA) as standard. The feasibility of the entire strategy at the proteomic scale is finally evaluated by using complex mixtures of proteolytic peptides. The effects of dansylation shown by Park *et al.* in MS are generalized to a large number of species and extend their results for LC/MALDI-MS/MS analysis.

EXPERIMENTAL

Chemicals

Tri(hydroxymethyl)aminomethane (Tris), 5-*N*,*N*-(dimethylamino)naphthalene-1-sulfonyl chloride (dansyl chloride, DNS-Cl), sodium carbonate and iodoacetamide (IAM) were purchased from Fluka. Bovine serum albumin (BSA), ethylenediaminetetraacetic acid (EDTA), trifluoroacetic acid (TFA), guanidine, trypsin, chymotrypsin, endoproteinase Glu-C, dithiothreitol (DTT), alpha-cyano-4-hydroxycinnamic acid (CHCA), and 2,5-dihydroxybenzoic acid (DHB) were purchased from Sigma (St. Louis, MO, USA). All the solvents were of the highest purity available from Baker. All other reagents were of the highest purity available from Sigma.

Standard protein digestion

Aliquots of BSA were dissolved in denaturing buffer (guanidine 6 M, Tris 150 mM, EDTA 10 mM, pH 8.0) to a final concentration of 0.2 μg/μL (3.0 pmol/μL), reduced with DTT (10-fold molar excess on the cysteine residues) for 2 h at 37°C and then alkylated with IAM (5-fold molar excess on the thiol residues) for 30 min at room temperature in the dark. Protein samples were desalted on size-exclusion cartridges (PD-10, Amersham). The elution was performed in Na_2CO_3 50 mM, pH 8.8. Protein elution was monitored at 220 and 280 nm. The fractions containing the proteins were pooled, concentrated and then digested. Trypsin, chymotrypsin and endoproteinase Glu-C digestions were carried out using an enzyme/substrate ratio of 1:50 (w/w) either at 37°C for 18 h or by microwave heating of the tubes in a water-bath and warming for 1 min in a microwave oven set at a power of 700 W.

Bacterial strains, growth conditions and protein extract preparation

Escherichia coli K12 strain was grown in aerobic conditions at 37°C in LB medium. After 16 h bacteria were harvested by centrifugation and re-suspended in Buffer Z (25 mM HEPES pH 7.6, 50 mM KCl, 12.5 mM $MgCl_2$, 1.0 mM DTT, 20% glycerol, 0.1% Triton) containing 1 μM phenylmethylsulfonyl fluoride. Cells were harvested by sonication. The suspension was centrifuged at 90 000 *g* for 30 min at 4°C. After centrifugation the protein concentration of the extract was determined by Bradford assay.

Peptide labeling

To 50 μL of the BSA peptide mixture (3.0 pmol/μL) were added 50 μL of a solution 5 ng/μL (18.5 nmol/μL) of DNS-Cl in acetonitrile (ACN). This results in an approximate reactive excess of 1:5000 (BSA/DNS-Cl). The reaction was carried out either for 45 min at 75°C[19] or warming the tubes in a water bath for 5 min in a microwave oven at a power of 700 W.

MALDI-MS/MS analysis

Peptide mixtures in Na_2CO_3 were diluted 10-fold in 0.1% aqueous TFA (v/v) and then 0.5 μL of the resulting solution was co-crystallized on a MALDI sample plate with 1 μL of a 4 mg/mL solution of CHCA in ACN/0.1% aqueous TFA (7:3, v/v). The spectra were automatically acquired with a 4800 MALDI-TOF/TOF instrument (Applied Biosystems) in MS mode, then the 25 most intense peaks with a S/N ratio above 100 were selected as precursors for further MS/MS analysis. The laser displacement on the spot was in 'random' mode. The MS spectra were recorded with 1200 laser shots at a laser intensity of 2100 arbitrary units (just above the desorption threshold). The fragmentation spectra were acquired with 2400 laser shots at a laser at 3500 arbitrary units, with a collision energy voltage of 2 kV, without collision gas (CID OFF mode) and with suppression of the metastable ions (metastable suppressor mode ON). BSA peptides assigned with PMF analysis and not automatically selected for MS/MS analysis were manually fragmented using *ad hoc* parameters changing the number of shots, the laser intensity and the number of the cumulated spectra.

LC/MALDI-MS/MS

NanoLC/MALDI-MS/MS experiments were performed on a 4800 TOF/TOF mass spectrometer (Applied Biosystems) coupled to an Ultimate 3000 LC system (Dionex) with an automat LC-Packings Probot (Dionex). Peptide mixtures

were loaded and desalted onto a reversed-phase pre-column cartridge (C18 PepMap 100 Dionex, 15 × 1 mm, 5 μm) at 20 μL/min with solvent A (ACN/0.9% aqueous formic acid, 2:98 v/v) for 5 min. Peptides were then eluted on a reversed-phase column (C18 PepMap 100 Dionex, 150 mm × 75 μm) at a flow rate of 0.2 μL/min with a 0–50% linear gradient of solvent B (ACN/0.9% aqueous formic acid, 10:90 v/v) in 35 min. The eluates were continuously mixed on-line with a solution of CHCA (5 mg/mL) at 436 nL/min by a T junction. A total of 180 spots were collected (one fraction each 10 s) on a MALDI sample plate with the Probot (Dionex). The resulting plate was analyzed in MS and in MS/MS mode by the 4800 TOF/TOF mass spectrometer. The method started with an MS analysis of all the spots to generate the list of precursors that were subsequently fragmented in MS/MS mode. The protocol for MS acquisition was the same as above except that 7 instead of 25 precursors *per* spot were selected for MS/MS analysis using 400 laser shots instead of 1200. The time duration of the MS/MS analysis is roughly 2 min for each spot.

Protein identification

The MS and MS/MS data were used for the database search. Peak lists were generated using the Applied Biosystems GPS tool that selected peaks with S/N ratio above 50 for the MS data analysis and above S/N ratio 30 for the MS/MS data. The peak lists were submitted to the Mascot search engine using the following research parameters: *other mammalia* and *E. coli* as taxonomy respectively for the analysis of BSA and the *E. coli* protein extract using the SwissProt database. Cysteine carbamidomethylation was selected as fixed modification and lysine N-terminal dansylation and methionine oxidation were selected as variable modifications. MudPIT scoring was selected for the protein score calculation. The MS mass tolerance was set at 50 ppm for the MS and 0.3 Da for the MS/MS. The instrument fragment ion type was the Mascot window 'MALDI-TOF/TOF' default setting. Mascot results were processed with myProMS[21] to combine the results obtained from the separate analyses of the unlabeled and dansylated samples. The peptides found in common between the two samples were considered only once using the best Mascot ion score. Only proteins identified with at least 2 peptides with distinct amino acid sequences, and individual ion score higher than 30 for each peptide (Mascot identity threshold), were validated.

Analysis of the *E. coli* proteome

E. coli protein extract (15 ng) was reduced and alkylated under denaturing conditions and then the excess of reagent was removed by size-exclusion chromatography eluting in 50 mM Na_2CO_3. Finally, *E. coli* proteins were digested by trypsin in a microwave oven. The resulting peptide mixture was divided in two aliquots, one of which was directly analyzed by LC/MALDI-MS/MS as described above. The second aliquot was microwave dansylated as described previously, dried to eliminate the ACN, re-suspended in the LC buffer A and finally analyzed by LC/MALDI-MS/MS. It was expected that 100 fmol of both native and tagged peptide mixtures were injected in separate runs.

RESULTS AND DISCUSSION

Peptide dansylation by DNS-Cl is a primary amine sulfonation that introduces one aromatic dimethylaminonaphthalene group. The sulfonyl chloride function of DNS-Cl is also reactive towards phenol hydroxyl groups at pH values higher than that normally used to modify peptide N-terminal amines.[22] Thus, tyrosine dansylation is considered as a partial side reaction.

Several experimental conditions for dansylation have been reported. The present work focuses on the set-up of a fast protocol based on microwave chemistry to reduce the time of manipulation. The use of microwave chemistry has become a common practice in proteomics.[23–26] Moreover, the advantages of microwave-assisted dansyl sulfonation in biogenic amines have been reported in previous studies.[27,28]

Optimization of the procedure

The reaction conditions, the acquisition parameters for the MS/MS analyses and the data processing were carefully evaluated and are fully described in the Supplemental Material using BSA as standard protein. Briefly, we found that performing the trypsin proteolysis and the peptide dansylation in a microwave oven, the analysis was improved in terms of identified peptides and manipulation time respect to the protocol proposed by Park *et al.*[19] The parameters for the MS/MS selection criteria and the database research were evaluated (see also the Experimental section). Moreover, the modification of the lysine side chain was not always quantitative, because the pH of the reaction was kept at 9.0 while the pKa value of the ε-amine lysine is 10.5. However, increasing the pH labeling conditions would increase the rate of dansyl chloride hydrolysis.[29] Thus, pH 9.0 was maintained for all experiments and in some cases the same peptide was detected twice, both with modified and unmodified lysine ε-amine. The limitations induced by this feature will be later discussed.

According to the procedure published by Park *et al.*,[19] the unlabeled sample was 2-fold more concentrated in comparison with dansylated samples, because of the dilution in the reagent solution. In order to study the effects of peptide dansylation, we diluted the unlabeled sample with a volume of ACN and we used it as control for the further experiments.

Understanding the effects of peptide dansylation on the MALDI-MS signal

As expected peptide dansylation changed the PMF of the standard protein BSA (see Supplemental Material). In agreement with Park *at al.*,[19] some new peptides were detected whereas others were lost after the dansylation (Table 1). A further investigation showed that many peptides were not automatically fragmented because their relative signal intensities were too low to pass the selection criteria for the MS/MS analysis. For example, the peptides (DNS)-SLHTLFGDELCK (*m/z* 1652.7) and (DNS)-RHPEYAVSVLLR (*m/z* 1672.7) were detected and manually sequenced after the dansylation even if they were not automatically selected for fragmentation. In contrat, the peptide (DNS)-SEIAHR (*m/z* 945.4) was automatically fragmented only after the N-terminal dansylation.

Table 1. Results of the automatic and manual MS/MS analyses of the microwave-digested/dansylated sample and for the diluted microwave-digested/unlabeled sample (control). No Mascot scores are reported for manually fragmented peptides because they are strongly dependent from the *ad hoc* parameters used to obtain good spectra. When the same peptide is detected in different dansylated forms only the best score is reported. Dansylated lysine residues are labeled with an asterisk

	Mass	Sequence	Score	Mass	Sequence (dansylated)	Score
	712.3	SEIAHR	-	945.4	SEIAHR	21.3
	927.4	YLYEIAR	37	1160.5	YLYEIAR	22
	1001.5	ALKAWSVAR	40	1234.6	ALKAWSVAR	36
	1419.7	SLHTLFGDELCK	48.3	1652.6	SLHTLFGDELCK	-
Common	1439.7	RHPEYAVSVLLR	42	1672.7	RHPEYAVSVLLR	-
peptides	1479.8	LGEYGFQNALIVR	54	1712.8	LGEYGFQNALIVR	76
	1567.7	DAFLGSFLYEYSR	52	1800.7	DAFLGSFLYEYSR	58
	1639.8	KVPQVSTPTLVEVSR	32	1957.8	MPCTEDYLSLILNR	44
	1724.8	MPCTEDYLSLILNR	51	2105.9	*KVPQVSTPTLVEVSR	38
	2004.8	VASLRETYGDMADCCEK	28	2237.9	VASLRETYGDMADCCEK	36
	1305.7	HLVDEPQNLIK	41	714.3	FGER	29
	1795.7	DDPHACYSTVFDKLK	-	778.3	VASLR	-
	1880.9	RPCFSALTPDETYVPK	27	805.3	QRLR	-
	1907.9	LFTFHADICTLPDTEK	36	842.3	AFDEK	-
	1927.7	CCAADDKEACFAVEGPK	-	882.3	IETMR	-
	2045.0	RHPYFYAPELLYYANK	-	891.3	QEPER	-
Unique	2113.9	VHKECCHGDLLECADDR	23	939.3	CASIQK	26
peptides	2148.0	LKPDPNTLCDEFKADEKK	-	922.3	AWSVAR	-
	2247.9	ECCHGDLLECADDRADLAK	-	1022.4	LVTDLTK	-
	2277.1	LFTFHADICTLPDTEKQIK	29	1051.4	ATEEQLK	34
	2487.1	YNGVFQECCQAEDKGACLLPK	-	1139.5	IETMREK	-
	2492.2	GLVLIAFSQYLQQCPFDEHVK	-	1301.4	QNCDQFEK	28
	2541.2	QEPERNECFLSHKDDSPDLPK	28	1371.4	CCTESLVNR	18
	2612.2	VHKECCHGDLLECADDRADLAK	19	1524.6	ECCDKPLLEK	-
				1659.8	DTHFKSEIAHR	-
				1632.7	CCT*KPESER	39
				1676.6	YICDNQDTISSK	40
				1696.8	TCVADESHAGCEK	45

The sequence coverage of the control sample was higher even if the same number of peptides were identified (Fig. S1, Supplemental Material). To understand this behavior, we extended the number of peptides to be manually sequenced. All the peptides that were identified as BSA proteolytic peptides by PMF analysis and that exhibited a S/N ratio below the threshold for automatic MS/MS analysis were manually fragmented. Excluding the 10 peptides identified in both samples, we obtained 14 unique peptides specific to the control sample, 13 of which in the range *m/z* 1795.8–2612.2. We also identified 18 peptides specific to the dansylated sample in the range *m/z* 714.4–1696.8 (Table 1). Dansylation improved the ionization of smaller peptides. Moreover, the mass shift of 233 Da allowed the detection of species with *m/z* values that would have been below the operative low mass limit (700 Da) without modification. The peptides unique to the control sample were preferentially in the higher mass range of the spectra, and 13 out of 14 had a C-terminal lysine residue. We hypothesized that the absence of this set of peptides in the dansylated sample might not be directly related to a suppression effect caused by the decreased lysine side-chain basicity after the modification because it has already been demonstrated that the weak ε-amine gas-phase basicity of lysine has no positive effects on the MALDI ionization.[2]

As already reported, it is very difficult to predict the MALDI ionization efficiency of a peptide from the knowledge of its amino acid sequence.[30] The evidence that dansylation improved the detection of shorter peptides suggested that hydrophobicity might be an important parameter to predict which species should have been better ionized and later identified by the MALDI-MS analysis.

To further investigate the effects of peptide dansylation on the MALDI-MS signal, we extended our study to a larger number of peptides generated by the BSA microwave digestion using two different proteases: chymotrypsin and endoproteinase Glu-C. Equal amounts of these peptide mixtures were microwave dansylated and analyzed by MALDI-TOF/TOF and compared to their control samples. Fragmentation spectra were automatically recorded both for the control and the dansylated samples. The related peak lists were used for Mascot identification. The relative chromatographic hydrophobicity of all the identified peptides was calculated using the software SSRCalculator version 3.0.[31] The data in Table 2 show that all the peptides specifically detected in their dansylated form had low values of relative hydrophobicity, confirming that dansylation promoted the analysis of hydrophilic peptides by MALDI-MS. Similar effects were also found by Pashkova *et al.*[3] using aromatic coumarin tags.

Others authors[19,20] have reported that peptide dansylation improves the S/N ratio in MALDI-MS mode. According to our data this was not always verified. To further investigate this effect, equal amounts of the peptide mixtures generated by the microwave-assisted proteolytic digestion using trypsin, chymotrypsin and Glu-C in the native and

DOI: 10.1002/rcm

Table 2. Unique BSA peptides found either in native or in dansylated forms. For each peptide the relative hydrophobicity is reported (calculated according to Krokhin *et al.*[31])

	Sequence (Native)	Relative hydrophobicity	Sequence (dansylated)	Relative hydrophobicity
	HLVDEPQNLIK	22,1	FGER	6,4
	DDPHACYSTVFDKLK	23,3	VASLR	9,2
	RPCFSALTPDETYVPK	27,6	QRLR	3,9
	LFTFHADICTLPDTEK	31,7	AFDEK	6,6
	CCAADDKEACFAVEGPK	17,3	IETMR	8,9
	RHPYFYAPELLYYANK	33,8	QEPER	−2,6
	VHKECCHGDLLECADDR	14,4	CASIQK	2,0
	LKPDPNTLCDEFKADEKK	21.5	AWSVAR	15,8
Trypsin	ECCHGDLLECADDRADLAK	22,6	LVTDLTK	16,3
	LFTFHADICTLPDTEKQIK	32,8	ATEEQLK	6,0
	YNGVFQECCQAEDKGACLLPK	28	IETMREK	7,5
	GLVLIAFSQYLQQCPFDEHVK	43,4	QNCDQFEK	8,7
	QEPERNECFLSHKDDSPDLPK	20.6	CCTESLVNR	12,2
	VHKECCHGDLLECADDRADLAK	19.0	DTH*KSEIAHR	2,5
			ECCDKPLLEK	14,8
			CCT*KPESER	2,6
			YICDNQDTISSK	13,2
			TCVADESHAGCEK	3,6
	KKFWGKYLYE	29.9	TMRE	0.9
	IARRHPYFYAPE	21.0	SHAGCE	−2.5
	DKGACLLPKIE	22.2	RMPCTE	7.7
Glu-C	RALKAWSVARLSQKFPKAE	30.6	LCKVASLRE	14.6
	LAKYICDNQDTISSKLKE	22.0	*KSHCIAE	2.2
	YAVSVLLRLAKEYE	33.6	QEPERNE	−1.1
	DYLSLILNRLCVLHE	44.2	YSRRHPE	2.3
	NFVAFVDKCCAADDKE	25.2	RMPCTE	7.7
	LSHKDDSPDLPKLKPDPNTLCDEF	26.1	KADE*KKF	5.3
	IKQNCDQFEKLGEY	20.9	EKLGEY	12.5
Chymotrypsin	VDKCCAADDKEACF	10.8	IVRY	10.1
	VNRRPCF	12.8	LYEY	18.4
	RLAKEYEATL	19.9	RCASIQKF	16.3
			RLAKEY	11.4

dansyl-tagged forms were spotted on a MALDI plate adding 20 fmol of Des-Arg1-bradykinin (*m/z* MH^+ 904.4) as internal standard (standard/sample 1:20 (mol/mol) according to the estimated amount of protein digests analyzed, 10 different spots per sample were analyzed). The averaged relative intensities of the peaks identified as common peptides in the native and dansylated samples were normalized with the internal standard. Relative standard deviation (RSD) values were between 10% and 20% (error bars are reported on the graphic in Fig. 1) using at least five mass spectra for the calculation of averaged relative intensities, indicating that the results are compatible with quantitation studies.[3] For each common peptide the normalized intensities of the dansylated and unmodified forms with the associated calculated hydrophobicity are visualized in Fig. 1. Although we did not find a find a simple relationship to correlate the signal intensity improvement and the peptide sequence, it was confirmed that increased signals were found when hydrophilic peptides were labeled. On the other hand, the signal intensities of the most hydrophobic peptides decreased after their N-terminal amine sulfonation with DNS-Cl.

The three different BSA peptide mixtures were also analyzed using the less hydrophobic matrix DHB (Fig. 1). For many hydrophilic peptides the increase in the MALDI-MS signal intensity was attenuated after the dansylation. Thus, we hypothesized that the introduction of a hydrophobic dimethylaminonaphthalene group by primary amine sulfonation might have two opposite effects: (a) it favoured the co-crystallization of more hydrophilic peptides with the matrix, increasing the ionization efficiency;[3] and (b) it decreased the N-terminal amine proton affinity with a negative influence on the peptide proton affinity. DNS-Cl labeling effects on peptide ionization efficiency may be a compromise between these two effects. For this reason the analysis of hydrophobic peptides was not improved and resulted in lower relative signal intensity. This behavior may explain the complementary features of the combined analysis proposed by Park *et al.* that was also confirmed by our MALDI-MS/MS data.

The preferential loss of lysine-containing peptides after the dansylation may be related to the hydrophobicity of the undetected peptides coupled to the unfavorable presence of a lysine residue. The fact that most of bi-dansylated peptides were hydrophilic (Table 2) also confirms our hypothesis.

Understanding the effects of peptide dansylation on the MALDI-MS/MS analysis

The MALDI-MS/MS features of dansyl-peptides in PSD-like experiments (CID OFF mode) were first assayed using BSA tryptic peptides.

Considering only the peptides that were automatically fragmented under the same operative conditions, it resulted that Mascot scores of dansylated peptides changed com-

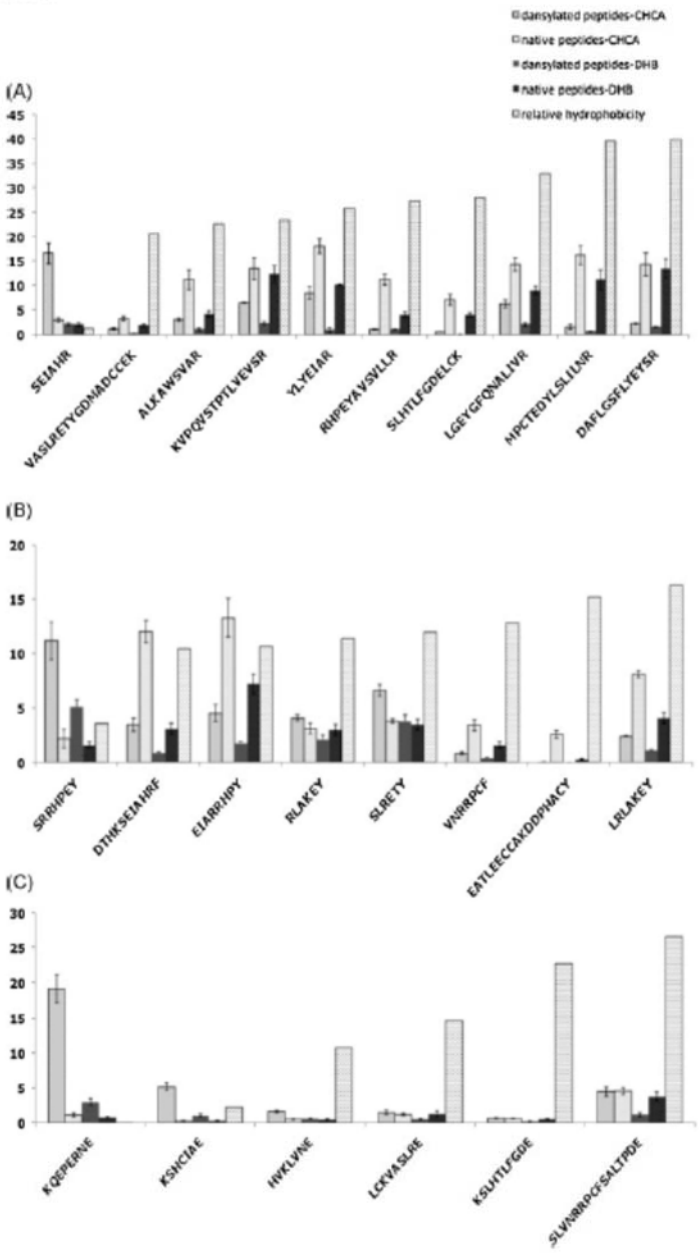

Figure 1. Des-Arg1-bradykinin was used as internal standard to normalize PMF of BSA proteolytic peptides generated by microwave-assisted trypsin (A), chymotrypsin (B) and endoproteinase Glu-C (C) digestions. Intensities of dansylated and native peptides are compared using both CHCA and DHB matrices. For each peptide the value of relative hydrophobicity is reported (calculated according to Krokhin *et al.*[31]).

DOI: 10.1002/rcm

pared to the associated unlabeled peptides: both increases or decreases are observed (Table 1). MS/MS results were not only correlated to the relative intensities of the precursor ions in MS mode (Fig. 1 and Table 1). In other words, the difference in ionization efficiency was not the only discriminatory parameter for the difference in quality of the MS/MS data between dansylated and native peptides because the fragmentation profiles are modified.

The fragmentation pattern of dansylated peptides exhibited enhanced *b*-ion series in PSD-like experiments (Fig. 2) compared to the native ones. This improvement in fragmentation could be attributed to the presence of the dansyl fluorescent moiety in peptide N-terminal position. This behavior was in agreement with previous reports where a fluorescent modification of peptide N-terminal amino acid induced a better generation of *b*-ion series.[3,13] To better understand this effect, the values of the relative signal intensities of *b*-ion series and their complementary *y*-ion series were evaluated for the automatically fragmented peptides. The tendency of a singly charged precursor ion to preferentially give rise to *b*- or *y*-fragment ions was monitored. The experimental relative intensities for each fragment ion detected in the MS/MS spectra related to the common BSA peptides are plotted in Figs. 3 and S2 of the Supplemental Material. The diagrams obtained gave a snapshot of the peptide sequence coverage by the MALDI-TOF/TOF analysis. In these diagrams the larger extent of the dotted plot indicated that the generation of *y*-ions was promoted. This was in agreement with a higher probability of a localization of the positive charge in the C-terminal position for singly charged tryptic peptides.[32] It was observed that the *y*-ion intensities were higher for the first

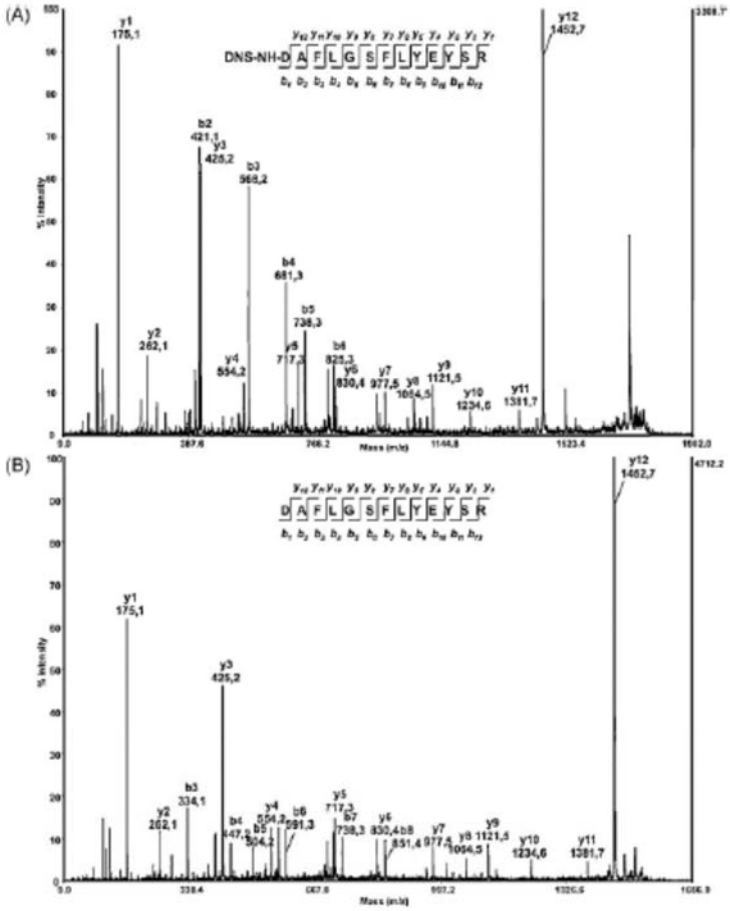

Figure 2. PSD-like fragmentation spectra of the BSA peptide DAFLGSFLYEYSR in dansylated (A) and native (B) forms.

DOI: 10.1002/rcm

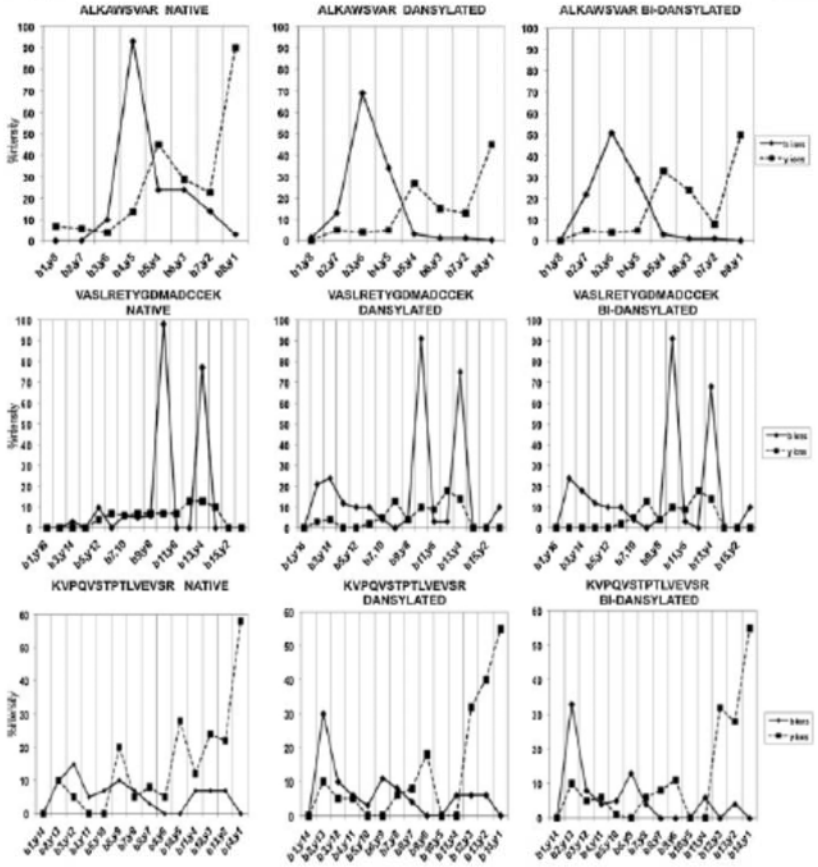

Figure 3. Relative intensities of *b*- and *y*-ion series for each native and dansylated BSA peptide. The intensities of the *b*-ions increase close to the N-terminal part of the dansylated peptides.

members of the series than in the higher mass range. This variation in intensity distribution could be attributed to the hybrid charge-directed/charge-remote fragmentation of tryptic peptides.[33] According to the mobile-proton model,[34] in the gas phase the charge is transferred from the basic sites to the vicinal amide bond leading to its destabilization and further fragmentation. This delocalization is statistically distributed along the peptide chain, generating a population of isomer ions. However, the charge localization on the C-terminal arginine or lysine basic-groups reduces the proton mobility and destabilizes the amide bond in the N-terminal region.

The graphics in Figs. 3 and S2 of the Supplemental Material showed a typical decrease of intensity in the high mass range for the *y*-ion series both for the native and dansylated peptides. Moreover, the *b*-ion series appeared higher for the dansylated peptides compared with the unmodified ones: the N-terminal amine dansylation increased the generation of *b* ions.

The intensity distribution of the *b*-ion series of the native peptides was not complementary to the *y*-ion series. This might be due to the lack of charge localization in the N-terminal side caused by the stronger basicity of the C-terminal of the peptide, meaning that the generation of *b*-ions is highly dependent on charge-directed fragmentation processes and the amide protonation is more probable at the central peptide bond. Therefore, it resulted that the N-terminal sequence of a native peptide was not always well covered by MALDI-MS/MS analysis although the distribution of MS/MS signal intensities should be influenced by the presence of proline, aspartate and glutamate residues that might locally increase the fragmentation efficiency. The intensity of the *b*-ion series of dansylated peptides was higher for the first member then decreased from the N-terminal region to the C-terminal region (Figs. 3 and S2 of the Supplemental Material) appearing more complementary to the *y*-ion series respect to native peptides. As a consequence, peptide dansylation improved the sequence

DOI: 10.1002/rcm

coverage in MS/MS. This could be rationalized considering that the effects of the N-terminal dansylation have a short-range nature: the peptide-bond fragmentation yield is increased at the N-terminal part. The generation of the *y*-ions could be less probable because of the decreased effect of C-terminus basicity in this region of the peptide chain. Moreover, the presence of the dansyl moiety could also play a role on the charge retention phenomenon. The fact that the intensity of the *y*-ion series did not decrease when the intensity of the *b*-ion series increased for singly charged precursor, one could hypothesize that the higher energy absorbed by dansylated peptides increased the proportion of fragmented precursor ions. The increased amount of precursor ions gave rise preferentially to *b*-ions. Two combined effects of the dansyl moiety on the peptide fragmentation should be considered. First, the UV-adsorbing naphthalene group might transfer the energy adsorbed from the laser radiation to the vicinal peptide bonds promoting a local destabilization, without the introduction of any additional mobile proton. Second, the dansyl moiety might also enhance the charge-retention process introducing a second amine group and also by the aromatic delocalization of the charge.

In order to study the effects of multi-dansylation on peptide fragmentation, we considered the MS/MS spectra of three BSA peptides found both in mono- and bi-dansylated forms (Fig. 3). The MS/MS spectra were acquired with the same mass spectrometer parameters. The BSA peptides, KVPQVSTPTLVEVSR, ALKAWSVAR, VASLRETYGD-MADCCEK, were detected with and without the lysine side chain dansylated. No changes between the fragmentation spectra of mono- and bi-dansylated forms of the peptides were observed. This finding could confirm that the dansyl moiety has a local effect on the peptide bond destabilization: if the lysine ε-amine is labeled, there is no long-range interaction along the peptide backbone, whereas the presence of the dansyl moiety was effective when it was directly linked to the peptide backbone by the N-terminal amine.

It is difficult to generalize the consequence of peptide dansylation on the Mascot ion score. For example, the peptide LGEYGFQNALIVR was identified with a higher ion score (ion sore 76) in the dansylated form as compared with the unmodified form (ion score 59), although its MS relative signal intensity is 50% weaker (Fig. 1). The increased intensities of b_2- to b_9-ions allowed a reduction in the number of 'most intense peaks' necessary to find the best match (Fig. S3, Supplemental Material). However, the peptide YLYEIAR was detected with a lower score in the dansylated form (ion score 22) than in the unmodified form (ion score 37). In this case, the increased intensities of b_2- and b_3-ions had no effect on the probabilistic assignation of the spectrum (Fig. S4, Supplemental Material). Even if the entire sequence was covered for the dansylated form, Mascot software used only 18 of the most 32 intense peaks for the dansylated form whereas the 22 of the 29 most intense peaks were used for the unmodified form. The four missing peaks for the labeled peptide were identified as internal fragments. Although it is not straightforward to predict when peptide dansylation would improve the Mascot ion score, the combination of the results obtained from unmodified and dansylated samples always led to better protein sequence coverage.

Application to a complex protein mixture

In order to validate the results obtained on the standard protein and to evaluate the feasibility of peptide dansylation on large-scale proteomic analysis, a soluble protein extract of *E. coli* underwent the labeling procedure (see Experimental section). To better underline differences in peptide recovery between the unlabeled and dansylated samples, a limited amount (15 ng) of protein digest was submitted to reversed-phase LC/MALDI-MS/MS analysis. The combination of a triplicate analysis allowed the detection of 79 *E. coli* proteins; 21 of them were not found using only the peak list related to the unmodified sample. Among them, six proteins were identified exclusively after dansylation. The remaining 15 proteins were identified uniquely by the combined search using the complementary data set of unmodified and dansylated samples that were both required to pass the validation criteria. This combination allowed identification of some proteins that would have been normally rejected (Table T2, Supplemental Material). The low number of identified protein is mainly due to the low amount of starting material.

As shown in Fig. 4(A), 73% of the identified proteins were identified separately in both samples with or without

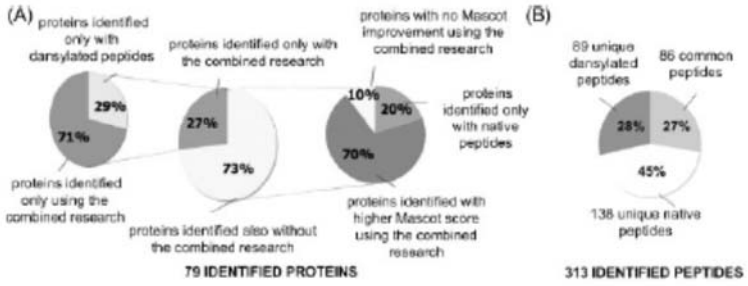

Figure 4. Combining the LC/MALDI-MS/MS analysis of native and dansylated *E. coli* trypsin digests enhances the number of identified proteins, their Mascot score and sequence coverage (A). (B) Distribution of assigned peptides in the separate runs.

DOI: 10.1002/rcm

dansylation. Only 27% of the 311 identified peptides were identified in both samples with or without dansylation (Fig. 4(B)) because many proteins were identified with peptides specific to one of the two samples only. To avoid any irrelevant increase of the probabilistic value because of data redundancy, peptides with the same sequence were considered only one time using the best ion score in all the combined database searches, by using myProMS software.[21] The combined analysis increased the sequence coverage and the Mascot score: 70% of the common proteins were identified with a better score when combining the two data sets. This improvement could also be due in some cases to higher peptides scores in the dansylated form compared to the unmodified form.

In the LC profiles, the percentage of identified peptides at earlier retention times (20–26 min) in reversed-phase LC was increased for dansylated samples (Fig. 5). This result is in agreement with the hypothesis that dansylation promoted the detection of more hydrophilic peptides (which in some cases may not be retained by the pre-concentration cartridge if not dansylated). Moreover, as shown in Fig. 5, peptide retention times were modified after the dansylation. The elution time distribution was centred in the middle of the chromatography at 26–28 min for the control sample, whereas the elution time distribution was broader for dansylated sample with more informative spots at lower and higher retention times.

This chromatographic behavior was correlated to the increased hydrophobicity of peptides after the dansylation, as shown in Fig. 6, where the retention times of the identified peptides present in both samples were plotted against their hydrophobicity values. From the similar B coefficients calculated from the linear relationship, it resulted that dansylation increased the peptide hydrophobicity of a constant factor which corresponded to a constant retention time increase of 4.5 min on our chromatographic system.

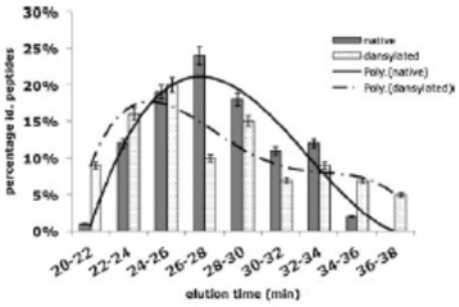

Figure 5. Percentage of MS/MS spectra submitted to the database search and associated to *E. coli* sequences vs. associated elution times (2 min interval). Interpolated polynomial graphs have been added as described in the legend. Informative MS/MS spectra for native peptide mixtures are obtained at higher retention times. Informative MS/MS spectra for dansylated peptides are obtained at earlier retention times, confirming that peptide dansylation improves the recovery of more hydrophilic species.

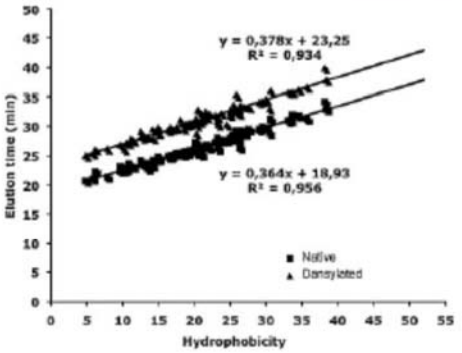

Figure 6. Elution times of *E. coli* trypsin proteolytic peptides are graphically plotted vs. their relative hydrophobicity for both the native and the dansylated peptide mixtures. Primary amine dansylation increases the peptide hydrophobicity by a constant increment.

In order to investigate if the partial lysine modification and eventual residual unlabeled peptides might interfere with the quality of the protein identification, we evaluated the efficiency of the analysis. Thus, the data were partitioned in different precursor S/N ratio ranges and, for each interval, the percentages of assigned spectra were compared to the total number of spectra submitted to the Mascot search (Fig. 7). In the lower S/N range the number of identified dansylated peptides is 5% less than the unmodified peptides: a larger number of MS/MS spectra were not informative enough for robust identification. This was mostly due to the presence of the low intensity precursor ions that generated rejected queries identified as redundant sequences (as for example multi-dansylated peptides) with lower ion score. Some of these species were also newly detected species that did not pass the validation criteria. On the contrary, the percentage of assigned peptides with a precursor S/N ratio higher then 500 was increased for the dansylated sample. This could be explained by the improved quality of MS signals of many dansylated peptides already detected in

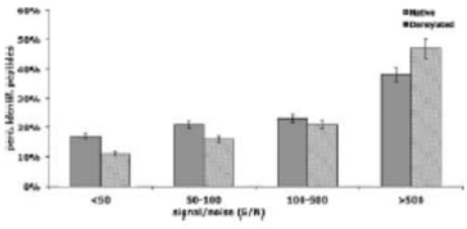

Figure 7. The percentage of *E. coli* identified peptides vs. the number of MS/MS spectra submitted to the database search is graphically plotted for different precursor ion S/N ranges. After dansylation a larger number of peptides are identified with higher S/N.

DOI: 10.1002/rcm

the unlabeled sample and by the high intensity of newly detected dansylated peptides in the low mass range of the MS spectra.

CONCLUSIONS

The PMF analysis could be improved by combining the data obtained from the MALDI-MS analysis of the dansylated and native samples.[19]

In this work an optimized dansylation protocol for proteomic studies by LC/MALDI-MS/MS analysis is presented. Peptide dansylation was demonstrated to be useful to optimize the sequence coverage of complex protein samples. Our experimental conditions for a microwave-based strategy reduced drastically the manipulation time to 1 h instead of 20 h. The experiments were realized in a domestic microwave oven. However, better results might be achieved using dedicated instruments with an accurate control of the different physical parameters such as pressure, temperature and microwave field power.

The MS features of peptide dansylation were evaluated to understand the complementary nature of MALDI identifications coming from the combined analysis of labeled and unmodified samples that was previously reported.[19] The introduction of the dimethylaminonaphthalene group by primary amine sulfonation allowed a better recovery of normally undetected hydrophilic peptides. This effect could be attributed to the increased hydrophobicity of labeled peptides that promotes the co-crystallization peptide/CHCA. On the contrary, the analysis of more hydrophobic peptides was not improved by the dansylation. Indeed, N-terminal primary amine conversion into sulfonamide could in some cases have a negative effect on the MALDI process and induce the loss of some species. This behavior was mainly observed for lysine C-terminal peptides whose ionization efficiency was already reported to be hindered in the native form compared to arginine C-terminal peptides.[2,4–6]

The combined data generated by the separate analysis of dansylated and unmodified peptide mixtures increased protein sequence coverage. For this reason this strategy helps in the recovery of post-translationally modified peptides as already evidenced in other reports.[19,20] Moreover, it should be interesting to evaluate the application of the present strategy to the study of specific post-translational modifications (PTMs) inducing an increase of the hydrophilicity of peptides (such as phosphorylation).

The fragmentation features of dansylated peptides were also explored. As for others UV-adsorbing reagents,[3,13] the presence of the dimethylaminonaphthalene group in the N-terminal position increased the peptide fragmentation and the generation of *b*-ions in PSD-like experiments, leading to a better coverage of the peptide sequence. This tendency could be rationalized considering that the UV-adsorbing naphthalene group in the N-terminal position could increase the energy transfer from the laser in PSD-like fragmentation, favoring the peptide bond destabilization/protonation. This effect appeared to have a short range nature, so preferentially the peptide bonds near the N-terminal were involved. Indeed, no improvement in fragmentation was found when lysine ε-amine was dansylated.

Even if the increased intensity of *b*-ions did not always improve the proportion of identified sequences in the MS/MS data, many dansylated peptides were identified with higher Mascot ion scores as compared to their related native form.

The LC/MALDI-MS/MS analysis of a whole *E. coli* protein extract confirmed our results on BSA. The enhanced number of identification is also related to the increased hydrophobicity due to dansylation of peptides. Peptides that are lost in the flow-through of the LC column in their unmodified hydrophilic form were recovered after dansylation. Moreover, the whole informative elution time window increased together with the proportion of informative collected spots for MALDI analysis.

The proposed strategy is a rapid and inexpensive tool to improve the results of an LC/MALDI-MS/MS analysis. Even if peptide dansylation might not be a standalone method for large-scale proteomics, it is a very useful complementary tool to validate the identification of ambiguous protein candidates and to increase the sequence coverage of proteins for the discovery of new PTMs by looking for hydrophilic species, which are usually lost.

SUPPORTING INFORMATION

Additional supporting information may be found in the online version of this article.

REFERENCES

1. Mollé D, Jardin J, Piot M, Pasco M, Léonil J, Gagnaire V. *J. Chromatogr. A* 2009; **1216**: 2424.
2. Valero ML, Giralt E, Andreu D. *Lett. Pept. Sci.* 1999; **6**: 109.
3. Pashkova A, Moskovets E, Karger BL. *Anal. Chem.* 2004; **76**: 4550.
4. Harrison AG. *Mass Spectrom. Rev.* 1997; **16**: 201.
5. Zenobi R, Knochenmuss R., *Mass Spectrom. Rev.* 1998; **17**: 337.
6. Brancia FL, Oliver SG, Gaskell SJ. *Rapid Commun. Mass Spectrom.* 2000; **14**: 2070.
7. Beardsley RL, Karty JA, Reilly JP. *Rapid Commun. Mass Spectrom.* 2000; **14**: 2147.
8. Pashkova A, Chen HS, Rejtar T, Zang X, Giese R, Andreev V, Moskovets E, Karger BL. *Anal Chem.* 2005; **77**: 2085.
9. Keough T, Lacey MP, Youngquist RS. *Rapid Commun. Mass Spectrom.* 2000; **14**: 2348.
10. Janek K, Wenschuh H, Bienert M, Krause E. *Rapid Commun. Mass Spectrom.* 2001; **15**: 1593.
11. Wang D, Kalb SR, Cotter RJ. *Rapid Commun. Mass Spectrom.* 2004; **8**: 96.
12. Nakagawa M, Yamagaky T, Nakinishi H. *Electrophoresis* 2000; **21**: 1651.
13. Nakagawa M, Nakanishi H. *Protein Pept. Lett.* 2004; **11**: 71.
14. Walker JM. *Methods Mol. Biol.* 1994; **32**: 329.
15. Amoresano A, Monti G, Cirulli C, Marino G. *Rapid Commun. Mass Spectrom.* 2006; **20**: 1400.
16. Cirulli C, Marino G, Amoresano A. *Rapid Commun. Mass Spectrom.* 2007; **21**: 2389.
17. Amoresano A, Chiappetta G, Pucci P, D'Ischia M, Marino G. *Anal. Chem.* 2007; **79**: 2109.
18. Guo K, Li L. *Anal Chem.* 2009; **81**: 3919.
19. Park SJ, Song JS, Kim HJ. *Rapid Commun. Mass Spectrom.* 2005; **19**: 3089.
20. Napoli A, Aiello D, Di Donna L, Moschidis P, Sindona G. *J. Proteome Res.* 2008; **7**: 2723.
21. Poullet P, Carpentier S, Barillot E. *Proteomics* 2007; **7**: 2553.
22. Naaesner M, Mergler M, Wolf K, Schuphan I. *J. Chromatogr. A* 2002; **945**: 133.

23. Lin S, Yun D, Qi D, Deng C, Li Y, Zhang X. *J. Proteome Res.* 2008; **7**: 1297.
24. Sun W, Gao S, Wang L, Chen Y, Wu S, Wang X, Zheng D, Gao Y. *Mol. Cell. Proteomics* 2006; **5**: 769.
25. Beaudry F, Guénette SA, Winterborn A, Marier JF, Vachon P. *J. Pharm. Biomed. Anal.* 2005; **39**: 411.
26. Sandoval WN, Pham V, Ingle ES, Liu PS, Lill JR. *Comb. Chem. High Throughput Screen.* 2007; **10**: 751.
27. Qi L, Zhang SF, Zuo M, Chen Y. *J. Pharm. Biomed. Anal.* 2006; **41**: 1620.
28. Cárdenes L, Ayala JH, González V, Afonso AM. *J. Chromatogr. A* 2002; **946**: 133.
29. Gros C, Labouesse B. *Eur. J. Biochem.* 1969; **7**: 463.
30. Baumgart S, Lindner Y, Kühne R, Oberemm A, Wenschuh H, Krause E. *Rapid Commun. Mass Spectrom.* 2004; **18**: 863.
31. Krokhin OV, Ying S, Cortens JP, Ghosh D, Spicer V, Ens W, Standing KG, Beavis RC, Wilkins JA. *Anal. Chem.* 2006; **78**: 6265.
32. van Dongen WD, Ruijters HF, Lunge HJ, Heerma W, Haverkamp J. *J. Mass Spectrom.* 1996; **31**: 1156.
33. Roth KDW, Huang ZH, Sadagopan N, Watson JT. *Mass Spectrom. Rev.* 1998; **17**: 255.
34. Dongré AR, Jones JL, Somogyi A, Wysocki VH. *J. Am. Chem. Soc.* 1996; **118**: 8365.

DOI: 10.1002/rcm

Annexe 3. Reversed-phase HPLC and hyphenated analytical strategies for peptidomics. Hesse AM, Ndiaye S, Vinh J. Methods Mol Biol. 2011;789:203-21. PMID: 21922410

Chapter 13

Reversed-Phase HPLC and Hyphenated Analytical Strategies for Peptidomics

Anne-Marie Hesse, Sega Ndiaye, and Joelle Vinh

Abstract

Peptide study and analysis widely involve liquid chromatography. Among the different strategies available, reversed-phase liquid chromatography (RP-HPLC) is one of the methods of choice to separate species in a nontargeted approach. The compounds are sorted according to their hydrophobicity, even though the experimental order of elution could change according to the nature of the mobile phase and the stationary phase. In our work, we have developed protocols to resolve hundred of peptidic species. To overcome the limitations of peak capacity of RP-HPLC alone, it has been coupled downstream to tandem mass spectrometry using two different ionization modes. To overcome the limitations of peak capacity of RP-HPLC MS/MS, it has been coupled upstream to strong cation exchange liquid chromatography. Multidimensional analysis allows for a deeper description of a sample because the limit of detection is often due to a lack of dynamic range of the detection itself rather than due to a lack of sensitivity. In this chapter, different protocols are presented. They should be considered as examples that could be used as starting point for new protocols optimization. Even if RP-HPLC is a universal peptide separation method, it should be optimized according to the specific characteristics of the peptide(s) of interest.

Key words: Reversed-phase liquid chromatography, Peptidomics, Mass spectrometry, ESI, MALDI, Peak capacity

1. Introduction

The study of peptides in biological fluids by separation techniques has been widely used for decades. Reversed-phase high-pressure liquid chromatography (RP-HPLC) is a method of choice for peptide characterization, because of its direct interface with mass spectrometry. It counts among several analytical techniques for the determination of neurotransmitters such as capillary electrophoresis, enzyme assays, sensors, and mass spectrometry (for a review see ref. 1). First dealing on the field of proteomics, this technique is

Adalberto Merighi (ed.), *Neuropeptides: Methods and Protocols*, Methods in Molecular Biology, vol. 789,
DOI 10.1007/978-1-61779-310-3_13, © Springer Science+Business Media, LLC 2011

also of high value for the separation and detection of endogenous peptides (2). The development of miniaturized approaches such as micro and nano-HPLC opened the way toward direct biological applications where sample amounts are limited such as the detection and characterization of bioactive peptides. These applications have been reviewed extensively. Saz and Marina have reviewed the works published since 2001 on the micro/nano-HPLC analysis of bioactive and biomarker peptides (3). Boonen et al. also have presented an overview of the strategies involving mass spectrometry for neuropeptide discovery and analysis (4, 5).

Briefly, the separation is based on the hydrophobic properties of the compounds. The peptides are injected in aqueous buffer at a controlled pH in a chromatographic column packed with a hydrophobic stationary phase. The most widely used stationary phase for peptides is the octadecyl carbon chain (C18) bonded silica in association with a mobile phase containing a mixture of acidic aqueous buffer and polar organic solvents. Other phases have been evaluated for diverse applications, working on different retention mechanisms (6, 7) or on the nature of the stationary phase, studying the influence of silica vs. polymeric beads (8), or looking for peak capacity optimization (9).

The elution of the peptides is sequentially obtained in isocratic mode by percolation of the mobile phase or with a gradient of the organic solvent concentration. The most frequent organic solvents are acetonitrile or methanol. The organic solvent should be miscible with water. The pH of the separation is an important parameter, since it controls the apparent charge of the peptides and can influence the strength of the interactions of the peptides with the stationary phase. A good separation resolution can be reached only if the injection volumes can be considered as negligible in comparison with the column volume itself.

Biological samples are often available at low concentrations in large volumes equivalent to several times the column volume and thus cannot be injected in the column as they are. Moreover, biological matrices contain high concentrations of salts that could interact with the analytical elution buffer. Sample cleanup has been studied and online configurations have been proposed (10, 11). A classical strategy to eliminate those two hindrances is the implementation of an upstream preconcentration and desalting step. Because very low amounts of material are targeted, the separation does not accept any external contamination that would hide the signal coming from the species of interest. With this aim, we have developed an online strategy for the efficient removal of plastic component from the buffer (12). Finally, a classic protocol for sample fractionation using strong cation exchange (SCX) chromatography is presented as a pseudoorthogonal approach to RP-HPLC when highly complex samples are studied.

The detection for such low amounts of sample requires high sensitivity and specificity: mass spectrometry is a method of choice

to detect eluted peptides. Two kinds of interfaces are presented, either associated to electrospray ionization (ESI) or matrix-assisted laser desorption/ionization (MALDI). To validate our experimental setup, the separation of a six-standard proteins tryptic digest is given as a reference at the end of the chapter. To minimize sample cross-contamination, we use a total flush method. Examples of such protocols are detailed in the following. However, one should keep in mind that those are only examples that are only given as a starting point. Each sample requires its own optimization according to the characteristics of the molecular species of interest and of the surrounding biological matrix.

2. Materials

2.1. Monodimensional RP-HPLC Hardware Configuration

As examples, three nano-HPLC hardware configurations are given (see Note 1).

1. Famos-Switchos-UltiMate (LC Packings, The Netherlands) *or* U3000 Dionex (Dionex, Sunnyvale, CA) *or* 1200 series Agilent HPLC (Agilent Technologies, Santa Clara, CA).
2. Nano-RP-HPLC column: Acclaim C18 PepMap100 (3 µm, 100 Å, 75 µm internal diameter (i.d.), 150 mm length – Dionex) *or* C18 Zorbax 300SB (3 µm, 300 Å, 75 µm i.d., 15 cm length – Agilent Technologies) (see Note 2).
3. Capillary SCX HPLC column: BioBasic SCX (300 Å, 5 µm, 320 µm i.d. 150 mm length – Thermo Fisher Scientific, Waltham, MA).
4. Regular precolumns for preconcentration and desalting: C18 PepMap100 (5 µm, 100 Å, 300 µm i.d., 5 mm length – Dionex) or C18 Zorbax300 SB (5 µm, 300 Å, 300 µm i.d., 5 mm length – Agilent Technologies).
5. Large precolumns for buffer cleanup: C18 PepMap100 (5 µm, 100 Å, 1 mm i.d., 15 mm length – Dionex).

2.2. Chemicals

1. MilliQ Water (Millipore, Billerica, MA – see Note 3).
2. Acetonitrile (ACN) (available from Fisher Scientific (Acetonitrile Optima® LC/MS packaged under nitrogen, 0.2 µm filtered) or from Mallinckrodt Baker, Phillipsburg, NJ (Ultra Gradient HPLC Grade Baker HPLC analyzed, packaged under nitrogen, 0.2 µm filtered)).
3. Isopropanol (IPA) (Fisher Scientific (2-Propanol Optima® LC/MS packaged under nitrogen, 0.2 µm filtered)).
4. Methanol (MeOH) (VWR Prolabo, West Chester, PA (HiPerSolv Chromanorm for HPLC – Isocratic grade)).

5. Formic acid (FA) (puriss. p.a. eluent additive for LC–MS, Fluka Analytical, Sigma Aldrich, St. Louis, MO) (see Note 4).
6. Trifluoroacetic acid (TFA – protein sequencing grade, protein sequencer reagent) (available from Applied Biosystems, Foster City, CA).
7. 25% Ammonia solution (Merck, Darmstadt, Germany).
8. α-Cyanohydroxycinnamic acid (CHCA – available from LaserBiolabs, Sophia-Antipolis, France).
9. Ammonium citrate (citric acid diammonium salt, 98% capillary GC – available from Sigma-Aldrich).
10. Tryptic digest consisting of six proteins with molecular weight from 11 to 135 kDa (cytochrome C, lysozyme, alcohol dehydrogenase, bovine serum albumin, serotransferrin, and β-galactosidase) (available from Dionex).

2.3. Buffers and Solvents (see Note 5)

1. Sample buffer: Sample is reconstituted in Solvent A or in 1–2% aqueous TFA/ACN 98:2 (v/v).
2. Solvent A: H_2O/ACN/FA, 98:2:0.1 (v/v/v).
3. Solvent B: ACN/H_2O/FA, 90:10:0.1 (v/v/v).
4. Flush buffer: ACN/IPA/MeOH 1:1:1 (v/v/v).
5. MALDI matrix solution: 5 mg/mL CHCA in 6:4 ACN/0.1% TFA in H_2O v/v, with 10 mM ammonium citrate (see Note 6).
6. Buffer A′: H_2O/ACN/FA, 95:5:0.1 (v/v/v).
7. Buffer B′: 100 mM ammonium formate in H_2O buffer directly prepared with formic acid and ammonia solution 25%. pH is adjusted to 2.5 with TFA. 5% ACN is added to give the final buffer B′.

2.4. Interface with ESI Hardware Configuration

1. Fused silica tubing (i.d. 20 µm).
2. Nanoelectrostray emitter (SilicaTip™ picotip emitter) with distal conductive coating, 360 µm outer diameter (o.d.), 20 µm i.d., 10 ± 1 µm tip i.d. (New Objective, Woburn, MA).
3. Electric contact for spray with a voltage 1.2–1.5 kV, for 10–20 nA ion current.

2.5. Interface with MALDI Hardware Configuration

1. Automat for MALDI sample preparation: Probot (Dionex).
2. Stainless steel MALDI target compatible with the mass spectrometer available.

2.6. Bidimensional HPLC Hardware Configuration

1. U3000 Dionex in dual configuration (see Note 7).
2. First dimension column: Capillary SCX HPLC (see Subheading 2.1, item 3).
3. Second dimension column: Nano-RP-HPLC (see Subheading 2.1, item 2).

3. Methods

3.1. Sample Enrichment and Desalting

The need to detect very low quantities of analytes from limited amount of diluted biological samples is one of the reasons of sample enrichment to achieve more sensitivity. Moreover, direct punctual injection of biological samples is generally not possible. Indeed, the typical nanocolumn volume is 0.5 µL (see Subheading 2). Injection volume should be less than 5 nL to be considered as punctual. To set the experiment above the detection limit, typical injection volume is 5–10 µL. This is the reason why sample enrichment is always performed for biological salts removal and peptide preconcentration. This procedure is identical for 1D- or 2D-liquid chromatography (LC) modes.

1. Trap peptides onto a regular precolumn.
2. Desalt and concentrate with a 15 µL/min flow of solvent A between 5 and 15 min according to the hydrophilic properties of the peptides and to the salt concentration in sample (see Fig. 1).

3.2. Monodimensional RP-HPLC (1D-LC) (see Notes 8 and 9)

1. Switch the valve V1 and elute the enriched and desalted sample from the regular precolumn toward the RP nanocolumn (see Fig. 1).
2. Separate peptides according to their hydrophobicity with an ACN gradient (see Notes 10 and 11).

3.3. RP-HPLC ESI MS/MS Coupling

1. Use a fused silica capillary with a conductive distal coating at an approximate distance of 2 mm with 1.4 kV potential in front of a grounded counter electrode at the entrance of the mass spectrometer to directly connect the RP-HPLC effluent to the nano-ESI probe (see Note 12).

3.4. RP-HPLC MALDI MS/MS Coupling

1. Use the Probot as LC-MALDI deposition device (Fig. 2) to collect and spot the RP-HPLC effluent on the stainless steel MALDI plate.
2. Begin collection 15 min after gradient start (the first part of the chromatogram usually corresponds to preconcentration, desalting and transfer from the trap column to the analytical column).
3. Mix continuously the matrix solution at 436 nL/min with the eluted sample using an external coaxial capillary added at the exit of the column.
4. Collect one fraction giving one MALDI spot every 10 s. For each run, a total of 240 spots are collected for 40 min.
5. Dry the MALDI samples under atmospheric pressure at 20°C.
6. Blown out any residual possible dust just before the introduction of the MALDI target in the mass spectrometer.

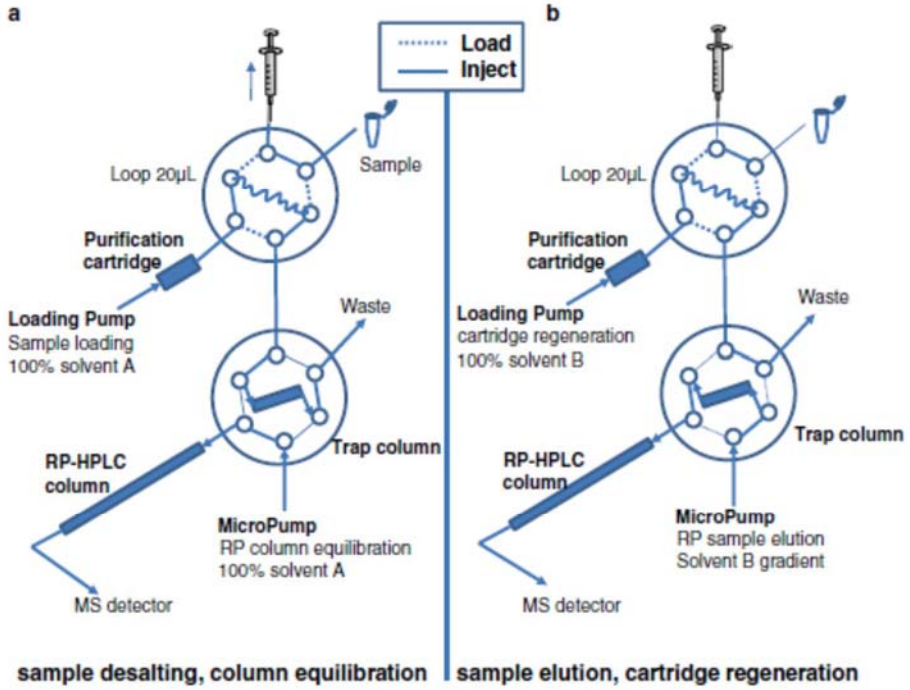

Fig. 1. Schematic representation of a classical 1D-LC system with a purification cartridge added to remove polymers. (**a**) Peptides are loaded into the sample loop using a syringe (load sample position), they are injected with 100% solvent A from the loading pump (inject position), they are retained and desalted on the regular trap column. In the mean time, contaminants are trapped on the purification large precolumn (purification cartridge). (**b**) Valve V1 switches, the trap column goes to the micropump fluidics pathway, the micropump delivers a positive gradient of solvent B (acetonitrile gradient) to elute peptides from the trap column for them to be separated into the analytical column. In the meantime, the purification cartridge is regenerated with 100% solvent B delivered by the loading pump in parallel of sample elution and RP gradient.

3.5. Bi-dimensional HPLC (2D-LC) (see Notes 8 and 9)

For very complex samples, such as tissues extracts or whole cells lysates, the total number of peptides widely exceeds the peak capacity of conventional RP-HPLC columns. Co-elution of tens of peptides decreases the percentage of peptides that can be further characterized and sequenced. This limits the sample coverage. In this case, 2D-LC offers an additional separation dimension that is useful to overcome this bottleneck. Even if strong cation exchange (SCX) and RP are not totally orthogonal, SCX-LC followed by RP-LC is the default coupling in proteomics and different protocols can be used (see Note 13). An online configuration is presented here.

1. Fractionate peptides on the capillary SCX column. For peptide fractionation, the gradient profile consists of a multilinear gradient from 0 to 100 mM ammonium formate (see Table 1). Micropump flow rate changes over separation time.

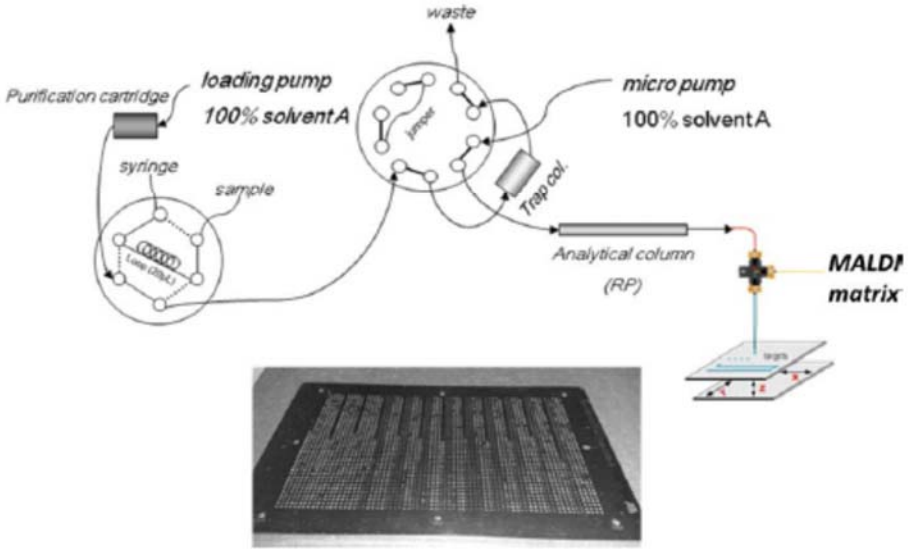

Fig. 2. Schematics of the RP-HPLC MALDI interface. The LC setup is analogous to the one detailed in Fig. 1. The effluent of the column is added a continuous flow of MALDI matrix solution at a flow-rate ratio sample–matrix 1:2 (v/v) roughly. As presented in the scheme, the matrix solution was added via a tee into an external metallic needle coaxial with the fused silica capillary containing the nano-LC effluent. The two solutions are mixed at the end of the metallic needle just at the contact with the MALDI target. In the picture, the collection frequency was set to 10 s/spot, the MALDI matrix solution was α-cyano-4-hydroxycinnamic acid at 5 mg/mL in 60% ACN, ammonium citrate 10 mM, at 436 nL/min. Up to 15 LC separations can be collected on the same plate.

2. Trap eluted peptides alternatively on the regular precolumn 1 or on the precolumn 2 (Trap Col 1 and 2, in Fig. 3). Valve V2 is switched every 71 min.
3. After the trapping and desalting step, switch valve V3 and elute the trapped peptides toward the analytical column for a RP-HPLC separation (see Note 14).
4. During last RP gradient, equilibrate the SCX column 100% buffer A′ for 1 h.

3.6. Online Buffer Purification and Total Flush

Continuous contamination with impurities can be highly detrimental to the quality of the LC profiles and to the efficiency of detection by mass spectrometry, as observed in our hands (12). It decreases sensitivity of detection and/or the contaminant signals overlap with compounds of interest. This observation has also been made in other laboratories with other equipments. Several peaks showing the well-known PEG MS pattern with m/z values 44.026 units apart are detected, covering approximately 4 min of retention time in every LC run. These compounds are eluted in the same elution window as peptides. It is difficult, if not impossible, to conclude about the source of contamination: solvent or liquid pathway bleeding or common contamination due to containers.

Table 1
Salt gradient characteristics for online SCX–RP-HPLC separation

	% of Buffer B′		
Time (min)	Start	End	Flow rate (µL/min)
From 0 to 17	0	0	4
From 17 to 230	0	3	4
From 230 to 301	3	5	3
From 301 to 372	5	7.1	2
From 372 to 443	7.1	8.8	2
From 443 to 514	8.8	10.9	2
From 514 to 585	10.9	17.3	1
From 585 to 656	17.3	24	1
From 656 to 727	24	46	1
From 727 to 798	46	100	1.5
From 798 to 869	100	100	4
From 869 to 929	0	0	0.5
From 929 to 934	0	0	4

Composition of buffer B′ is detailed in Subheading 2. RP-HPLC gradient is given in the Subheading 3. A new RP gradient is started every 71 min for a total SCX gradient time of 934 min

1. To remove contamination in 1D-LC, insert a large precolumn in LC fluidics pathway between the micropump outlet and the injection valve (Fig. 1).
2. Regenerate the purification cartridge by independent flushing at 40 µL/min with 100% solvent B in parallel during the analytical gradient period.
3. At the end of the run, equilibrate the cartridge with solvent A for 15 min.

A similar approach is used in our 2D-LC system:

1. Insert a first large precolumn after loading pump 2 and a second identical precolumn after micropump 1 (Fig. 4).
2. Flush the first cartridge at 40 µL/min with 100% solvent B in parallel of each RP gradient.
3. Flush the second precolumn with solvent B after the last SCX fraction (see Note 15).

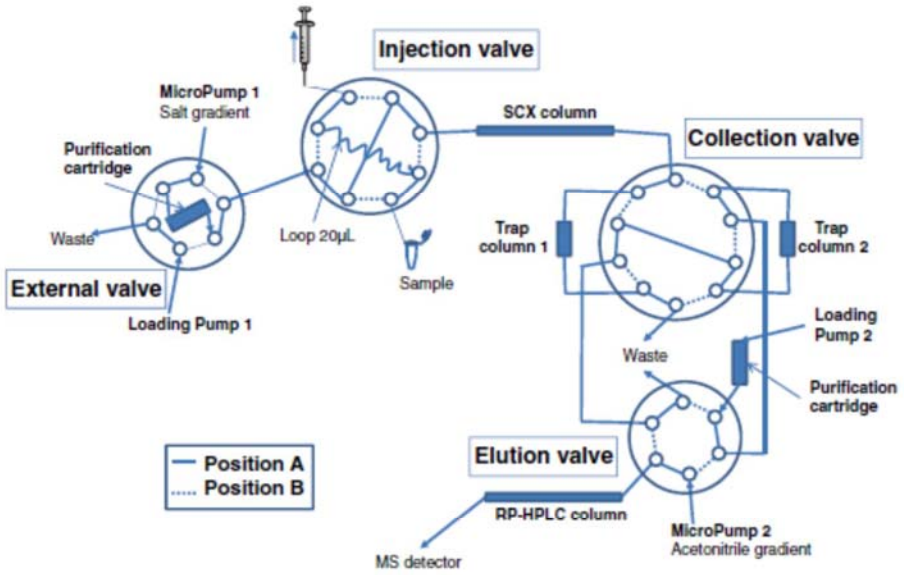

Fig. 3. Schematics of the online 2D-LC configuration. Injection valve: in position A, sample is loaded; in position B, sample is injected on the SCX column. External valve: in position A, the micropump 1 delivers a salt gradient to separate peptides on the SCX column; in position B, the cartridge 2 is regenerated after the last SCX fraction at a high flow rate of solvent B using loading pump 1. Collection valve V2: in position A, peptides are collected on the trap column 1 during desalting and sample elution from trap column 2; in position B, it is the opposite. Elution valve V3: in position A, the loading pump 2 is used for desalting, the RP column is equilibrated; in position B, the micropump 2 delivers the acetonitrile gradient to separate compounds on the RP column, the loading pump 2 delivers solvent B at high flow rate to regenerate the purification cartridge 1.

4. Notes

1. All nano-HPLC hardware configurations are equipped with a loading pump (two solvent channels, isocratic mode for flow rates between 5 and 50 µL/min are required), a nanopump (three solvent channels, isocratic and gradient modes for flow rates between 50 and 350 nL/min are required), a refrigerated autosampler (set at 4°C) for injection volumes between 1 and 20 µL, a solvent organizer with online desalting, and a column oven (stable temperature at 20°C is used).
2. The stationary phases presented in this work are the one we use, but it does not exclude other phases. One should be aware that different C18 silica phases can give different LC profiles with different elution orders. According to the peptide(s) of interest, the C18 phase of choice will change.
3. Unless stated otherwise, all solutions should be prepared in water that has a resistivity of 18.2 MΩ cm and total organic

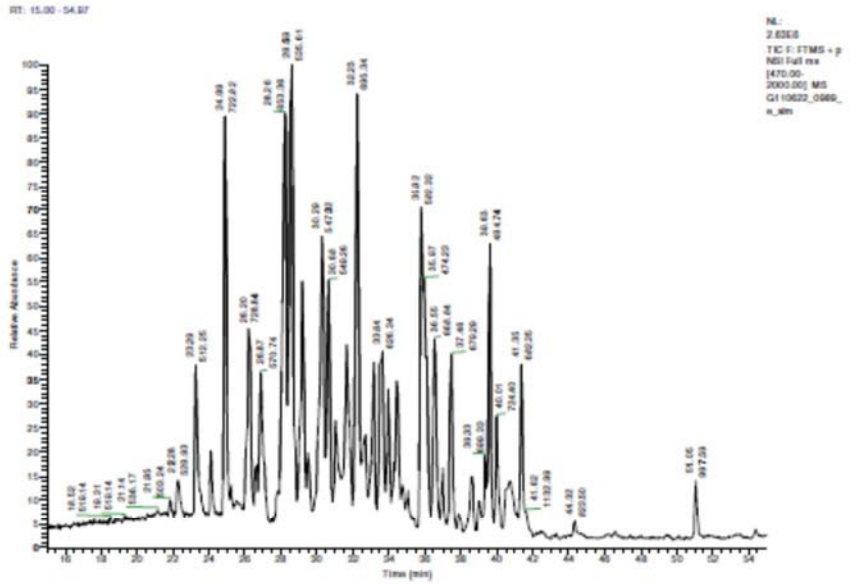

Fig. 4. LC chromatogram from the tryptic digest of 20 fmol of six standard proteins mixture (see Subheading 2). Presented here is a chromatogram detected with the total ion current recorded in nano-ESI interface: more than 400 species have been detected, selected and 100 distinct peptides have been successfully sequenced online by mass spectrometry. The profile illustrates the lack of peak capacity even for a simple peptidic mixture, with many peaks overlapping, for a MHWH of 30 s, which is a good average value for gradient separation in RP-HPLC. This profile was obtained using the RP-HPLC U3000 setup (see Subheading 2 and 3), using a Pepmap Acclaim column coupled to a nano-ESI LTQ-FT mass spectrometer (Thermo Fisher Scientific). The signal was filtered to select only the total ion current from the Fourier Transform Mass Spectrometry full survey scan on 470–2,000 Da mass range.

content of less than five parts per billion. This standard is referred to as "H_2O" in the text.

4. Instead of FA, TFA can be used in mobile phases when an LC-MALDI setup is chosen. It will enhance peptides resolution. In the case of a LC-ESI setup, FA is preferred because TFA is known to suppress the ESI signals of analytes due to ion pair formation.
5. LC buffers should be at least weekly prepared if not daily. The bottles should be changed and washed carefully each time. The last step should be a thorough rinse with MilliQ H_2O.
6. The MALDI matrix solution should be prepared extemporaneously and stored in dark.
7. For 2D-LC experiments, two loading pumps are needed (two solvent channels, isocratic mode for flow rates between 5 and 50 µL/min are required) a micropump (three solvent channels, isocratic and gradient modes for flow rate between 0.5 and 4 µL/min are required), a nanopump (three solvent

channels, isocratic and gradient modes for flow rates between 50 and 350 nL/min are required), a refrigerated autosampler (set at 4°C) for injection volumes between 1 and 20 µL, a solvent organizer, and a column oven (stable temperature at 20°C is used).

8. LC setups should be regularly checked for performances in terms of peptides retention times and intensities. Pressure profile should be stable. We used a 20-fmol mix of six proteins tryptic digest for sample recovery control. The proteins and the associated proteolytic peptides that are detected and identified on a routine basis are described in Table 2 and are our reference for validation.
9. If the LC system should be kept on standby for a while, do not stop the mobile phase flow rate completely in the RP-HPLC nanocolumn. RP column and trap columns are kept in ACN–H2O, 50:50 (v/v), and SCX column in water.
10. For the Dionex column, the flow rate is 220 nL/min. The default gradient profile consists in a linear gradient from 0 to 50% solvent B in 35 min, then in an isocratic step of 10 min 100% solvent B, and finally 20 min of 100% solvent A as the final equilibration step.
11. For the Agilent column the flow rate is 300 nL/min. The linear gradient starts from 1 to 13% solvent B in 3 min, then from 13 to 44% solvent B in 42 min, 15 min 100% solvent B, and finally 15 min 100% solvent A.
12. The dead volume between the exit of the analytical column and the nano-ESI probe should be as low as possible. We selected a connection in fused silica with 20 µm i.d. as short as possible to maintain the column in the column oven regulated at 20°C. The connections between the exit of the column, the fused silica capillary, and the nano-ESI needle are realized with pieces of Teflon tubing (10 mm length max), since there is negligible pressure drop between these three parts. The voltage is applied at the outer surface of the coated nano-ESI needle with no contact with the sample itself.
13. This protocol can be adapted for different peptidic samples. For example, very complex mixtures may require increasing the separation time by lowering the gradient slope. Starting from endogenous peptidic extract, it is likely that all species will not be resolved with overlapping peaks. Therefore, the coupling of the LC with mass spectrometry is highly informative since it allows the detection of different coeluted species.
14. Peptides samples could be very easily lost by nonspecific adsorption in the plastic vials. This phenomenon increases with storage time and temperature. It is also more pronounced for very low concentrations. Therefore, it is advisory to store the sample

Table 2
Identification of 20 fmol of a tryptic digest of six standard proteins mixture in RP–HPLC

Protein	t_r (min)	t_r/t_m	Theorical MW (Th)	ΔM (ppm)	Peptide Sequence	Peptide Modification(s)
ALBU_BOVINE (Serum albumin, *Bos Taurus*, MW = 69,248 Da)	22.22	1.02	1249.6208	−0.31	FKDLGEEHFK	
	23.17	1.06	1534.7474	−1.22	LKEccDKPLLEK	2 CaM (C)
	24.64	1.13	1444.6257	−0.26	YIcDNQDTISSK	CaM (C)
	26.4	1.21	1480.4915	0.11	ETYGDMADccEK	2 CaM (C)
	26.53	1.21	1422.4854	−0.34	ETYGDMADcCEK	CaM (C)
	26.76	1.23	1140.4657	−0.33	ccTESLVNR	2 CaM (C)
	27.13	1.24	1902.8534	−0.28	NEcFLSHKDDSPDLPK	CaM (C)
	28.49	1.30	1504.5814	−0.3	EYEATLEEccAK	2 CaM (C)
	28.93	1.32	1108.4976	−0.33	EAcFAVEGPK	CaM (C)
	29.03	1.33	1439.8108	−0.73	RHPEYAVSVLLR	
	29.23	1.34	1305.7169	0.57	HLVDEPQNLIK	
	30.25	1.39	1639.9368	−0.65	KVPQVSTPTLVEVSR	
	30.41	1.39	1930.7511	0.33	ccAADDKEAcFAVEGPK	3 CaM (C)
	30.63	1.40	1749.6732	0.06	YNGVFQEccQAEDK	2 CaM (C)
	30.82	1.41	1752.6153	0.37	EccHGDLLEcADDR	2 CaM (C)
	31	1.42	1555.6357	−0.85	DDPHAcYSTVFDK	CaM (C)
	31.79	1.46	1142.7139	−0.41	KQTALVELLK	
	32.73	1.50	1577.7507	−0.62	LKPDPNTLcDEFK	CaM (C)

	33.54	1.54	1283.7104	−0.23	HPEYAVSVLLR	
	34.69	1.59	1511.8415	−0.88	VTQVSTPTLVEVSR	
	34.87	1.60	1881.9042	−0.53	RPcFSALTPDETYVPK	CaM (C)
	35.72	1.64	1163.6294	−1.15	LVNELTEFAK	
	35.85	1.64	1002.5823	−0.75	LVVSTQTALA	
	35.86	1.64	1420.6781	0.23	SLHTLFGDELcK	CaM (C)
	38.51	1.76	1014.6195	0.09	QTALVELLK	
	38.6	1.77	1415.6851	−1.8	TVmENFVAFVDK	Ox (M)
	40.38	1.85	1479.7948	−0.49	LGEYGFQNALIVR	
	40.96	1.88	1888.9261	−0.4	HPYFYAPELLYYANK	
	44.49	2.04	1399.6912	−1.04	TVMENFVAFVDK	
TRFE_BOVINE (Serotransferrin, *Bos Taurus*, MW = 77,703 Da)	23.45	1.07	1347.5999	0.02	WcTISTHEANK	CaM (C)
	26.04	1.19	1483.6840	−0.42	KNYELLcGDNTR	CaM (C)
	26.32	1.21	1167.5721	0.5	KENFEVLcK	CaM (C)
	27.72	1.27	1768.8586	−1.54	HSTVFDNLPNPEDRK	
	27.98	1.28	1216.6030	−0.08	LLEAcTFHKP	CaM (C)
	28	1.28	1311.6540	0.04	ELPDPQESIQR	
	28.49	1.30	1757.8595	−0.65	DKPDNFQLFQSPHGK	
	28.55	1.31	1604.8061	−0.42	DNPQTHYYAVAVVK	
	28.77	1.32	1594.7389	0.33	KTYDSYLGDDYVR	
	30.56	1.40	1122.5791	0.05	DLLFRDDTK	

(continued)

Table 2
(continued)

Protein	t_r (min)	t_r/t_{r0}	Theorical MW (Th)	ΔM (ppm)	Peptide Sequence	Peptide Modification(s)
	30.67	1.40	1464.7774	0.41	ILESGPFVScVKK	CaM (C)
	31.55	1.44	1640.7653	−0.69	HSTVFDNLPNPEDR	
	32.13	1.47	1389.6756	−0.16	TSDANINWNNLK	
	32.13	1.47	1039.4764	−0.13	ENFEVLcK	CaM (C)
	32.15	1.47	1355.5892	−0.3	NYELLcGDNTR	CaM (C)
	34.06	1.56	1466.6421	−0.91	TYDSYLGDDYVR	
	34.39	1.57	1413.6374	−1.07	cLmEGAGDVAFVK	CaM (C); Ox (M)
	35.08	1.61	1996.7841	0	cAcSNHEPYFGYSGAFK	2 CaM (C)
	36.48	1.67	1336.6804	−1	ILESGPFVScVK	CaM (C)
	38.37	1.76	1846.8515	−0.72	GEADAmSLDGGYLYIAGK	Ox (M)
	38.44	1.76	1645.6932	−1.21	FDEFFSAGcAPGSPR	CaM (C)
	39.24	1.80	1397.6433	−0.57	cLMEGAGDVAFVK	CaM (C)
	40.04	1.83	1996.8269	0.25	SVTDcTSNFcLFQSNSK	2 CaM (C)
	41.9	1.92	1830.8573	−0.35	GEADAMSLDGGYLYIAGK	
	42.17	1.93	1566.7979	−0.42	TAGWNIPmGLLYSK	Ox (M)
	42.31	1.94	1363.6931	0.33	cGLVPVLAENYK	CaM (C)
	46.48	2.13	1550.8020	−1.08	TAGWNIPMGLLYSK	
BGAL_ECOHS (Beta-Galactosidase, *Escherichia coli*, MW = 116,388 Da)	21.84	1.00	1507.69578	−0.04	YSQQQLMETSHR	
	25.42	1.16	1299.62365	0.55	ELNYGPHQWR	

Table 2
(continued)

Protein	t_r (min)	t_r/t_{r0}	Theorical MW (Th)	ΔM (ppm)	Peptide Sequence	Peptide Modification(s)
	31.42	1.44	1386.7400	−0.76	ANGTTVLVGMPAGAK	
	33.05	1.51	1013.5983	−0.72	ANELLINVK	
	33.55	1.54	1251.6686	−0.54	SISIVGSYVGNR	
	34.38	1.57	1618.8430	−0.36	VLGIDGGEGKEELFR	
	37.35	1.71	1357.5755	−0.58	ccSDVFNQVVK	2 CaM (C)
	39.88	1.83	1447.8033	−0.73	VVGLSTLPEIYEK	
	40.7	1.86	968.4832	−0.44	EALDFFAR	
	42.64	1.95	1312.6781	−0.22	SIGGEVFIDFTK	
CYC_BOVINE (Cytochrome C, *Bos_Taurus*, MW = 11,696 Da)	22.27	1.02	1584.76492	−0.25	KTGQAPGFSYTDANK	
	26.16	1.20	1456.67011	−0.17	TGQAPGFSYTDANK	
	30.02	1.37	1434.79502	−0.11	KGEREDLIAYLK	
	32.02	1.47	1168.62131	−0.78	TGPNLHGLFGR	
	33.74	1.54	1092.62942	−0.51	EDLIAYLKK	
	34.48	1.58	1306.69913	−0.82	GEREDLIAYLK	
	39.52	1.81	964.53419	−0.85	EDLIAYLK	
LYSC_CHICK (Lysozyme C, Gallus gallus, MW = 16, 228 Da)	24.92	1.14	1428.64926	−0.71	FESNFNTQATNR	
	31.79	1.46	1334.65191	−0.22	cKGTDVQAWIR	CaM (C)
	33.54	1.54	1045.54217	−0.38	GTDVQAWIR	

	36.08	1.65	1753.83343	−1.01	NTDGSTDYGILQINSR	
	37.46	1.72	1691.79451	−0.85	IVSDGNGmNAWVAWR	Ox (M)
	38.99	1.79	1326.61325	−1.13	GYSLGNWVcAAK	CaM (C)
	41.34	1.89	1675.79986	−0.7	IVSDGNGMNAWVAWR	

The setup used a PepMap Acclaim column (see Subheadings 2 and 3) and the schematics are given in Fig. 1. Chromatographic characteristics are given: t_R is the experimental retention time, the relative retention factor k' is calculated using the first identified peptide as a reference (ESKPPDSSKDEC(CaM)M(Ox)VK from bovine serotransferrin, where CaM stands for a carboxymethyl on Cys and Ox stands for an oxidized Met) because no experimental t_0 is measured in our setup on a routine basis. According to tandem mass spectrometry analysis, sequences and observed peptide modifications are summarized, and the theoretical masses are calculated from the elucidated structure of the peptide. The protein associated to each proteolytic peptide is given in the first column

as concentrated as possible and to analyze the sample immediately after its preparation. The surface of the storage vial seems to have a great influence (13). Use vial with low protein adsorption properties.

15. In the case of persistent contamination, the whole system should be flushed for 4–6 h, and all the valves should be switched every 30–45 min. As described in Subheading 2, we selected a mixture of solvent with strong elution power. However, the use of isopropanol increases the pressure drop during the transition between water–acetonitrile and methanol–acetonitrile–isopropanol, so the transition between the two solvent systems should be done at lower flow rates during the equilibration steps in both directions.

Acknowledgments

The authors would like to thank Emmanuelle Demey and Iman Haddad for technical assistance. The 2D-LC work was part of A.M. Hesse's PhD work, which was cofinanced by the CNRS (Centre National de la Recherche Scientifique) and by L'Oréal. The nano-LC-MALDI work was part of S. Ndiaye's PhD work, which was financed by UPMC Paris 6. The hardware configuration was financed by the town of Paris (ESPCI ParisTech) for the dual LC configuration and by the Réseau National des Genopoles (RNG) for the monodimensional LC configurations.

References

1. Perry, M., Li, Q., and Kennedy, R.T. (2009) Review of recent advances in analytical techniques for the determination of neurotransmitters. *Analytica Chimica Acta* **653**, 1–22.
2. Fricker, L.D., Lim, J., Pan, H., and Che, F.Y. (2006) Peptidomics: identification and quantification of endogenous peptides in neuroendocrine tissues. *Mass. Spec. Rev.* **25**, 327–344.
3. Saz, J.M., and Marina, M.L. (2008) Application of micro- and nano-HPLC to the determination and characterization of bioactive and biomarker peptides. *J. Sep. Sci.* **31**, 446–458.
4. Boonen, K., Landuyt, B., Baggerman G., et al (2008) Peptidomics: The integrated approach of MS, hyphenated techniques and bioinformatics for neuropeptide analysis. *J. Sep. Sci.* **31**, 427–445.
5. Boonen, K., Husson, S.J., Landuyt, B., et al (2010) Identification and relative quantification of neuropeptides from the endocrine tissues. In: Soloviev, M. (ed.), Peptidomics, Meth. Mol. Biol. 615 Humana Press, Springer Science.
6. Pesek, J.J., Matyska, M.T., and Pindi Venkat, J. (2008) Evaluation of protein, peptide, and amino acid retention on C5 hydride-based stationary phases. *J. Sep. Sci.* **31**, 2560–2566.
7. Wujcik, C.E., Tweed, J., and Kadar, E.P. (2010) Application of hydrophilic interaction chromatography retention coefficients for predicting peptide elution with TFA and methanesulfonic acid ion-pairing reagents. *J. Sep. Sci.* **33**, 826–833.
8. Li, Y., and Lee, M.L. (2009) Biocompatible polymeric monoliths for protein and peptide separations. *J. Sep. Sci.* **32**, 3369–3378.
9. Donato, P., Dugo, P., Cacciola, F., et al (2009) High peak capacity separation of peptides through the serial connection of LC shell-packed columns. *J. Sep. Sci.* **32**, 1129–1136.

10. Machtejevas, E., Marko-Varga, G., Lindberg,C. et al (2009) Profiling of endogenous peptides by multidimensional liquid chromatography: On-line automated sample cleanup for biomarker discovery in human urine, *J. Sep. Sci.* **32**, 2223–2232.

11. Storme, M.L., t'Kindt, R.S., and Van Bocxlaer, J.F. (2009) Improved analyte detectability of proteins and peptide lysates by means of multiple large-volume injection in LC-MS. *J. Sep. Sci.* **32**, 2346–2352.

12. Hesse, A.M., Marcelo, P., Rossier, J. et al (2008) Simple and universal tool to remove on-line impurities in mono- or two-dimensional liquid chromatography-mass spectrometry analysis. *J. Chromatogr. A* **1189**, 175–182.

13. Kraut, A., Marcellin, M., Adrait, A. et al. (2009) Peptide storage: are you getting the best return on your investment? Defining optimal storage conditions for proteomics samples. *J. Proteome Res.* **8**, 3778–3785.

Annexe 4. Tableaux Identification des protéines en présence d'amyloïde bêta après une séparation chromatographique d'une heure.

Sample: abeta gradient 1 heure							
Analysis: abeta gradient 1 heure							
Identifier	Description	Score	peptides	Coverage (%)	Peptide data (distinct in best Analysis)		
			All		#	Sequence	Score
AT1A3_RAT	Sodium/potassium-transporting ATPase subunit alpha-3	1378.82	19	24.2	1	MSVEEVCR	54.28
					2	KYNTDCVQGLTHSK	91.78
					3	NMVPQQALVIR	44.93
					4	VDNSSLTGESEPQTR	99.62
					5	SPDCTHDNPLETR	70.74
					6	NLEAVETLGSTSTICSDK	123.06
					7	GGQDNIPVLK	43.94
					8	DVAGDASESALLK	91.91
					9	CIELSSGSVK	54.48
					10	VAEIPFNSTNK	52.11
					11	YQLSIHETEDPNDNR	76.6
					12	EQPLDEEMK	35.44
					13	VIMVTGDHPITAK	75.64
					14	GVGIISEGNETVEDIAAR	95.23
					15	LNIPVSQVNPR	45.81
					16	ACVIHGTDLK	45.53
					17	LIIVEGCQR	70.2
					18	QGAIVAVTGDGVNDSPALK	123.17
					19	TVNDLEDSYGQQWTYEQR	84.35
TBB5_RAT	Tubulin beta-5 chain	1083.17	17	44.6	1	EIVHIQAGQCGNQIGAK	113.19
					2	ISVYYNEATGGK	65.25
					3	AILVDLEPGTMDSVR	94.22
					4	SGPFGQIFRPDNFVFGQSGAGNNWAK	40.76
					5	GHYTEGAELVDSVLDVVR	37.19
					6	IMNTFSVVPSPK	59.05
					7	FPGQLNADLR	60.69
					8	KLAVNMVPFPR	58.49
					9	LHFFMPGFAPLTSR	38.9
					10	NMMAACDPR	44.2
					11	YLTVAAVFR	50.86
					12	EVDEQMLNVQNK	78.84
					13	EVDEQMLNVQNK	78.08
					14	NSSYFVEWIPNNVK	84.96
					15	TAVCDIPPR	65.04
					16	ISEQFTAMFR	54.81

					17	ISEQFTAMFR	58.64
TBB2A_RAT	Tubulin beta-2A chain	1062.24	16	41.8	1	EIVHIQAGQCGNQIGAK	113.19
					2	INVYYNEAAGNK	91.01
					3	AILVDLEPGTMDSVR	94.22
					4	SGPFGQIFRPDNFVFGQSGAGNNWAK	40.76
					5	GHYTEGAELVDSVLDVVR	37.19
					6	FPGQLNADLR	60.69
					7	KLAVNMVPFPR	58.49
					8	LHFFMPGFAPLTSR	38.9
					9	NMMAACDPR	44.2
					10	YLTVAAIFR	63.22
					11	EVDEQMLNVQNK	78.84
					12	EVDEQMLNVQNK	78.08
					13	NSSYFVEWIPNNVK	84.96
					14	TAVCDIPPR	65.04
					15	ISEQFTAMFR	54.81
					16	ISEQFTAMFR	58.64
TBB2C_RAT	Tubulin beta-2C chain	900.33	16	43.4	1	FWEVISDEHGIDPTGTYHGDSDLQLER	30.29
					2	INVYYNEATGGK	59.53
					3	SGPFGQIFRPDNFVFGQSGAGNNWAK	40.76
					4	GHYTEGAELVDSVLDVVR	37.19
					5	IMNTFSVVPSPK	59.05
					6	FPGQLNADLR	60.69
					7	KLAVNMVPFPR	58.49
					8	LHFFMPGFAPLTSR	38.9
					9	NMMAACDPR	44.2
					10	YLTVAAVFR	50.86
					11	EVDEQMLNVQNK	78.84
					12	EVDEQMLNVQNK	78.08
					13	NSSYFVEWIPNNVK	84.96
					14	TAVCDIPPR	65.04
					15	ISEQFTAMFR	54.81
					16	ISEQFTAMFR	58.64
TBB3_RAT	Tubulin beta-3 chain	852.46	13	31.1	1	EIVHIQAGQCGNQIGAK	113.19
					2	ISVYYNEASSHK	62.7
					3	AILVDLEPGTMDSVR	94.22
					4	GHYTEGAELVDSVLDVVR	37.19
					5	IMNTFSVVPSPK	59.05
					6	FPGQLNADLR	60.69
					7	KLAVNMVPFPR	58.49
					8	NMMAACDPR	44.2
					9	EVDEQMLAIQSK	58.57
					10	EVDEQMLAIQSK	65.75
					11	NSSYFVEWIPNNVK	84.96

					12	ISEQFTAMFR	58.64
					13	ISEQFTAMFR	54.81
TBA1A_RAT	Tubulin alpha-1A chain	800.4	12	38.4	1	TIGGGDDSFNTFFSETGAGK	107.88
					2	AVFVDLEPTVIDEVR	67.8
					3	QLFHPEQLITGK	38.56
					4	QLFHPEQLITGK	45.5
					5	NLDIERPTYTNLNR	51.39
					6	LIGQIVSSITASLR	41.01
					7	IHFPLATYAPVISAEK	63.46
					8	AYHEQLSVAEITNACFEPANQMVK	47.45
					9	DVNAAIATIK	75.28
					10	TIQFVDWCPTGFK	73.92
					11	VGINYQPPTVVPGGDLAK	82.14
					12	AVCMLSNTTAIAEAWAR	106.01
ACTG_RAT	Actin, cytoplasmic 2	691.03	11	39.2	1	EEEIAALVIDNGSGMCK	109.66
					2	AGFAGDDAPR	75.05
					3	HQGVMVGMGQK	44.54
					4	IWHHTFYNELR	42.31
					5	VAPEEHPVLLTEAPLNPK	74.8
					6	TTGIVMDSGDGVTHTVPIYEGYALPHAILR	51.97
					7	GYSFTTTAER	63.9
					8	SYELPDGQVITIGNER	100.88
					9	EITALAPSTMK	34.07
					10	EITALAPSTMK	42.12
					11	QEYDESGPSIVHR	51.73
AT1A2_RAT	Sodium/potassium-transporting ATPase subunit alpha-2	818.81	11	14.5	1	NMVPQQALVIR	44.93
					2	VDNSSLTGESEPQTR	99.62
					3	SPEFTHENPLETR	32.91
					4	NLEAVETLGSTSTICSDK	123.06
					5	CIELSCGSVR	56.13
					6	VAEIPFNSTNK	52.11
					7	VIMVTGDHPITAK	75.64
					8	GVGIISEGNETVEDIAAR	95.23
					9	LNIPVSQVNPR	45.81
					10	LIIVEGCQR	70.2
					11	QGAIVAVTGDGVNDSPALK	123.17
K2C5_RAT	Keratin, type II cytoskeletal 5	666.38	11	19.1	1	WTLLQEQGTK	51.29
					2	NKYEDEINKR	39.04
					3	YEDEINKR	31.95
					4	DVDAAYMNKVELEAK	58.97
					5	VDALMDEINFMK	95.38
					6	SLDLDSIIAEVK	100.04
					7	SRTEAESWYQTK	61.49
					8	YEELQQTAGR	55.84

					9	EYQELMNTK	33.79
					10	LALDVEIATYR	86.76
					11	KLLEGEECR	51.83
TBA1B_RAT	Tubulin alpha-1B chain	765.66	11	35.5	1	TIGGGDDSFNTFFSETGAGK	107.88
					2	AVFVDLEPTVIDEVR	67.8
					3	QLFHPEQLITGK	38.56
					4	QLFHPEQLITGK	45.5
					5	NLDIERPTYTNLNR	51.39
					6	LISQIVSSITASLR	80.19
					7	IHFPLATYAPVISAEK	63.46
					8	AYHEQLSVAEITNACFEPANQMVK	47.45
					9	DVNAAIATIK	75.28
					10	VGINYQPPTVVPGGDLAK	82.14
					11	AVCMLSNTTAIAEAWAR	106.01
TBA1C_RAT	Tubulin alpha-1C chain	709.99	10	29.2	1	TIGGGDDSFNTFFSETGAGK	107.88
					2	AVFVDLEPTVIDEVR	67.8
					3	QLFHPEQLITGK	38.56
					4	QLFHPEQLITGK	45.5
					5	NLDIERPTYTNLNR	51.39
					6	LISQIVSSITASLR	80.19
					7	IHFPLATYAPVISAEK	63.46
					8	DVNAAIATIK	75.28
					9	TIQFVDWCPTGFK	73.92
					10	AVCMLSNTTAIAEAWAR	106.01
AT1A1_RAT	Sodium/potassium-transporting ATPase subunit alpha-1	707.7	9	12.4	1	NMVPQQALVIR	44.93
					2	VDNSSLTGESEPQTR	99.62
					3	NLEAVETLGSTSTICSDK	123.06
					4	AVAGDASESALLK	43.9
					5	IVEIPFNSTNK	31.95
					6	VIMVTGDHPITAK	75.64
					7	GVGIISEGNETVEDIAAR	95.23
					8	LIIVEGCQR	70.2
					9	QGAIVAVTGDGVNDSPALK	123.17
STXB1_RAT	Syntaxin-binding protein 1	581.33	9	15.5	1	VLVVDQLSMR	66.83
					2	ADDPTMGEGPDK	58.03
					3	SQLLILDR	42.25
					4	YETSGIGEAR	35.4
					5	HIAEVSQEVTR	61.46
					6	YSTHLHLAEDCMK	61.23
					7	VEQDLAMGTDAEGEK	91.16
					8	VEQDLAMGTDAEGEK	70.74
					9	SSASFSTTAVSAR	94.23
TBA4A_RAT	Tubulin alpha-4A chain	581.84	9	29.0	1	AVFVDLEPTVIDEIR	67.14
					2	QLFHPEQLITGK	38.56

					3	QLFHPEQLITGK	45.5
					4	NLDIERPTYTNLNR	51.39
					5	LISQIVSSITASLR	80.19
					6	IHFPLATYAPVISAEK	63.46
					7	AYHEQLSVAEITNACFEPANQMVK	47.45
					8	VGINYQPPTVVPGGDLAK	82.14
					9	AVCMLSNTTAIAEAWAR	106.01
CLH_RAT	Clathrin heavy chain 1	505.95	8	6.0	1	HSSLAGCQIINYR	45.65
					2	VIQCFAETGQVQK	91.96
					3	IHEGCEEPATHNALAK	65.59
					4	IYIDSNNNPER	57.82
					5	SVNESLNNLFITEEDYQALR	125.87
					6	HELIEFR	37.38
					7	DAMQYASESK	44.63
					8	VDKLDASESLR	37.05
ACTC_RAT	Actin, alpha cardiac muscle 1	392.01	7	19.9	1	AGFAGDDAPR	75.05
					2	HQGVMVGMGQK	44.54
					3	YPIEHGIITNWDDMEK	53.04
					4	IWHHTFYNELR	42.31
					5	SYELPDGQVITIGNER	100.88
					6	EITALAPSTMK	34.07
					7	EITALAPSTMK	42.12
EAA2_RAT	Excitatory amino acid transporter 2	431.88	7	10.5	1	KNDEVSSLDAFLDLIR	96.88
					2	NDEVSSLDAFLDLIR	91.55
					3	CLEDNLGIDKR	38.86
					4	SELDTIDSQHR	66.29
					5	MHEDIEMTK	41.77
					6	SADCSVEEEPWK	39.46
					7	SADCSVEEEPWKR	57.07
K2C1_RAT	Keratin, type II cytoskeletal 1	415.91	7	8.5	1	FLEQQNQVLQTK	90.29
					2	WELLQQVDTSTR	77.67
					3	YEDEINKR	31.95
					4	TNAENEFVTIK	58.18
					5	TNAENEFVTIKK	64.43
					6	DYQELMNTK	36.67
					7	DYQELMNTK	56.72
TBA8_RAT	Tubulin alpha-8 chain	477.71	7	19.6	1	QLFHPEQLITGK	38.56
					2	QLFHPEQLITGK	45.5
					3	NLDIERPTYTNLNR	51.39
					4	LISQIVSSITASLR	80.19
					5	TIQFVDWCPTGFK	73.92
					6	VGINYQPPTVVPGGDLAK	82.14
					7	AVCMLSNTTAIAEAWAR	106.01
1433Z_RAT	14-3-3 protein zeta/delta	376.37	6	27.8	1	MDKNELVQK	51.3

					2	YDDMAACMK	69.26
					3	SVTEQGAELSNEER	101.51
					4	DICNDVLSLLEK	65.88
					5	FLIPNASQPESK	33.87
					6	YLAEVAAGDDKK	54.55
AT1B1_RAT	Sodium/potassium-transporting ATPase subunit beta-1	371.27	6	23.4	1	TEISFRPNDPK	39.74
					2	SYEAYVLNIIR	75.83
					3	YKDSAQKDDMIFEDCGSMPSEPK	37.2
					4	YNPNVLPVQCTGK	63.19
					5	AYGENIGYSEK	68.37
					6	AYGENIGYSEKDR	86.94
K1C17_RAT	Keratin, type I cytoskeletal 17	341.02	6	14.1	1	LASYLDKVR	35.86
					2	VLDELTLAR	63.86
					3	NHEEEMNALR	46.49
					4	EVATNSELVQSGK	79.97
					5	CEMEQQNQEYK	64.95
					6	LEQEIATYR	49.89
K22E_RAT	Keratin, type II cytoskeletal 2 epidermal	359.1	6	8.8	1	GFSSGSAVVSGGSR	97.39
					2	VDPEIQNVK	39.14
					3	YEDEINKR	31.95
					4	DYQELMNVK	52.03
					5	LALDVEIATYR	86.76
					6	KLLEGEECR	51.83
SYT1_RAT	Synaptotagmin-1	262.42	6	15.2	1	VFLLPDKK	36.31
					2	TLNPVFNEQFTFK	44.56
					3	VPYSELGGK	31.1
					4	DLQSAEKEEQEK	57.19
					5	MDVGGLSDPYVK	43.59
					6	HWSDMLANPR	49.67
GNAO_RAT	Guanine nucleotide-binding protein G(o) subunit alpha	306.75	5	14.1	1	IIHEDGFSGEDVK	64.35
					2	AMDTLGVEYGDK	46.77
					3	AMDTLGVEYGDKER	65.45
					4	MVCDVVSR	48.07
					5	IGAADYQPTEQDILR	82.11
HSP7C_RAT	Heat shock cognate 71 kDa protein	286.87	5	10.4	1	VEIIANDQGNR	75.52
					2	TTPSYVAFTDTER	36.5
					3	NQVAMNPTNTVFDAK	78.08
					4	RFDDAVVQSDMK	31.52
					5	STAGDTHLGGEDFDNR	65.25
K1C10_RAT	Keratin, type I cytoskeletal 10	329.52	5	9.1	1	VTMQNLNDR	67.57
					2	LKYENEVALR	62.07
					3	QSVEADINGLR	80.07
					4	DAEAWFNEK	57.26
					5	LENEIQTYR	62.55

K1C14_RAT	Keratin, type I cytoskeletal 14	326.24	5	10.5	1	VTMQNLNDR	67.57
					2	VLDELTLAR	63.86
					3	EVATNSELVQSGK	79.97
					4	CEMEQQNQEYK	64.95
					5	LEQEIATYR	49.89
K2C6A_RAT	Keratin, type II cytoskeletal 6A	392.34	5	10.3	1	TAAENEFVTLKK	63.19
					2	SLDLDSIIAEVK	100.04
					3	SRAEAESWYQTK	66.12
					4	YEELQITAGR	76.23
					5	LALDVEIATYR	86.76
K2C75_RAT	Keratin, type II cytoskeletal 75	336.7	5	9.6	1	YEDEINKR	31.95
					2	SLDLDSIIAEVK	100.04
					3	SRAEAESWYQTK	66.12
					4	LALDVEIATYR	86.76
					5	KLLEGEECR	51.83
NSF_RAT	Vesicle-fusing ATPase	301.95	5	5.9	1	DYQSGQHVMVR	49.79
					2	YVGESEANIR	66.72
					3	KLFADAEEEQR	64.7
					4	LFADAEEEQR	48.99
					5	GHQLLSADVDIK	71.75
ATPA_RAT	ATP synthase subunit alpha, mitochondrial	242.17	4	9.4	1	TGTAEMSSILEER	36.45
					2	TGAIVDVPVGDELLGR	65.57
					3	VVDALGNAIDGK	74.09
					4	HALIIYDDLSK	66.06
ATPB_RAT	ATP synthase subunit beta, mitochondrial	264.17	4	11.5	1	TVLIMELINNVAK	71.26
					2	AHGGYSVFAGVGER	30.51
					3	VALVYGQMNEPPGAR	77.91
					4	AIAELGIYPAVDPLDSTSR	84.49
CN37_RAT	2',3'-cyclic-nucleotide 3'-phosphodiesterase	261.22	4	11.4	1	LDEDLAGYCR	61.83
					2	VLVLDDTNHER	48.89
					3	ATGAEEYAQQDVVR	86.45
					4	GGSQGEEVGELPR	64.05
DPYL2_RAT	Dihydropyrimidinase-related protein 2	244.52	4	9.6	1	QIGENLIVPGGVK	45.79
					2	SITIANQTNCPLYVTK	87.99
					3	SAAEVIAQAR	66.27
					4	MDENQFVAVTSTNAAK	44.47
G3P_RAT	Glyceraldehyde-3-phosphate dehydrogenase	306.94	4	21.0	1	IVSNASCTTNCLAPLAK	99.38
					2	VIHDNFGIVEGLMTTVHAITATQK	75.04
					3	GAAQNIIPASTGAAK	43.37
					4	VPTPNVSVVDLTCR	89.15
K1C42_RAT	Keratin, type I cytoskeletal 42	199.77	4	8.4	1	TKYETELNLR	39.53
					2	VLDELTLAR	63.86
					3	NHEEEMNALR	46.49
					4	LEQEIATYR	49.89

K2C8_RAT	Keratin, type II cytoskeletal 8	198.8	4	6.2	1	NKYEDEINKR	39.04
					2	YEDEINKR	31.95
					3	AQYEEIANR	60.49
					4	LALDIEIATYR	67.32
KCC2A_RAT	Calcium/calmodulin-dependent protein kinase type II subunit alpha	276.46	4	10.7	1	FTEEYQLFEELGK	95.59
					2	VLAGQEYAAK	55.82
					3	DLKPENLLLASK	32.67
					4	ESSESTNTTIEDEDTK	92.38
SPTA2_RAT	Spectrin alpha chain, brain	215.5	4	2.3	1	KFEEFQTDLAAHEER	32.24
					2	SQLLGSAHEVQR	56.39
					3	LIQSHPESAEDLKEK	37.15
					4	LSDDNTIGQEEIQQR	89.72
1433G_RAT	14-3-3 protein gamma	156.31	3	13.4	1	VDREQLVQK	30.79
					2	NVTELNEPLSNEER	78.02
					3	YLAEVATGEK	47.5
GBB1_RAT	Guanine nucleotide-binding protein G(I)/G(S)/G(T) subunit beta-1	195.22	3	10.3	1	LLVSASQDGK	75.14
					2	ELAGHTGYLSCCR	65.95
					3	LFVSGACDASAK	54.13
GBB2_RAT	Guanine nucleotide-binding protein G(I)/G(S)/G(T) subunit beta-2	175.09	3	10.3	1	LLVSASQDGK	75.14
					2	ELPGHTGYLSCCR	49.85
					3	TFVSGACDASIK	50.1
HS90A_RAT	Heat shock protein HSP 90-alpha	115.53	3	4.2	1	ELISNSSDALDK	33.07
					2	YIDQEELNK	51.94
					3	HIYFITGETK	30.52
K1C15_RAT	Keratin, type I cytoskeletal 15	167.29	3	6.0	1	VTMQNLNDR	67.57
					2	LASYLDKVR	35.86
					3	VLDELTLAR	63.86
K2C1B_RAT	Keratin, type II cytoskeletal 1b	161.28	3	4.2	1	FLEQQNQVLQTK	90.29
					2	NKYEDEINKR	39.04
					3	YEDEINKR	31.95
K2C73_RAT	Keratin, type II cytoskeletal 73	209.44	3	5.8	1	FLEQQNQVLQTK	90.29
					2	LALDIEIATYR	67.32
					3	KLLEGEECR	51.83
KCRB_RAT	Creatine kinase B-type	231.96	3	12.6	1	LAVEALSSLDGDLSGR	76.33
					2	LGFSEVELVQMVVDGVK	110.61
					3	LEQGQPIDDLMPAQK	45.02
LDHB_RAT	L-lactate dehydrogenase B chain	199.16	3	12.3	1	SLADELALVDVLEDK	66.54
					2	IVADKDYSVTANSK	61.7
					3	VIGSGCNLDSAR	70.92
MYPR_RAT	Myelin proteolipid protein	210.16	3	12.6	1	GLSATVTGGQK	52.43
					2	TSASIGSLCADAR	101.79
					3	VCGSNLLSICK	55.94
QCR2_RAT	Cytochrome b-c1 complex subunit 2, mitochondrial	171.11	3	7.5	1	RWEVAALR	36.88
					2	AVAFQNPQTR	39.07

					3	AVAQGNLSSADVQAAK	95.16
RAB3A_RAT	Ras-related protein Rab-3A	276.67	3	12.3	1	ILIIGNSSVGK	30.46
					2	MSESLDTADPAVTGAK	135.99
					3	MSESLDTADPAVTGAK	110.22
SYPH_RAT	Synaptophysin	145.81	3	7.8	1	MDVVNQLVAGGQFR	57.27
					2	MATDPENIIK	50.8
					3	MATDPENIIK	37.74
TPIS_RAT	Triosephosphate isomerase	230.91	3	14.1	1	IAVAAQNCYK	60.65
					2	CNVSEGVAQCTR	82.18
					3	IIYGGSVTGATCK	88.08
1433B_RAT	14-3-3 protein beta/alpha	124.53	2	10.2	1	AVTEQGHELSNEER	82.14
					2	YLSEVASGDNK	42.39
1433T_RAT	14-3-3 protein theta	158.72	2	10.2	1	AVTEQGAELSNEER	107.27
					2	YLAEVACGDDR	51.45
ALBU_RAT	Serum albumin	89.11	2	3.9	1	YMCENQATISSK	54
					2	LQACCDKPVLQK	35.11
AT2A2_RAT	Sarcoplasmic/endoplasmic reticulum calcium ATPase 2	92.68	2	2.3	1	TGTLTTNQMSVCR	56.78
					2	EFDELSPSAQR	35.9
AT2B2_RAT	Plasma membrane calcium-transporting ATPase 2	154.3	2	2.3	1	MVTGDNINTAR	83.05
					2	QVVAVTGDGTNDGPALK	71.25
ATP5H_RAT	ATP synthase subunit d, mitochondrial	120.17	2	15.5	1	ANVDKPGLVDDFK	43.15
					2	NCAQFVTGSQAR	77.02
GNAI1_RAT	Guanine nucleotide-binding protein G(i) subunit alpha-1	81.01	2	7.3	1	IIHEAGYSEEECK	45.78
					2	EIYTHFTCATDTK	35.23
HBA_RAT	Hemoglobin subunit alpha-1/2	123.03	2	21.8	1	IGGHGGEYGEEALQR	67.08
					2	TYFSHIDVSPGSAQVK	55.95
HS90B_RAT	Heat shock protein HSP 90-beta	102.64	2	2.8	1	YIDQEELNK	51.94
					2	EQVANSAFVER	50.7
K1C13_RAT	Keratin, type I cytoskeletal 13	129.96	2	4.6	1	QSVEADINGLR	80.07
					2	LEQEIATYR	49.89
KCC2B_RAT	Calcium/calmodulin-dependent protein kinase type II subunit beta	125.74	2	5.2	1	DLKPENLLLASK	32.67
					2	ESSDSTNTTIEDEDAK	93.07
MBP_RAT	Myelin basic protein S	92.85	2	11.8	1	YLATASTMDHAR	45.75
					2	GAYDAQGTLSK	47.1
MDHC_RAT	no description	128.08	2	N/A	1	VIVVGNPANTNCLTASK	70.96
					2	GEFITTVQQR	57.12
PGAM1_RAT	Phosphoglycerate mutase 1	119.98	2	10.2	1	HYGGLTGLNK	31.5
					2	YADLTEDQLPSCESLK	88.48
QCR1_RAT	Cytochrome b-c1 complex subunit 1, mitochondrial	128.68	2	4.6	1	LCTSATESEVTR	77.73
					2	IEEVDAQMVR	50.95
SEPT7_RAT	Septin-7	95.72	2	5.3	1	FEDYLNAESR	44.85
					2	ADTLTPEECQQFK	50.87
SNAB_RAT	Beta-soluble NSF attachment protein	98.63	2	7.7	1	IEEACEMYTR	49.23
					2	SIQGDGEGDGDLK	49.4

SV2A_RAT	Synaptic vesicle glycoprotein 2A	101.01	2	3.1	1	GGLSDGEGPPGGR	47.71
					2	HLQAVDYAAR	53.3
VGLU1_RAT	Vesicular glutamate transporter 1	79.05	2	2.1	1	KYIEDAIGESAK	33.63
					2	YIEDAIGESAK	45.42

Annexe 5. Tableaux Identification des protéines en présence d'amyloïde bêta après une séparation chromatographique de quatre heures.

Sample: abeta 4 heures							
Analysis: abeta 4 heures							
Identifier	Description	Score	Matching peptides	Coverage (%)	Peptide data (distinct in best Analysis)		
			All		#	Sequence	Score
SPTA2_RAT	Spectrin alpha chain, brain	1492.93	31	14.8	1	VLETAEDIQER	52.33
					2	KFEEFQTDLAAHEER	33.95
					3	LFGAAEVQR	46.09
					4	DVDETIGWIK	44.08
					5	DLASVQALLR	71.55
					6	REELITNWEQIR	42.12
					7	DLTSWVTEMK	47.32
					8	AALLELWELR	37.46
					9	DTEQVDNWMSK	35.65
					10	AQLADSFHLQQFFR	34.48
					11	MNEVISLWK	42.99
					12	IDGITIQAR	46.45
					13	DVEDEETWIR	31.86
					14	DLIGVQNLLK	43.85
					15	GNAMVEEGHFAAEDVK	43.28
					16	EANELQQWINEK	52.58
					17	SLQQLAEER	37.44
					18	DVTGAEALLER	51.02
					19	LGESQTLQQFSR	65.75
					20	DVDEIEAWISEK	38.87
					21	LAALADQWQFLVQK	61.36
					22	DLASVNNLLK	31.18
					23	LKDLNSQADSLMTSSAFDTSQVK	30.93
					24	LLVSSEDYGR	39.44
					25	LSDDNTIGQEEIQQR	51.26
					26	ADVVESWIGEK	37.59
					27	DLSSVQTLLTK	70.42
					28	SSLSSAQADFNQLAELDR	101.59
					29	SSEEIESAFR	73.62
					30	EELYQNLTR	38.33

					31	ELPTAFDYVEFTR	58.09
ATPB_RAT	ATP synthase subunit beta, mitochondrial	1632.23	27	53.3	1	LVLEVAQHLGESTVR	86.1
					2	TIAMDGTEGLVR	40.98
					3	TIAMDGTEGLVR	55.99
					4	VLDSGAPIKIPVGPETLGR	53.95
					5	IPVGPETLGR	49.89
					6	IMNVIGEPIDER	49.2
					7	IMNVIGEPIDER	73.09
					8	VVDLLAPYAK	49.92
					9	IGLFGGAGVGK	58.66
					10	TVLIMELINNVAK	77.96
					11	TVLIMELINNVAK	66.48
					12	AHGGYSVFAGVGER	66.46
					13	TREGNDLYHEMIESGVINLK	30.15
					14	EGNDLYHEMIESGVINLK	38.84
					15	VALVYGQMNEPPGAR	43.65
					16	VALVYGQMNEPPGAR	86.29
					17	VALTGLTVAEYFR	94.38
					18	DQEGQDVLLFIDNIFR	64.85
					19	FTQAGSEVSALLGR	81.05
					20	IPSAVGYQPTLATDMGTMQER	30.06
					21	IPSAVGYQPTLATDMGTMQER	80.32
					22	IPSAVGYQPTLATDMGTMQER	60.07
					23	AIAELGIYPAVDPLDSTSR	95.67
					24	IMDPNIVGSEHYDVAR	36.59
					25	IMDPNIVGSEHYDVAR	70.95
					26	SLQDIIAILGMDELSEEDKLTVSR	50.27
					27	FLSQPFQVAEVFTGHMGK	40.41
TBB2A_RAT	Tubulin beta-2A chain	1756.47	26	52.1	1	MREIVHIQAGQCGNQIGAK	30.39
					2	EIVHIQAGQCGNQIGAK	94.42
					3	INVYYNEAAGNK	80.44
					4	AILVDLEPGTMDSVR	75.91
					5	AILVDLEPGTMDSVR	74.97
					6	SGPFGQIFRPDNFVFGQSGAGNNWAK	32.03
					7	GHYTEGAELVDSVLDVVR	93.45
					8	IMNTFSVMPSPK	97.41
					9	FPGQLNADLR	55.58
					10	KLAVNMVPFPR	65.12
					11	LAVNMVPFPR	80.39
					12	LAVNMVPFPR	43.01
					13	LHFFMPGFAPLTSR	43.6
					14	LHFFMPGFAPLTSR	46.88
					15	ALTVPELTQQMFDSK	85.17
					16	ALTVPELTQQMFDSK	48.58

					17	NMMAACDPR	53.57
					18	YLTVAAIFR	53.09
					19	EVDEQMLNVQNK	68.86
					20	EVDEQMLNVQNK	78.49
					21	NSSYFVEWIPNNVK	58.26
					22	TAVCDIPPR	51.11
					23	MSATFIGNSTAIQELFK	113.67
					24	MSATFIGNSTAIQELFK	91.89
					25	ISEQFTAMFR	72.11
					26	ISEQFTAMFR	68.07
TBB2B_RAT	Tubulin beta-2B chain	1720.02	26	52.1	1	MREIVHIQAGQCGNQIGAK	30.39
					2	EIVHIQAGQCGNQIGAK	94.42
					3	INVYYNEATGNK	43.99
					4	AILVDLEPGTMDSVR	75.91
					5	AILVDLEPGTMDSVR	74.97
					6	SGPFGQIFRPDNFVFGQSGAGNNWAK	32.03
					7	GHYTEGAELVDSVLDVVR	93.45
					8	IMNTFSVMPSPK	97.41
					9	FPGQLNADLR	55.58
					10	KLAVNMVPFPR	65.12
					11	LAVNMVPFPR	80.39
					12	LAVNMVPFPR	43.01
					13	LHFFMPGFAPLTSR	43.6
					14	LHFFMPGFAPLTSR	46.88
					15	ALTVPELTQQMFDSK	85.17
					16	ALTVPELTQQMFDSK	48.58
					17	NMMAACDPR	53.57
					18	YLTVAAIFR	53.09
					19	EVDEQMLNVQNK	68.86
					20	EVDEQMLNVQNK	78.49
					21	NSSYFVEWIPNNVK	58.26
					22	TAVCDIPPR	51.11
					23	MSATFIGNSTAIQELFK	113.67
					24	MSATFIGNSTAIQELFK	91.89
					25	ISEQFTAMFR	72.11
					26	ISEQFTAMFR	68.07
TBB2C_RAT	Tubulin beta-2C chain	1629.44	25	47.9	1	INVYYNEATGGK	69.22
					2	AVLVDLEPGTMDSVR	65.08
					3	AVLVDLEPGTMDSVR	74.97
					4	SGPFGQIFRPDNFVFGQSGAGNNWAK	32.03
					5	GHYTEGAELVDSVLDVVR	93.45
					6	IMNTFSVVPSPK	45.73
					7	IMNTFSVVPSPK	78.49
					8	FPGQLNADLR	55.58

					9	KLAVNMVPFPR	65.12
					10	LAVNMVPFPR	80.39
					11	LAVNMVPFPR	43.01
					12	LHFFMPGFAPLTSR	43.6
					13	LHFFMPGFAPLTSR	46.88
					14	ALTVPELTQQMFDAK	76.33
					15	ALTVPELTQQMFDAK	42.78
					16	NMMAACDPR	53.57
					17	YLTVAAVFR	60.75
					18	EVDEQMLNVQNK	68.86
					19	EVDEQMLNVQNK	78.49
					20	NSSYFVEWIPNNVK	58.26
					21	TAVCDIPPR	51.11
					22	MSATFIGNSTAIQELFK	113.67
					23	MSATFIGNSTAIQELFK	91.89
					24	ISEQFTAMFR	72.11
					25	ISEQFTAMFR	68.07
TBB5_RAT	Tubulin beta-5 chain	1559.4	25	52.3	1	MREIVHIQAGQCGNQIGAK	30.39
					2	EIVHIQAGQCGNQIGAK	94.42
					3	ISVYYNEATGGK	61.91
					4	AILVDLEPGTMDSVR	75.91
					5	AILVDLEPGTMDSVR	74.97
					6	SGPFGQIFRPDNFVFGQSGAGNNWAK	32.03
					7	GHYTEGAELVDSVLDVVR	93.45
					8	IMNTFSVVPSPK	45.73
					9	IMNTFSVVPSPK	78.49
					10	FPGQLNADLR	55.58
					11	KLAVNMVPFPR	65.12
					12	LAVNMVPFPR	80.39
					13	LAVNMVPFPR	43.01
					14	LHFFMPGFAPLTSR	43.6
					15	LHFFMPGFAPLTSR	46.88
					16	ALTVPELTQQVFDAK	66.23
					17	NMMAACDPR	53.57
					18	YLTVAAVFR	60.75
					19	EVDEQMLNVQNK	68.86
					20	EVDEQMLNVQNK	78.49
					21	NSSYFVEWIPNNVK	58.26
					22	TAVCDIPPR	51.11
					23	MAVTFIGNSTAIQELFK	60.07
					24	ISEQFTAMFR	72.11
					25	ISEQFTAMFR	68.07
DHE3_RAT	Glutamate dehydrogenase 1, mitochondrial	1356.25	23	47.0	1	MVEGFFDR	44.61
					2	GASIVEDKLVEDLK	67.79

					3	RDDGSWEVIEGYR	37.64
					4	DDGSWEVIEGYR	74.64
					5	YSTDVSVDEVK	62.9
					6	ALASLMTYK	50.1
					7	CAVVDVPFGGAK	49.61
					8	KGFIGPGIDVPAPDMSTGER	72.48
					9	GFIGPGIDVPAPDMSTGER	77.24
					10	GFIGPGIDVPAPDMSTGER	57.4
					11	TFVVQGFGNVGLHSMR	77.92
					12	CVGVGESDGSIWNPDGIDPK	91.89
					13	VYEGSILEADCDILIPAASEK	68.15
					14	IIAEGANGPTTPEADK	54.02
					15	IIAEGANGPTTPEADKIFLER	49.19
					16	NIMVIPDLYLNAGGVTVSYFEWLK	39.55
					17	DSNYHLLMSVQESLER	59.98
					18	HGGTIPVVPTAEFQDR	60.07
					19	DIVHSGLAYTMER	38.7
					20	DIVHSGLAYTMER	58.94
					21	YNLGLDLR	49.39
					22	TAAYVNAIEK	58.37
					23	VYNEAGVTFT	55.67
NSF_RAT	Vesicle-fusing ATPase	1225.05	23	34.3	1	CPTDELSLSNCAVVNEK	91.64
					2	DYQSGQHVMVR	36.5
					3	NIDSNPYDTDK	32.89
					4	DIEAMDPSILK	50.14
					5	AENSSLNLIGK	54.34
					6	QSIINPDWNFEK	39.14
					7	QSIINPDWNFEK	34.23
					8	GILLYGPPGCGK	45.57
					9	VVNGPEILNK	33.8
					10	YVGESEANIR	54.64
					11	KLFADAEEEQR	33.9
					12	LFADAEEEQR	60.13
					13	GSMAGSTGVHDTVVNQLLSK	60.57
					14	MEIGLPDEK	32.89
					15	GHQLLSADVDIK	52.58
					16	NFSGAELEGLVR	65.69
					17	VLDDGELLVQQTK	78.53
					18	TPLVSVLLEGPPHSGK	48.13
					19	IAEESNFPFIK	46.68
					20	SQLSCVVVDDIER	108.55
					21	LLDYVPIGPR	57.57
					22	FSNLVLQALLVLLK	69.87
					23	LLIIGTTSR	37.07

TBB3_RAT	Tubulin beta-3 chain	1428.49	23	43.8	1	MREIVHIQAGQCGNQIGAK	30.39
					2	EIVHIQAGQCGNQIGAK	94.42
					3	ISVYYNEASSHK	45.72
					4	AILVDLEPGTMDSVR	75.91
					5	AILVDLEPGTMDSVR	74.97
					6	GHYTEGAELVDSVLDVVR	93.45
					7	IMNTFSVVPSPK	45.73
					8	IMNTFSVVPSPK	78.49
					9	FPGQLNADLR	55.58
					10	KLAVNMVPFPR	65.12
					11	LAVNMVPFPR	80.39
					12	LAVNMVPFPR	43.01
					13	LHFFMPGFAPLTAR	36.08
					14	ALTVPELTQQMFDAK	76.33
					15	ALTVPELTQQMFDAK	42.78
					16	NMMAACDPR	53.57
					17	YLTVATVFR	59.63
					18	EVDEQMLAIQSK	53.15
					19	EVDEQMLAIQSK	63.07
					20	NSSYFVEWIPNNVK	58.26
					21	MSSTFIGNSTAIQELFK	62.26
					22	ISEQFTAMFR	72.11
					23	ISEQFTAMFR	68.07
ADT1_RAT	ADP/ATP translocase 1	1359.99	22	65.4	1	GDQALSFLK	72.52
					2	GDQALSFLKDFLAGGIAAAVSK	45.92
					3	DFLAGGIAAAVSK	92
					4	LLLQVQHASK	48.86
					5	EQGFLSFWR	37.72
					6	YFPTQALNFAFK	70.42
					7	QIFLGGVDR	61.94
					8	QIFLGGVDR	45.11
					9	YFAGNLASGGAAGATSLCFVYPLDFAR	89.45
					10	EFNGLGDCLTK	59.8
					11	GLYQGFSVSVQGIIIYR	51.97
					12	AAYFGVYDTAK	67.82
					13	GMLPDPKNVHIIVSWMIAQSVTAVAGLVSYPFDTVR	33.75
					14	GMLPDPKNVHIIVSWMIAQSVTAVAGLVSYPFDTVR	32.49
					15	KGADIMYTGTVDCWR	68.47
					16	KGADIMYTGTVDCWR	79.28
					17	GADIMYTGTVDCWR	75.39
					18	GADIMYTGTVDCWR	93.37
					19	GMGGAFVLVLYDEIK	60.29
					20	GMGGAFVLVLYDEIK	52.4
					21	GMGGAFVLVLYDEIKK	62.36

					22	GMGGAFVLVLYDEIKK	58.66
NDUS1_RAT	NADH-ubiquinone oxidoreductase 75 kDa subunit, mitochondrial	1326.72	22	40.0	1	VVAACAMPVMK	65.16
					2	GWNILTNSEK	32.55
					3	FASEIAGVDDLGTTGR	96.45
					4	GNDMQVGTYIEK	61.29
					5	MHEDINEEWISDK	62.59
					6	GLLTYTSWEDALSR	87.8
					7	VAGMLQSFEGK	55.73
					8	AVAAIAGGLVDAEALVALK	56.17
					9	VDSDTLCTEEIFPNEGAGTDLR	49.43
					10	FEAPLFNAR	50.74
					11	VALIGSPVDLTYR	72.04
					12	ILQDIASGNHEFSK	63.71
					13	KPMVVLGSSALQR	64.61
					14	DDGAAILAAVSSIAQK	88.05
					15	VASGAAAEWK	33.46
					16	LLFLLGADGGCITR	88.23
					17	SATYVNTEGR	44.88
					18	VAVTPPGLAR	33.63
					19	ALSEIAGITLPYDTLDQVR	56.19
					20	LGEVSPNLVR	50.6
					21	DFYMTDSISR	37.9
					22	AVTEGAQAVEEPSIC	75.51
ADT2_RAT	ADP/ATP translocase 2	1245.41	21	54.4	1	TDAAVSFAK	80.71
					2	TDAAVSFAKDFLAGGVAAAISKTAVAPIER	39.33
					3	DFLAGGVAAAISK	107.57
					4	LLLQVQHASK	48.86
					5	EQGVLSFWR	45.56
					6	YFPTQALNFAFK	70.42
					7	QIFLGGVDK	46.96
					8	QIFLGGVDKR	39.97
					9	QIFLGGVDKR	32.96
					10	TQFWRYFAGNLASGGAAGATSLCFVYPLDFAR	31.54
					11	YFAGNLASGGAAGATSLCFVYPLDFAR	89.45
					12	GLYQGFNVSVQGIIIYR	55.07
					13	AAYFGIYDTAK	62.48
					14	KGTDIMYTGTLDCWR	82.66
					15	KGTDIMYTGTLDCWR	43.11
					16	GTDIMYTGTLDCWR	72.29
					17	GTDIMYTGTLDCWR	62.76
					18	GMGGAFVLVLYDEIK	60.29
					19	GMGGAFVLVLYDEIK	52.4
					20	GMGGAFVLVLYDEIKK	62.36
					21	GMGGAFVLVLYDEIKK	58.66

AT1A3_RAT	Sodium/potassium-transporting ATPase subunit alpha-3	1268.51	20	26.1	1	KYNTDCVQGLTHSK	34.68
					2	YNTDCVQGLTHSK	58.93
					3	DGPNALTPPPTTPEWVK	40.59
					4	NMVPQQALVIR	36.66
					5	VDNSSLTGESEPQTR	86.49
					6	SPDCTHDNPLETR	38.87
					7	NLEAVETLGSTSTICSDK	115.86
					8	SSHTWVALSHIAGLCNR	40.43
					9	GGQDNIPVLK	46.69
					10	DVAGDASESALLK	88.35
					11	YQLSIHETEDPNDNR	53.83
					12	EAFQNAYLELGGLGER	72.58
					13	VIMVTGDHPITAK	57.94
					14	GVGIISEGNETVEDIAAR	114.14
					15	LNIPVSQVNPR	43.34
					16	LIIVEGCQR	49.5
					17	QGAIVAVTGDGVNDSPALK	71.65
					18	QGAIVAVTGDGVNDSPALK	97.79
					19	KADIGVAMGIAGSDVSK	55.76
					20	TVNDLEDSYGQQWTYEQR	64.43
MAP1B_RAT	Microtubule-associated protein 1B	1090.42	20	11.1	1	AIGNIELGIR	70.07
					2	ASLTLFCPEEGDWK	42.97
					3	SVGNAIEPVILFQK	61.68
					4	DLTGQVSTPPVK	32.25
					5	DFEELKAEEIDVAK	33.8
					6	SVNFSLTPNEIK	69.26
					7	ASDAEIMSSQSALALDER	87.92
					8	DMSLYASLASEK	38.85
					9	SDISPLTPR	39.14
					10	ESSPTYSPGFSDSTSGAK	43.88
					11	TIQAHDVGGYYYEK	30.19
					12	SPCDSGYSYETIEK	63.74
					13	TPEDGGYSCEITEK	54.45
					14	TPEEGGYSYEISEK	84.1
					15	TPEVSGYTYEK	40.43
					16	ITSFPESESYSYETTTK	60.13
					17	SPDTSAYCYETMEK	45.44
					18	TPQASTYSYETSDR	69.04
					19	SSYYVVSGNDPAAEEPSR	77.34
					20	AVLDALLEGK	45.74
SYN2_RAT	Synapsin-2	1207.28	20	38.7	1	RPPPAQAPAPQPAPQPAPTPSVGSSFFSSLSQAVK	35.43
					2	QTAASAGLVDAPAPSAASR	90.33
					3	QTAASAGLVDAPAPSAASR	109.74
					4	VLLVVDEPHTDWAK	66.41

					5	ILGDYDIK	36.04
					6	SFRPDFVLIR	41.79
					7	QHAFGMAENEDFR	36.53
					8	FPLIEQTYYPNHR	30.98
					9	EMLTLPTFPVVVK	55.72
					10	EMLTLPTFPVVVK	36.37
					11	TNTGSAMLEQIAMSDR	117.62
					12	TNTGSAMLEQIAMSDR	91.38
					13	TNTGSAMLEQIAMSDR	90.27
					14	QLITDLVISK	60.4
					15	QLITDLVISK	50.84
					16	TPALSPQRPLTTQQPQSGTLK	31.72
					17	TPALSPQRPLTTQQPQSGTLKEPDSSK	39.05
					18	TPPQRPAPQGGPGQPQGMQPPGK	41.15
					19	SQSLTNAFSFSESSFFR	107.95
					20	KSFASLFSD	37.56
ATPA_RAT	ATP synthase subunit alpha, mitochondrial	1254.73	19	45.0	1	TGTAEMSSILEER	82.39
					2	TGTAEMSSILEER	63.94
					3	ILGADTSVDLEETGR	113.49
					4	VLSIGDGIAR	55.06
					5	NVQAEEMVEFSSGLK	86.7
					6	GMSLNLEPDNVGVVVFGNDK	67.85
					7	GMSLNLEPDNVGVVVFGNDK	46.02
					8	TGAIVDVPVGDELLGR	77
					9	VVDALGNAIDGK	76.77
					10	AVDSLVPIGR	65.09
					11	TSIAIDTIINQK	79.7
					12	YTIVVSATASDAAPLQYLAPYSGCSMGEYFR	31.73
					13	HALIIYDDLSK	60.07
					14	EAYPGDVFYLHSR	72.69
					15	GIRPAINVGLSVSR	59.92
					16	EVAAFAQFGSDLDAATQQLLSR	66.77
					17	FESAFLSHVVSQHQSLLGNIR	39.64
					18	LKEIVTNFLAGFEP	52.16
					19	EIVTNFLAGFEP	57.74
ACTB_RAT	Actin, cytoplasmic 1	1068.08	18	54.4	1	DDDIAALVVDNGSGMCK	93.35
					2	AGFAGDDAPR	81.35
					3	HQGVMVGMGQK	46.69
					4	DSYVGDEAQSK	54
					5	IWHHTFYNELR	42.86
					6	VAPEEHPVLLTEAPLNPK	75.01
					7	DLTDYLMK	30.01
					8	GYSFTTTAER	56.7
					9	LCYVALDFEQEMATAASSSSLEK	45.14

					10	SYELPDGQVITIGNER	86.93
					11	KDLYANTVLSGGTTMYPGIADR	46.76
					12	DLYANTVLSGGTTMYPGIADR	83.51
					13	DLYANTVLSGGTTMYPGIADR	101.51
					14	EITALAPSTMK	53.02
					15	EITALAPSTMK	41.54
					16	YSVWIGGSILASLSTFQQMWISK	31.27
					17	QEYDESGPSIVHR	43.15
					18	QEYDESGPSIVHR	55.28
ACTG_RAT	Actin, cytoplasmic 2	1076.58	18	54.4	1	EEEIAALVIDNGSGMCK	101.85
					2	AGFAGDDAPR	81.35
					3	HQGVMVGMGQK	46.69
					4	DSYVGDEAQSK	54
					5	IWHHTFYNELR	42.86
					6	VAPEEHPVLLTEAPLNPK	75.01
					7	DLTDYLMK	30.01
					8	GYSFTTTAER	56.7
					9	LCYVALDFEQEMATAASSSSLEK	45.14
					10	SYELPDGQVITIGNER	86.93
					11	KDLYANTVLSGGTTMYPGIADR	46.76
					12	DLYANTVLSGGTTMYPGIADR	83.51
					13	DLYANTVLSGGTTMYPGIADR	101.51
					14	EITALAPSTMK	53.02
					15	EITALAPSTMK	41.54
					16	YSVWIGGSILASLSTFQQMWISK	31.27
					17	QEYDESGPSIVHR	43.15
					18	QEYDESGPSIVHR	55.28
ECHA_RAT	Trifunctional enzyme subunit alpha, mitochondrial	924.16	18	30.4	1	MVGVPAAFDMMLTGR	32.29
					2	MGLVDQLVDPLGPGIK	72.61
					3	TIEYLEEVAVNFAK	38.09
					4	LTSYAMTIPFVR	77.32
					5	TGLEQGNDAGYLAESEK	104.4
					6	ALMGLYNGQVLCK	39.49
					7	DSIFSNLIGQLDYK	59.97
					8	ADMVIEAVFEDLAVK	34.86
					9	MQLLEIITTDK	63.16
					10	DTTASAVAVGLK	61.44
					11	DGPGFYTTR	30.24
					12	ILQEGVDPK	30.05
					13	FGGGSVELLK	48.53
					14	GFYIYQSGSK	49.67
					15	NLNSEIDNILVNLR	38.22
					16	LPAKPEVSSDEDIQYR	65.05
					17	FVDLYGAQK	34.1

					18	YESAYGTQFTPCQLLR	44.67
IDH3B_RAT	Isocitrate dehydrogenase [NAD] subunit beta, mitochondrial	927.77	17	44.7	1	VEGAFPVTMLPGDGVGPELMHAVK	36.15
					2	AAAVPVEFK	33.39
					3	EHHLSEVQNMASEEK	47.03
					4	LEQVLSSMK	46.88
					5	GELASYDMQLR	39.64
					6	GELASYDMQLR	61.65
					7	RKLDLFANVVHVK	38.29
					8	KLDLFANVVHVK	54.23
					9	LDLFANVVHVK	41.72
					10	HNNLDLVIIR	68.65
					11	EQTEGEYSSLEHESAR	68.43
					12	LGDGLFLQCCEEVAELYPK	42.15
					13	NIANPTAMLLSASNMLR	115.65
					14	NIANPTAMLLSASNMLR	59.86
					15	HLNLEYHSSMIADAVK	45.49
					16	DMGGYSTTTDFIK	51.7
					17	DMGGYSTTTDFIK	76.86
SYN1_RAT	Synapsin-1	971.65	17	31.4	1	QTTAAAAATFSEQVGGGSGGAGR	113.46
					2	EMLSSTTYPVVVK	48.6
					3	EMLSSTTYPVVVK	76.1
					4	VKVDNQHDFQDIASVVALTK	43.56
					5	TYATAEPFIDAK	55.76
					6	TNTGSAMLEQIAMSDR	117.62
					7	TNTGSAMLEQIAMSDR	91.38
					8	TNTGSAMLEQIAMSDR	90.27
					9	DHIIEVVGSSMPLIGDHQDEDK	45.77
					10	QLIVELVVNK	45.68
					11	GSHSQTPSPGALPLGR	37.33
					12	QTSQQPAGPPAQQRPPPQGGPPQPGPGPQR	39.75
					13	LPSPTAAPQQSASQATPMTQGQGR	34.39
					14	LPSPTAAPQQSASQATPMTQGQGR	31.57
					15	QASISGPAPPK	30.53
					16	QGPPQKPPGPAGPIR	32.32
					17	KSFASLFSD	37.56
TBA1A_RAT	Tubulin alpha-1A chain	1159.15	17	53.0	1	TIGGGDDSFNTFFSETGAGK	85.98
					2	AVFVDLEPTVIDEVR	89.63
					3	QLFHPEQLITGK	48.01
					4	QLFHPEQLITGKEDAANNYAR	49.8
					5	QLFHPEQLITGKEDAANNYAR	33.23
					6	EIIDLVLDR	52.61
					7	LADQCTGLQGFLVFHSFGGGTGSGFTSLLMER	39.52
					8	LIGQIVSSITASLR	90.9
					9	FDGALNVDLTEFQTNLVPYPR	76.91

					10	IHFPLATYAPVISAEK	72.97
					11	AYHEQLSVAEITNACFEPANQMVK	35.43
					12	YMACCLLYR	38.23
					13	DVNAAIATIK	68.56
					14	TIQFVDWCPTGFK	75.26
					15	VGINYQPPTVVPGGDLAK	91.54
					16	AVCMLSNTTAIAEAWAR	118.56
					17	AVCMLSNTTAIAEAWAR	92.01
TBA1B_RAT	Tubulin alpha-1B chain	1148.55	17	53.0	1	TIGGGDDSFNTFFSETGAGK	85.98
					2	AVFVDLEPTVIDEVR	89.63
					3	QLFHPEQLITGK	48.01
					4	QLFHPEQLITGKEDAANNYAR	49.8
					5	QLFHPEQLITGKEDAANNYAR	33.23
					6	EIIDLVLDR	52.61
					7	LADQCTGLQGFLVFHSFGGGTGSGFTSLLMER	39.52
					8	LISQIVSSITASLR	74.82
					9	FDGALNVDLTEFQTNLVPYPR	76.91
					10	IHFPLATYAPVISAEK	72.97
					11	AYHEQLSVAEITNACFEPANQMVK	35.43
					12	YMACCLLYR	38.23
					13	DVNAAIATIK	68.56
					14	SIQFVDWCPTGFK	80.74
					15	VGINYQPPTVVPGGDLAK	91.54
					16	AVCMLSNTTAIAEAWAR	118.56
					17	AVCMLSNTTAIAEAWAR	92.01
AT1A1_RAT	Sodium/potassium-transporting ATPase subunit alpha-1	1042.53	16	19.1	1	LSLDELHR	31.83
					2	DGPNALTPPPTTPEWVK	40.59
					3	NMVPQQALVIR	36.66
					4	VDNSSLTGESEPQTR	86.49
					5	SPDFTNENPLETR	67.62
					6	GIVVYTGDR	38.21
					7	NLEAVETLGSTSTICSDK	115.86
					8	TSATWFALSR	71.15
					9	AVAGDASESALLK	81.64
					10	IVEIPFNSTNK	34.93
					11	VIMVTGDHPITAK	57.94
					12	GVGIISEGNETVEDIAAR	114.14
					13	LNIPVNQVNPR	46.53
					14	LIIVEGCQR	49.5
					15	QGAIVAVTGDGVNDSPALK	97.79
					16	QGAIVAVTGDGVNDSPALK	71.65
CH60_RAT	60 kDa heat shock protein, mitochondrial	1121.7	16	38.6	1	TVIIEQSWGSPK	73.86
					2	LVQDVANNTNEEAGDGTTTATVLAR	151.95
					3	RGVMLAVDAVIAELKK	48.09

					4	DIGNIISDAMK	65.13
					5	TLNDELEIIEGMK	30.42
					6	TLNDELEIIEGMK	84.97
					7	GYISPYFINTSK	41.45
					8	CEFQDAYVLLSEK	71.1
					9	ISSVQSIVPALEIANAHR	50.16
					10	VGEVIVTKDDAMLLK	53.32
					11	IQEITEQLDITTSEYEK	94.86
					12	VGGTSDVEVNEK	84.06
					13	VTDALNATR	57.4
					14	AAVEEGIVLGGGCALLR	114.24
					15	NAGVEGSLIVEK	61.9
					16	DPGMGAMGGMGGGMGGGMF	38.79
IMMT_RAT	Mitochondrial inner membrane protein (Fragment)	881.39	16	31.5	1	LFGMVLGSAPYTVPLPK	44.75
					2	SLEDALNQTATVTR	72.54
					3	QTITAQNAAVQAVK	92.51
					4	QTITAQNAAVQAVK	66.17
					5	TAMDNSEIAGEK	31.05
					6	AVDEAADALLK	44.16
					7	EIAGATPYITAAEEK	51.42
					8	VVSQYHELVVQAR	63.38
					9	ELDSITPDITPGWK	52.12
					10	QHIELALER	57.25
					11	FEFEQDLSEK	72.76
					12	SQEQMDNFTLDINTAYAR	34.46
					13	GIEQAVQSHAVAEEEAR	49.85
					14	TSSAEMPTIPLGSAVEAIR	51.14
					15	TSSAEMPTIPLGSAVEAIR	43.86
					16	GVYSEETLR	53.97
OPA1_RAT	Dynamin-like 120 kDa protein, mitochondrial	939.55	16	21.0	1	DFFTAGTPGETAFR	62.86
					2	IDQLQEELLHTQLK	40.69
					3	TSVLEMIAQAR	83.2
					4	EFDLTKEEDLAALR	38.21
					5	EGCTVSPETISLNVK	32.34
					6	SIVTDLVSQMDPHGR	81.93
					7	ALGYFAVVTGK	80.43
					8	GNSSESIEAIR	49.1
					9	EYEEEFFQNSK	69.31
					10	NLSLAVSDCFWK	72.07
					11	ESVEQQADSFK	43.23
					12	FNLETEWK	38.95
					13	AVEVAWETLQDEFSR	82.42
					14	VNDEHPAYLASDEITTVR	51.92
					15	MLAITANTLR	61.99

					16	EVLEDFAEDGEK	50.9
TBA4A_RAT	Tubulin alpha-4A chain	1119.14	16	46.2	1	TIGGGDDSFTTFFCETGAGK	105.03
					2	AVFVDLEPTVIDEIR	98.87
					3	QLFHPEQLITGK	48.01
					4	QLFHPEQLITGKEDAANNYAR	49.8
					5	QLFHPEQLITGKEDAANNYAR	33.23
					6	EIIDPVLDR	37.21
					7	LISQIVSSITASLR	74.82
					8	FDGALNVDLTEFQTNLVPYPR	76.91
					9	IHFPLATYAPVISAEK	72.97
					10	AYHEQLSVAEITNACFEPANQMVK	35.43
					11	YMACCLLYR	38.23
					12	DVNAAIAAIK	65.78
					13	SIQFVDWCPTGFK	80.74
					14	VGINYQPPTVVPGGDLAK	91.54
					15	AVCMLSNTTAIAEAWAR	118.56
					16	AVCMLSNTTAIAEAWAR	92.01
CN37_RAT	2',3'-cyclic-nucleotide 3'-phosphodiesterase	855.44	15	28.6	1	ADFSEEYK	41.23
					2	RLDEDLAGYCR	57.96
					3	LDEDLAGYCR	73.47
					4	VLVLDDTNHER	47.53
					5	EKNQWQLSLDDLK	48.76
					6	NQWQLSLDDLK	55.15
					7	NQWQLSLDDLKK	45.29
					8	DFLPLYFGWFLTK	71.26
					9	KAGQVFLEELGNHK	46.18
					10	AGQVFLEELGNHK	88.75
					11	EKLDLVSYFGK	35.95
					12	LDLVSYFGK	41.03
					13	ATGAEEYAQQDVVR	74.96
					14	LSISALFVTPK	47.94
					15	GGSQGEEVGELPR	79.98
EFTU_RAT	Elongation factor Tu, mitochondrial	908.38	15	38.7	1	DKPHVNVGTIGHVDHGK	32.7
					2	KYEEIDNAPEER	74.82
					3	YEEIDNAPEER	67.13
					4	GITINAAHVEYSTAAR	91.44
					5	QIGVEHVVVYVNK	53.29
					6	QIGVEHVVVYVNK	54.97
					7	ELLTEFGYK	32.32
					8	GEETPVIVGSALCALEQR	92.91
					9	LLDAVDTYIPVPTR	63.2
					10	GTVVTGTLER	52.92
					11	TVVTGIEMFHK	48.69
					12	AEAGDNLGALVR	82.86

					13	GLVMVKPGSIQPHQK	36.98
					14	VEAQVYILSK	57.52
					15	TIGTGLVTDVPAMTEEDK	66.63
QCR2_RAT	Cytochrome b-c1 complex subunit 2, mitochondrial	1002.92	15	36.3	1	TSAPGGVPLQPQELEFTK	63.54
					2	LPNGLVIASLENYAPLSR	86.51
					3	YENYNYLGTSHLLR	97.41
					4	RWEVAALR	41.19
					5	AVAFQNPQTR	53.05
					6	IIENLHDVAYK	69.11
					7	NALANPLYCPDYR	68.29
					8	MALVGLGVSHSILK	45.06
					9	MALVGLGVSHSILK	75.71
					10	EVAEQFLNIR	81.13
					11	RGNNTTSLLSQSVAK	49.95
					12	GNNTTSLLSQSVAK	86.94
					13	AVAQGNLSSADVQAAK	90.15
					14	SMTASGNLGHTPFLDEL	46.38
					15	SMTASGNLGHTPFLDEL	48.5
TBA1C_RAT	Tubulin alpha-1C chain	1016.1	15	43.9	1	TIGGGDDSFNTFFSETGAGK	85.98
					2	AVFVDLEPTVIDEVR	89.63
					3	QLFHPEQLITGK	48.01
					4	QLFHPEQLITGKEDAANNYAR	49.8
					5	QLFHPEQLITGKEDAANNYAR	33.23
					6	EIIDLVLDR	52.61
					7	LADQCTGLQGFLVFHSFGGGTGSGFTSLLMER	39.52
					8	LISQIVSSITASLR	74.82
					9	FDGALNVDLTEFQTNLVPYPR	76.91
					10	IHFPLATYAPVISAEK	72.97
					11	YMACCLLYR	38.23
					12	DVNAAIATIK	68.56
					13	TIQFVDWCPTGFK	75.26
					14	AVCMLSNTTAIAEAWAR	118.56
					15	AVCMLSNTTAIAEAWAR	92.01
AT1A2_RAT	Sodium/potassium-transporting ATPase subunit alpha-2	934.96	14	17.7	1	DGPNALTPPPTTPEWVK	40.59
					2	NMVPQQALVIR	36.66
					3	VDNSSLTGESEPQTR	86.49
					4	NLEAVETLGSTSTICSDK	115.86
					5	DTAGDASESALLK	71.68
					6	VLGFCQLNLPSGK	47.33
					7	FDTDELNFPTEK	36.91
					8	VIMVTGDHPITAK	57.94
					9	GVGIISEGNETVEDIAAR	114.14
					10	LNIPVSQVNPR	43.34
					11	DMTSEQLDEILR	65.08

					12	LIIVEGCQR	49.5
					13	QGAIVAVTGDGVNDSPALK	97.79
					14	QGAIVAVTGDGVNDSPALK	71.65
CLH_RAT	Clathrin heavy chain 1	839.92	14	11.1	1	TLQIFNIEMK	41.88
					2	WLLLTGISAQQNR	81.86
					3	VVGAMQLYSVDR	71.28
					4	NNLAGAEELFAR	96.86
					5	FNALFAQGNYSEAAK	37.07
					6	VIQCFAETGQVQK	63.47
					7	GQFSTDELVAEVEK	56.48
					8	LLLPWLEAR	46.5
					9	IYIDSNNNPER	46.48
					10	GQCDLELINVCNENSLFK	31.3
					11	NLQNLLILTAIK	73.79
					12	LLYNNVSNFGR	49.2
					13	LASTLVHLGEYQAAVDGAR	47.39
					14	TSIDAYDNFDNISLAQR	96.36
LPPRC_RAT	Leucine-rich PPR motif-containing protein, mitochondrial	800.54	14	12.6	1	SGSQFDWALMR	40.19
					2	SGSPGSNQALLLLR	57.24
					3	LIAAYCSVGDIEGASK	83.69
					4	DETSSSFGSFFLR	80.1
					5	NVQGIIDILK	47.47
					6	STTFAQAEVR	35.03
					7	SMNIDLWSK	30.41
					8	TSQFTSSDLESTLEK	117.81
					9	SSLSSSSPSAGDTVTEK	49.35
					10	AALDLEQVPSELAVTR	31.46
					11	LIQALALQGDVK	84.85
					12	GLDAIELSR	42.82
					13	MVFINNIALAQMK	58.99
					14	TLLELIPELR	41.13
AINX_RAT	Alpha-internexin	834.31	13	32.3	1	SFGSEHYLCSASSYR	70.39
					2	SNVASTAACSSASSLGLGLAYR	104.41
					3	RLPASDGLDLSQAAAR	34.49
					4	LPASDGLDLSQAAAR	86.35
					5	ALEAELAALR	77.17
					6	DGLAEEVQR	30.5
					7	KVESLLDELAFVR	78.46
					8	NLQSAEEWYK	40.71
					9	FANLNEQAAR	70.54
					10	TIEIEGLR	39.58
					11	HSAEVAGYQDSIGQLESDLR	50.76
					12	VGESFEETLEETVVSTK	81.32
					13	STIEEITTSSSQK	69.63

ODPB_RAT	Pyruvate dehydrogenase E1 component subunit beta, mitochondrial	785.67	13	34.8	1	EAINQGMDEELER	53.33
					2	EAINQGMDEELERDEK	47.4
					3	VFLLGEEVAQYDGAYK	93.55
					4	TYYMSAGLQPVPIVFR	74.06
					5	TYYMSAGLQPVPIVFR	68.17
					6	VVSPWNSEDAK	42.03
					7	EGIECEVINLR	73.79
					8	TIRPMDIEAIEASVMK	46.5
					9	IMEGPAFNFLDAPAVR	74.51
					10	IMEGPAFNFLDAPAVR	53.29
					11	VTGADVPMPYAK	53.45
					12	VTGADVPMPYAK	39.59
					13	ILEDNSIPQVK	66
SYGP1_RAT	Ras GTPase-activating protein SynGAP	702.81	13	14.7	1	AGYVGLVTVPVATLAGR	59.06
					2	YQTMSILPMELYK	36.44
					3	MLCAVLEPALNVK	68.13
					4	GKEEVASALVHILQSTGK	35.3
					5	ALYESEENCEVDPIK	57.48
					6	LISASLFLR	54.34
					7	LLSDISTALR	45.62
					8	DLNSSIDLQSFMAR	33.69
					9	SSPAYCTSSSDITEPEQK	49.26
					10	SVSMLDLQGDGPGGR	67.8
					11	LSQGSGSSITAAGMR	75.17
					12	LSQMGVTTDGVPAQQLR	89.77
					13	QHSQTPSTLNPTMPASER	30.75
DYN1_RAT	Dynamin-1	605.7	12	17.1	1	GMEDLIPLVNR	33.6
					2	SSVLENFVGR	50.2
					3	LEIEAETDR	44.78
					4	VPVGDQPPDIEFQIR	40.63
					5	DMLMQFVTK	47.5
					6	LDLMDEGTDAR	53.02
					7	LQSQLLSIEK	48.48
					8	IEGSGDQIDTYELSGGAR	93.12
					9	TGLFTPDLAFEATVK	40.94
					10	TSGNQDEILVIR	57.66
					11	QLELACETQEEVDSWK	40.32
					12	NLVDSYMAIVNK	55.45
GLSK_RAT	Glutaminase kidney isoform, mitochondrial	649.76	12	25.5	1	GGTPPQQQQQQQQQPGASPPAAPGPK	35.58
					2	CVQSNIVLLTQAFR	67.2
					3	VADYIPQLAK	35.22
					4	FSPDLWGVSVCTVDGQR	82.34
					5	YAIAVNDLGTEYVHR	66.56
					6	FDYVMQFLNK	58.45

					7	MAGNEYVGFSNATFQSER	91.21
					8	NFAIGYYLK	31.32
					9	FALSAMDMEQR	37.04
					10	FALSAMDMEQR	65.56
					11	TALHVAAAEGHVEVVK	46.85
					12	ILQEYQVQYTPQGDSDDGKENQTVHK	32.43
ODO1_RAT	2-oxoglutarate dehydrogenase, mitochondrial	539.16	12	13.5	1	SWDIFFR	41.9
					2	NTNAGAPPGTAYQSPLSLSR	49.26
					3	LVEDHLAVQSLIR	52.88
					4	FEEFLQR	30.89
					5	FGLEGCEVLIPALK	46.01
					6	LNVLANVIR	41.85
					7	ELEQIFCQFDSK	52.62
					8	SSPYPTDVAR	36.11
					9	DVVVDLVCYR	65.79
					10	VIPEDGPAAQNPDK	36.13
					11	DMAEEVAITR	47.21
					12	FLDTAFDLDAFK	38.51
DHSA_RAT	Succinate dehydrogenase [ubiquinone] flavoprotein subunit, mitochondrial	526.68	11	23.3	1	AAFGLSEAGFNTACLTK	78.46
					2	NTIIATGGYGR	51.7
					3	TYFSCTSAHTSTGDGTAMVTR	42.94
					4	GEGGILINSQGER	58.92
					5	LGANSLLDLVVFGR	32.76
					6	ANAGEESVMNLDK	54.27
					7	VGSVLQEGCEK	41.04
					8	VSQLYGDLQHLK	46.16
					9	IDEYDYSKPIEGQQK	44.57
					10	VTLDYRPVIDK	38.79
					11	TLNEADCATVPPAIR	37.07
DYHC1_RAT	Cytoplasmic dynein 1 heavy chain 1	642.57	11	3.0	1	LNTQEIFDDWAR	48.07
					2	LAETVFNFQEK	34.09
					3	DSAIQQQVANLQMK	57.38
					4	VQVALEELQDLK	53.43
					5	INEWLTLVEK	65.81
					6	LGGSPFGPAGTGK	31.05
					7	IQFVGACNPPTDPGR	43.5
					8	DLFQVAFNR	72.92
					9	VQGLTVEQAEAVAR	78.98
					10	SACDTVDTWLDDTAK	78.28
					11	VLLTTQGVDMISK	79.06
KCC2A_RAT	Calcium/calmodulin-dependent protein kinase type II subunit alpha	698.01	11	30.5	1	FTEEYQLFEELGK	106.18
					2	VLAGQEYAAK	35.31
					3	DLKPENLLLASK	35.65
					4	AGAYDFPSPEWDTVTPEAK	66.66

					5	GAILTTMLATR	48.84
					6	GAILTTMLATR	78.72
					7	ESSESTNTTIEDEDTK	66.91
					8	VTEQLIEAISNGDFESYTK	59
					9	MCDPGMTAFEPEALGNLVEGLDFHR	47.83
					10	FYFENLWSR	64.23
					11	ITQYLDAGGIPR	88.68
MDHM_RAT	Malate dehydrogenase, mitochondrial	570.19	11	43.5	1	VAVLGASGGIGQPLSLLLK	50.71
					2	GYLGPEQLPDCLK	35.32
					3	GCDVVVIPAGVPR	64.46
					4	IFGVTTLDIVR	57.39
					5	TIIPLISQCTPK	46.19
					6	VDFPQDQLATLTGR	50.27
					7	AGAGSATLSMAYAGAR	79.25
					8	FVFSLVDAMNGK	44.44
					9	EGVIECSFVQSK	37.98
					10	ETECTYFSTPLLLGK	61.54
					11	MIAEAIPELK	42.64
MPCP_RAT	Phosphate carrier protein, mitochondrial	607.54	11	41.0	1	YYALCGFGGVLSCGLTHTAVVPLDLVK	64.17
					2	GIFNGFSITLK	59.05
					3	GWAPTLIGYSMQGLCK	51.45
					4	GWAPTLIGYSMQGLCK	75.97
					5	FGFYEVFK	37.69
					6	ALYSNILGEENTYLWR	67.91
					7	IQTQPGYANTLR	59.51
					8	MYKEEGLNAFYK	46.49
					9	MYKEEGLNAFYK	60.26
					10	AEQLVVTFVAGYIAGVFCAIVSHPADSVVSVLNK	31.37
					11	GSTASQVLQR	53.67
MYO5A_RAT	Myosin-Va	604.05	11	7.5	1	NQSIIVSGESGAGK	70.12
					2	VLASNPIMESIGNAK	76.38
					3	LGILDLLDEECK	63.67
					4	VEYQCEGFLEK	36.6
					5	ACGVLETIR	41.06
					6	WTYQEFFSR	52.69
					7	LTNLEGVYNSETEK	58.61
					8	NTMTDSTILLEDVQK	40.66
					9	LTNENLDLMEQLEK	69.01
					10	YNVSQLEEWLR	61.81
					11	VLNLYTPVNEFEER	33.44
NDUA9_RAT	NADH dehydrogenase [ubiquinone] 1 alpha subcomplex subunit 9, mitochondrial	536.97	11	33.4	1	SSVSGVVATVFGATGFLGR	41.98
					2	MGSQVIIPYR	65.78
					3	AVQHSNVVINLIGR	81.38
					4	NFDFEDVFVNIPR	60.1

					5	FIHVSHLNASMK	34.01
					6	FLNHFANYR	31.47
					7	WFLAVPLVSLGFK	32.84
					8	QPVYVADVSK	51.32
					9	QPVYVADVSK	45.89
					10	LFGLSPFEPWTTK	39.1
					11	WLSSEIEETKPAK	53.1
NFL_RAT	Neurofilament light polypeptide	592.5	11	23.4	1	SSFSYEPYFSTSYK	36.54
					2	SAYSSYSAPVSSSLSVR	90.54
					3	VLEAELLVLR	66.84
					4	ALYEQEIR	30.29
					5	EGLEETLR	31.92
					6	YEEEVLSR	37.79
					7	IDSLMDEIAFLK	57.1
					8	NMQNAEEWFK	51.68
					9	FTVLTESAAK	40.73
					10	QNADISAMQDTINK	53.92
					11	SAYSGLQSSSYLMSAR	95.15
ODPA_RAT	Pyruvate dehydrogenase E1 component subunit alpha, somatic form, mitochondrial	548.66	11	28.2	1	NFANDATFEIK	30.05
					2	LEEGPPVTTVLTR	65.42
					3	AILAELTGR	34.79
					4	LPCIFICENNR	39.92
					5	YGMGTSVER	46.62
					6	RGDFIPGLR	30.57
					7	VDGMDILCVR	69.62
					8	VDGMDILCVR	53.74
					9	GPILMELQTYR	58.45
					10	YHGHSMSDPGVSYR	39.48
					11	MVNSNLASVEELK	80
SYT1_RAT	Synaptotagmin-1	678.49	11	27.1	1	TLNPVFNEQFTFK	57.86
					2	TLVMAVYDFDR	65.76
					3	HDIIGEFK	34.4
					4	VPMNTVDFGHVTEEWR	64.12
					5	LGDICFSLR	74.36
					6	LTVVILEAK	60.85
					7	KMDVGGLSDPYVK	37.88
					8	MDVGGLSDPYVK	66.29
					9	VQVVVTVLDYDK	68.25
					10	VFVGYNSTGAELR	89.31
					11	HWSDMLANPR	59.41
ACTC_RAT	Actin, alpha cardiac muscle 1	504.56	10	31.0	1	AGFAGDDAPR	81.35
					2	HQGVMVGMGQK	46.69
					3	DSYVGDEAQSK	54
					4	YPIEHGIITNWDDMEK	36.89

					5	IWHHTFYNELR	42.86
					6	DLTDYLMK	30.01
					7	SYELPDGQVITIGNER	86.93
					8	EITALAPSTMK	53.02
					9	EITALAPSTMK	41.54
					10	YSVWIGGSILASLSTFQQMWISK	31.27
GFAP_RAT	Glial fibrillary acidic protein	577.09	10	27.2	1	ALAAELNQLR	55.52
					2	LADVYQAELR	80.47
					3	DNLTQDLGTLR	64.04
					4	LEAENNLAVYR	59.64
					5	KVESLEEEIQFLR	43.49
					6	FADLTDVASR	61.54
					7	QLQALTCDLESLR	59.29
					8	LEEEGQSLKEEMAR	56.02
					9	LALDIEIATYR	39.13
					10	ITIPVQTFSNLQIR	57.95
K6PF_RAT	6-phosphofructokinase, muscle type	598.77	10	17.4	1	GITNLCVIGGDGSLTGADTFR	108.63
					2	SEWSDLLNDLQK	44.48
					3	TFVLEVMGR	42.1
					4	LPLMECVQVTK	34.46
					5	VLVVHDGFEGLAK	64.7
					6	GQIEEAGWSYVGGWTGQGGSK	89.32
					7	NLEQISANITK	50.13
					8	DLQVNVEHLVQK	58.65
					9	IFANTPDSGCVLGMR	55.53
					10	ALVFQPVTELK	50.77
K6PP_RAT	6-phosphofructokinase type C	582.86	10	18.9	1	SDQDSSTSSTSFPK	50.35
					2	AIGVLTSGGDAQGMNAAVR	112.22
					3	EWSGLLEELAK	51.39
					4	TFVLEVMGR	42.1
					5	ELVVTNLGFDTR	78.93
					6	LPLMECVQMTQDVQK	60.2
					7	SNCNVAIINVGAPAAGMNAAVR	32.22
					8	EIGWGDVGGWTGQGGSILGTK	36.59
					9	FVSDDSICVLGIQK	72.84
					10	YEASYDMSDVGK	46.02
SFXN1_RAT	Sideroflexin-1	542.08	10	37.9	1	WDQSTFIGR	51.61
					2	NILLTNEQLENAR	81.36
					3	QGIVPAGLTENELWR	47.09
					4	QGIVPAGLTENELWR	51.92
					5	YAYDSAFHPDTGEK	55.42
					6	TTPAVLFWQWINQSFNAVVNYTNR	30.46
					7	FVPFAAVAAANCINIPLMR	36.75
					8	QAITQVVISR	66.88

					9	QAITQVVISR	46.67
					10	SSMSVTSLEDDLQASIQK	73.92
SRCN1_RAT	SRC kinase signaling inhibitor 1	473.53	10	12.3	1	FALAWWER	43.35
					2	SPGVLFLQFGEETR	63.49
					3	NVFYELEDVR	53.31
					4	LGGAPTSQGVSPSPSAILER	47.08
					5	AGAGGPLYGDGYGFR	35.11
					6	STGASTAGAPPSELFPGPGER	39.44
					7	SSGATPVSGPPPPAVSSTPAGQPTAVSR	41.99
					8	GLQNSASDLR	42.54
					9	VVTDTLAQIR	60.39
					10	LLEETQAELLK	46.83
ATPG_RAT	ATP synthase subunit gamma, mitochondrial	472.75	9	34.4	1	VYGTGSLALYEK	67.64
					2	HLIIGVSSDR	43.85
					3	GLCGAIHSSVAK	43.13
					4	NDMAALTAAGK	76.15
					5	EVMIVGIGEK	38.47
					6	EVMIVGIGEK	37.48
					7	THSDQFLVSFK	46.75
					8	NASDMIDKLTLTFNR	77.86
					9	ELIEIISGAAALD	41.42
G3P_RAT	Glyceraldehyde-3-phosphate dehydrogenase	671.7	9	27.9	1	VIISAPSADAPMFVMGVNHEK	44.53
					2	IVSNASCTTNCLAPLAK	87.74
					3	GAAQNIIPASTGAAK	103.83
					4	VPTPNVSVVDLTCR	92.56
					5	LISWYDNEYGYSNR	77.26
					6	VVDLMAYMASK	81.3
					7	VVDLMAYMASK	63.95
					8	VVDLMAYMASK	71.74
					9	VVDLMAYMASKE	48.79
GNAO_RAT	Guanine nucleotide-binding protein G(o) subunit alpha	501.48	9	28.2	1	IIHEDGFSGEDVK	50.91
					2	AMDTLGVEYGDK	57.66
					3	AMDTLGVEYGDKER	83.28
					4	MVCDVVSR	46.35
					5	MEDTEPFSAELLSAMMR	49.54
					6	LWGDSGIQECFNR	68.46
					7	YYLDSLDR	38.7
					8	IGAADYQPTEQDILR	61.05
					9	TTGIVETHFTFK	45.53
IDH3A_RAT	Isocitrate dehydrogenase [NAD] subunit alpha, mitochondrial	455.6	9	27.9	1	APIQWEER	63.7
					2	NVTAIQGPGGK	39.55
					3	TPIAAGHPSMNLLLR	39.22
					4	TPYTDVNIVTIR	65.84
					5	IAEFAFEYAR	49.68

					6	MSDGLFLQK	38.04
					7	DMANPTALLLSAVMMLR	33.53
					8	IEAACFATIK	67.45
					9	CSDFTEEICR	58.59
KCC2B_RAT	Calcium/calmodulin-dependent protein kinase type II subunit beta	578.54	9	18.6	1	FTDEYQLYEDIGK	86.31
					2	DLKPENLLLASK	35.65
					3	AGAYDFPSPEWDTVTPEAK	66.66
					4	NLINQMLTINPAK	63.76
					5	GAILTTMLATR	48.84
					6	GAILTTMLATR	78.72
					7	QTTAPATMSTAASGTTMGLVEQAK	61.33
					8	QTTAPATMSTAASGTTMGLVEQAK	89.94
					9	FYFENLLAK	47.33
LETM1_RAT	LETM1 and EF-hand domain-containing protein 1, mitochondrial	416.21	9	16.9	1	LEEGGPVYSPPAQVVVK	39.85
					2	FLQDTIEEMALK	53.51
					3	DFSAFFQK	34.23
					4	LLELQSIGTNNFLR	63.03
					5	LISEEGVDSLTVK	65.04
					6	AMYLPDTLSPADQLK	62.49
					7	STLQTLPEIVAK	34.58
					8	DIQPEVAEATVPGRPGAELQPK	31.91
					9	LISLTSALDENK	31.57
MAP2_RAT	Microtubule-associated protein 2	436.38	9	7.6	1	VTEGSQPFAPVFFQSDDK	51.96
					2	STGLGSDYYELSDSR	44.58
					3	VTGGQTTQVETSSESPFPAK	82.25
					4	DLATDLSLIEVK	42.3
					5	VSDFGQMASGMSVDAGK	46.79
					6	ETSPETSLIQDEVALK	34.66
					7	SDTLQITDLLVPGSR	32.63
					8	SILTEQLETIPK	38.95
					9	TTATSGESAQAPSAFK	62.26
NDUAA_RAT	NADH dehydrogenase [ubiquinone] 1 alpha subcomplex subunit 10, mitochondrial	509.55	9	25.6	1	YGLLASILGDK	70.76
					2	VITVDGNICSGK	56.03
					3	LQSWLYASR	43.77
					4	SIYSDFVFLEAMYNQGFIR	52.89
					5	VTSAYLQDIEDAYK	70.53
					6	VTSAYLQDIEDAYKK	58.2
					7	VVEDIEYLNYNK	75.7
					8	KYAPGYNADVGDK	35.06
					9	YAPGYNADVGDK	46.61
NDUV2_RAT	NADH dehydrogenase [ubiquinone] flavoprotein 2, mitochondrial	556.71	9	48.8	1	DTPENNPDTPFDFTPENYER	69.05
					2	AAAVLPVLDLAQR	59.5
					3	QNGWLPISAMNK	59.29
					4	VAEVLQVPPMR	48.82

					5	VYEVATFYTMYNR	85.33
					6	YHIQVCTTTPCMLR	31.1
					7	DSDSILETLQR	59.01
					8	DIEEIIDELR	77.32
					9	FCCEPAGGLTSLTEPPK	67.29
ODP2_RAT	Dihydrolipoyllysine-residue acetyltransferase component of pyruvate dehydrogenase complex, mitochondrial	524.33	9	19.0	1	VPLPSLSPTMQAGTIAR	95.94
					2	DVPLGTPLCIIVEK	50.48
					3	DIDSFVPTK	45.31
					4	AAPAAAAAAPPGPR	43.89
					5	VAPTPAGVFIDIPISNIR	75.82
					6	ISVNDFIIK	31.09
					7	VPEANSSWMDTVIR	62.47
					8	GLETIASDVVSLASK	82.54
					9	YLEKPVTMLL	36.79
SFXN3_RAT	Sideroflexin-3	513.2	9	39.3	1	GDLPLNINIQEPR	60.16
					2	AGVVTPGLTEDQLWR	63.78
					3	YVYDSAFHPDTGEK	57.03
					4	TPTVVFWQWVNQSFNAIVNYSNR	39.79
					5	FVPFAAVAAANCINIPLMR	36.75
					6	ELQVGIPVTDEAGQR	61.06
					7	QGIFQVVVSR	47.96
					8	QGIFQVVVSR	71.07
					9	AQIQAQKPSIDVVYYNK	75.6
TBA8_RAT	Tubulin alpha-8 chain	660.14	9	23.2	1	QLFHPEQLITGK	48.01
					2	QLFHPEQLITGKEDAANNYAR	49.8
					3	QLFHPEQLITGKEDAANNYAR	33.23
					4	LISQIVSSITASLR	74.82
					5	FDGALNVDLTEFQTNLVPYPR	76.91
					6	TIQFVDWCPTGFK	75.26
					7	VGINYQPPTVVPGGDLAK	91.54
					8	AVCMLSNTTAIAEAWAR	118.56
					9	AVCMLSNTTAIAEAWAR	92.01
ACON_RAT	Aconitate hydratase, mitochondrial	425.92	8	14.5	1	IVYGHLDDPANQEIER	40.55
					2	VGLIGSCTNSSYEDMGR	83.78
					3	SQFTITPGSEQIR	47.9
					4	DGYAQILR	39.56
					5	FKLEAPDADELPR	30.29
					6	NAVTQEFGPVPDTAR	48.9
					7	WVVIGDENYGEGSSR	84.88
					8	QGLLPLTFADPSDYNK	50.06
ACSL6_RAT	Long-chain-fatty-acid--CoA ligase 6	412.48	8	15.1	1	RAEFLGSGLLQHDCK	34.41
					2	LVILMEPFDDALR	49.87
					3	VGFFQGDIR	49.87
					4	MIVTGAAPASPTVLGFLR	59.23

					5	LVDAEELNYWTSK	75.04
					6	SEPVAQIYVHGDSLK	43.53
					7	GIEGNYQELCK	50.53
					8	AILDDMVMLGK	50
AT2B1_RAT	Plasma membrane calcium-transporting ATPase 1	414.76	8	9.2	1	IQESYGDVYGICTK	46.28
					2	TSPNEGLSGNPADLER	52.51
					3	HLDACETMGNATAICSDK	31.95
					4	TVIEPMASEGLR	31.91
					5	MVTGDNINTAR	47.02
					6	GIIDSTVSEQR	54.53
					7	QVVAVTGDGTNDGPALK	95.34
					8	EASDIILTDDNFTSIVK	55.22
ATPO_RAT	ATP synthase subunit O, mitochondrial	417.5	8	47.9	1	LVRPPVQVYGIEGR	35.46
					2	YATALYSAASK	70.58
					3	VSLAVLNPYIK	67.23
					4	FSPLTANLMNLLAENGR	63.18
					5	LGNTQGVISAFSTIMSVHR	49.95
					6	TVLNSFLSK	40.17
					7	GQILNLEVK	46.38
					8	TDPSIMGGMIVR	44.55
GRP75_RAT	Stress-70 protein, mitochondrial	467.25	8	15.5	1	TTPSVVAFTPDGER	55.64
					2	QAVTNPNNTFYATK	41.17
					3	DAGQISGLNVLR	68.21
					4	VINEPTAAALAYGLDK	79.42
					5	AQFEGIVTDLIK	65.2
					6	SDIGEVILVGGMTR	56.97
					7	VQQTVQDLFGR	42.49
					8	QAASSLQQASLK	58.15
HXK1_RAT	Hexokinase-1	378.56	8	10.2	1	GDFIALDLGGSSFR	63.69
					2	IDEAVLITWTK	39.03
					3	HIDLVEGDEGR	36.03
					4	GAAMVTAVAYR	68.1
					5	QIEETLAHFR	31.38
					6	MISGMYLGEIVR	41.75
					7	CTVSFLLSEDGSGK	45.84
					8	GAALITAVGVR	52.74
KCC2G_RAT	Calcium/calmodulin-dependent protein kinase type II subunit gamma	458.67	8	18.6	1	FTDDYQLFEELGK	75.73
					2	DLKPENLLLASK	35.65
					3	AGAYDFPSPEWDTVTPEAK	66.66
					4	NLINQMLTINPAK	63.76
					5	GAILTTMLVSR	63.2
					6	QSSAPASPAASAAGLAGQAAK	32.45
					7	QSSAPASPAASAAGLAGQAAK	74.82
					8	FYFENLLSK	46.4

M2OM_RAT	Mitochondrial 2-oxoglutarate/malate carrier protein	474.09	8	28.3	1	TSFHALTSILK	43.31
					2	GIYTGLSAGLLR	81.44
					3	LGIYTVLFER	75.39
					4	LTGADGTPPGFLLK	65.34
					5	NVFNALIR	31.57
					6	EEGVPTLWR	40.04
					7	AVVVNAAQLASYSQSK	81.05
					8	YEGFFSLWK	55.95
MCCB_RAT	Methylcrotonoyl-CoA carboxylase beta chain, mitochondrial	485.1	8	20.8	1	LYGEEEVPAGGIITGIGR	60.4
					2	VSGVECMIVANDATVK	74.02
					3	LPCIYLVDSGGANLPR	89.78
					4	IFYNQAIMSSK	56.84
					5	FLYMWPNAR	41.26
					6	ISVMGGEQAATVLATVAR	44.29
					7	QFSSAEEAALKEPIIK	43.37
					8	LWDDGIIDPVDTR	75.14
MYH10_RAT	Myosin-10	395.98	8	5.4	1	QLLQANPILESFGNAK	37.8
					2	SDLLLEGFNNYR	47.11
					3	NTDQASMPENTVAQK	32.77
					4	ALELDPNLYR	40.42
					5	IAECSSQLAEEEEK	72.09
					6	ALEQQVEEMR	34.17
					7	TTLQVDTLNTELAAER	66.91
					8	ELDDATEANEGLSR	64.71
NDUS2_RAT	NADH dehydrogenase [ubiquinone] iron-sulfur protein 2, mitochondrial	436.56	8	17.9	1	LVLELSGEMVR	45.89
					2	LVLELSGEMVR	83.08
					3	TYLQALPYFDR	38.88
					4	MFEFYER	35.74
					5	IDEVEEMLTNNR	85.46
					6	GSGIQWDLR	53.53
					7	LYTEGYQVPPGATYTAIEAPK	43.54
					8	APGFAHLAGLDK	50.44
QCR1_RAT	Cytochrome b-c1 complex subunit 1, mitochondrial	456	8	16.7	1	NNGAGYFLEHLAFK	51.93
					2	EVESIGAHLNAYSTR	50.99
					3	LCTSATESEVTR	69.33
					4	NALISHLDGTTPVCEDIGR	75.27
					5	RIPLAEWESR	36.98
					6	IPLAEWESR	61.47
					7	IEEVDAQMVR	73.08
					8	IEEVDAQMVR	36.95
STXB1_RAT	Syntaxin-binding protein 1	468.6	8	15.5	1	VLVVDQLSMR	51.87
					2	LAEQIATLCATLK	70.68
					3	DNALLAQLIQDK	97.57
					4	SQLLILDR	37.46

					5	HIAEVSQEVTR	32.28
					6	VEQDLAMGTDAEGEK	53.56
					7	ISEQTYQLSR	49.34
					8	SSASFSTTAVSAR	75.84
BDH_RAT	D-beta-hydroxybutyrate dehydrogenase, mitochondrial	451.94	7	27.1	1	AVLVTGCDSGFGFSLAK	73.33
					2	GFLVFAGCLLK	63.23
					3	TIQLNVCNSEEVEK	62.81
					4	VVNISSMLGR	57.45
					5	FGVEAFSDCLR	52.32
					6	VSVVEPGNFIAATSLYSPER	89.47
					7	MWDELPEVVR	53.33
ECHB_RAT	Trifunctional enzyme subunit beta, mitochondrial	334.08	7	14.1	1	NIVVVEGVR	36.82
					2	IPFLLSGTSYK	43.03
					3	AALSGLLYR	41.27
					4	EAALGAGFSDK	44.93
					5	DQLLLGPTYATPK	65.04
					6	AMDSDWFAQNYMGR	36.16
					7	AMDSDWFAQNYMGR	66.83
LONM_RAT	Lon protease homolog, mitochondrial	324.87	7	9.4	1	QLEVEPEGLEPEAENK	47.5
					2	DIIALNPLYR	33.51
					3	ESVLQMMQAGQR	51.15
					4	HVMDVVDEELSK	53.7
					5	LALLDNHSSEFNVTR	42.26
					6	VLEFIAVSQLR	66.53
					7	AQLSATVLTLLIK	30.22
MBP_RAT	Myelin basic protein S	426.8	7	36.9	1	YLATASTMDHAR	54.87
					2	YLATASTMDHAR	60.9
					3	DTGILDSIGR	73.76
					4	TTHYGSLPQK	32.03
					5	TQDENPVVHFFK	74.65
					6	FSWGAEGQKPGFGYGGR	66.36
					7	GAYDAQGTLSK	64.23
MFN2_RAT	Mitofusin-2	429	7	12.5	1	NTELDPVTTEEQVLDVK	75.14
					2	STVINAMLWDK	69.64
					3	CTSFLVDELGVVDR	55.8
					4	AQGMPEGGGALAEGFQVR	77.19
					5	MFEFQNFER	41.73
					6	LIMDSLHIAAQEQR	64.78
					7	DNLEQEIAAMNK	44.72
MYPR_RAT	Myelin proteolipid protein	374.92	7	23.1	1	GLLECCAR	36.34
					2	LIETYFSK	34.63
					3	GLSATVTGGQK	57.51
					4	TSASIGSLCADAR	75.4
					5	MYGVLPWNAFPGK	45.57

					6	MYGVLPWNAFPGK	72.41
					7	VCGSNLLSICK	53.06
PCCA_RAT	Propionyl-CoA carboxylase alpha chain, mitochondrial	332.54	7	12.2	1	MADEAVCVGPAPTSK	47.77
					2	FSSQEAASSFGDDR	76.86
					3	VVEEAPSIFLDPETR	54.47
					4	NFYFLEMNTR	33.41
					5	QEDIPISGWAVECR	35.43
					6	MEDALDSYVIR	48.06
					7	FLSDVYPDGFK	36.54
RAB3A_RAT	Ras-related protein Rab-3A	374.97	7	28.6	1	ESSDQNFDYMFK	53.42
					2	ILIIGNSSVGK	42.97
					3	QLADHLGFEFFEASAK	41.65
					4	QLADHLGFEFFEASAK	36.86
					5	LVDVICEK	33.3
					6	MSESLDTADPAVTGAK	91.53
					7	MSESLDTADPAVTGAK	75.24
SFXN5_RAT	Sideroflexin-5	349.67	7	32.2	1	ADTATTASAASAAASASNASSDAPPFQLGKPR	49.75
					2	FQQTSFYGR	38.83
					3	HFLDIIDPR	32.38
					4	EAVQLLEDYK	61.05
					5	HGTLRPGVTNEQLWSAQK	36.32
					6	YGELEEGIDVLDADGNLVGSSK	94.76
					7	HALLETALTR	36.58
SYT2_RAT	Synaptotagmin-2	384.72	7	17.8	1	TLVMAIYDFDR	45.14
					2	VPMNTVDLGQPIEEWR	65.06
					3	KMDVGGLSDPYVK	37.88
					4	MDVGGLSDPYVK	66.29
					5	VQVVVTVLDYDK	68.25
					6	IFVGSNATGTELR	42.69
					7	HWSDMLANPR	59.41
THIL_RAT	Acetyl-CoA acetyltransferase, mitochondrial	501.3	7	23.3	1	TPIGSFLGSLASQPATK	81.56
					2	LGTIAIQGAIEK	61.03
					3	EVYMGNVIQGGEGQAPTR	105.52
					4	QATLGAGLPIATPCTTVNK	53.91
					5	QATLGAGLPIATPCTTVNK	83.93
					6	FANEITPITISVK	71.6
					7	VNVHGGAVSLGHPIGMSGAR	43.75
TOM70_RAT	Mitochondrial import receptor subunit TOM70	344.53	7	16.9	1	ASPALGSGPDGSGDSLEMSSLDR	82.52
					2	YEQAIQCYTEAISLCPTEK	57.24
					3	NREPLMPSPQFIK	40.88
					4	YMAEALLLR	37.92
					5	QAYTANNSSQVQAAMK	51.76
					6	CIDLEPDNATTYVHK	33.78
					7	GLLQLQWK	40.43

VDAC3_RAT	Voltage-dependent anion-selective channel protein 3	441.01	7	32.5	1	CSTPTYCDLGK	43.64
					2	VCNYGLIFTQK	51
					3	WNTDNTLGTEISWENK	57.07
					4	LTVDTIFVPNTGK	62.58
					5	LCQNNFALGYK	77.22
					6	VNNASLIGLGYTQSLRPGVK	77.39
					7	LTLSALVDGK	72.11
WDR7_RAT	WD repeat-containing protein 7	353.97	7	6.4	1	ISPDWISSMSIIR	32.2
					2	LPASCLPASDSFR	46.72
					3	TTTCISLQDAFDK	67.05
					4	LQTLATNLLASEASDK	63.88
					5	DSPPASSNIVQGQIK	43.85
					6	EAAQALLLAELR	47.44
					7	GPITAVSFAPDGR	52.83
AOFA_RAT	Amine oxidase [flavin-containing] A	332.17	6	13.7	1	INVLVLEAR	64.22
					2	WVDVGGAYVGPTQNR	101.12
					3	EIPVDAPWQAR	38.25
					4	YVISAIPPILTAK	43.59
					5	DIWVEEPESK	35.39
					6	DVPAIEITHTFLER	49.6
ATP5H_RAT	ATP synthase subunit d, mitochondrial	283.46	6	52.2	1	TIDWVSFVEIMPQNQK	31.27
					2	LASLSEKPPAIDWAYYR	33.48
					3	ANVDKPGLVDDFK	48.28
					4	YTALVDAEEKEDVK	68.66
					5	NCAQFVTGSQAR	63.15
					6	YPYWPHQPIENL	38.62
BSN_RAT	Protein bassoon	232.94	6	2.1	1	AQGLSGQEAEGPR	34.3
					2	ATSVPGPTQATAPPEVGR	46.08
					3	QVEQAVQTAPYR	30.87
					4	YLGQGLQYGSFTDLR	53.03
					5	DACEPESGPDPSTVR	36.65
					6	YLELGITQR	32.01
DLG4_RAT	Disks large homolog 4	310.26	6	11.6	1	NTYDVVYLK	38.08
					2	EQLMNSSLGSGTASLR	73.12
					3	DCGFLSQALSFR	76.52
					4	FIEAGQYNSHLYGTSVQSVR	34.62
					5	HCILDVSANAVR	38.65
					6	VIEDLSGPYIWVPAR	49.27
DPYL2_RAT	Dihydropyrimidinase-related protein 2	257.25	6	12.2	1	QIGENLIVPGGVK	32.77
					2	QIGENLIVPGGVK	32.4
					3	SITIANQTNCPLYVTK	58.7
					4	SAAEVIAQAR	46.97
					5	IVLEDGTLHVTEGSGR	35
					6	GLYDGPVCEVSVTPK	51.41

ETFA_RAT	Electron transfer flavoprotein subunit alpha, mitochondrial	361.18	6	27.3	1	LGGEVSCLVAGTK	64.47
					2	LNVAPVSDIIEIK	42.4
					3	TIYAGNALCTVK	49.51
					4	GTSFEAAAASGGSASSEK	88.12
					5	APSSSSAGISEWLDQK	64.22
					6	AAVDAGFVPNDMQVGQTGK	52.46
HCD2_RAT	3-hydroxyacyl-CoA dehydrogenase type-2	361.99	6	37.9	1	GLVAVITGGASGLGLSTAK	76.74
					2	LVGQGATAVLLDVPNSEGETEAK	54.97
					3	LGGNCIFAPANVTSEK	38.96
					4	LVAGVMGQNEPDQGGQR	61.79
					5	GGIVGMTLPIAR	55.81
					6	NFLASQVPFPSR	73.72
IDHG1_RAT	Isocitrate dehydrogenase [NAD] subunit gamma 1, mitochondrial	280.76	6	24.9	1	HTVTMIPGDGIGPELMLHVK	44.42
					2	HACVPVDFEEVHVSSNADEEDIR	35.42
					3	TSLDLYANVIHCK	52.72
					4	DIDILIVR	46.62
					5	ENTEGEYSSLEHESVAGVVESLK	34.85
					6	LGDGLFLQCCR	66.73
K1C10_RAT	Keratin, type I cytoskeletal 10	302.49	6	11.6	1	VTMQNLNDR	53.11
					2	LKYENEVALR	32.87
					3	QSVEADINGLR	46.46
					4	DAEAWFNEK	32.18
					5	QSLEASLAETEGR	85.4
					6	LENEIQTYR	52.47
KCC2D_RAT	Calcium/calmodulin-dependent protein kinase type II subunit delta	321.47	6	12.8	1	FTDEYQLFEELGK	55.86
					2	DLKPENLLLASK	35.65
					3	AGAYDFPSPEWDTVTPEAK	66.66
					4	GAILTTMLATR	48.84
					5	GAILTTMLATR	78.72
					6	ENFSGGTSLWQNI	35.74
KPCG_RAT	Protein kinase C gamma type	331.97	6	11.5	1	QGLQCQVCSFVVHR	56.36
					2	APTSDEIHITVGEAR	34.23
					3	LSVEVWDWDR	51.48
					4	FEACNYPLELYER	54.21
					5	DVIVQDDDVDCTLVEK	101.87
					6	LGSGPDGEPTIR	33.82
MAP1A_RAT	Microtubule-associated protein 1A	285.76	6	2.6	1	SIEEACLTLQHLNR	37.8
					2	LGIQAEPLYR	37.97
					3	LDMYVLNPVK	65.62
					4	SSLLLDTVTSIPSSR	42.88
					5	DTDLQQTQATEPR	55.75
					6	AVLDALLEGK	45.74
MAP6_RAT	Microtubule-associated protein 6	549.93	6	16.2	1	AVAIETQPAQGESDAVAR	85.66
					2	SGLGLGAASGSTSGSGPADSVMR	108.4

					3	DPEGAGGAGVPAAGK	55.48
					4	AGPAWMVTR	41.28
					5	TEGHEEKPLPPAQSQTQEGGPAAGK	35.92
					6	EEVTSTVSSSYR	63.43
NFM_RAT	Neurofilament medium polypeptide	302.7	6	7.1	1	SYTLDSLGNPSAYR	61.81
					2	QASHAQLGDAYDQEIR	78.08
					3	QASHAQLGDAYDQEIR	34.39
					4	LRDDTEAAIR	31.63
					5	VQSLQDEVAFLR	65.13
					6	SIELESVR	31.66
PYC_RAT	Pyruvate carboxylase, mitochondrial	310.3	6	7.0	1	ADFAQACQDAGVR	61.2
					2	GANAVGYTNYPDNVVFK	46.81
					3	GTPLDTEVPLER	30.79
					4	VFDYSEYWEGAR	55.35
					5	AEAEAQAEELSFPR	55.87
					6	DFTATFGPLDSLNTR	60.28
RP3A_RAT	Rabphilin-3A	271.27	6	14.6	1	KQEELTDEEKEIINR	40.95
					2	TKPQQPAGEPATQEQPTPESR	45.48
					3	TGPTGGFQAAPHTAGPYSQAAPAR	39.84
					4	GMALYEEEQVER	43.16
					5	SLDISVWDYDIGK	31.53
					6	SNDYIGGCQLGISAK	70.31
SAM50_RAT	Sorting and assembly machinery component 50 homolog	267.22	6	16.4	1	VTGQFPWSSLR	53.08
					2	GVSAEYSFPLCK	48.4
					3	SSLSHAMVIDSR	41.18
					4	FYLGGPTSVR	43.1
					5	THFFLNAGNLCNLNYGEGPR	42.82
					6	ICDGVQFGAGIR	38.64
SV2A_RAT	Synaptic vesicle glycoprotein 2A	369.66	6	9.0	1	FEEEEDDDDFPAPADGYYR	97.81
					2	MADGAPLAGVR	49.51
					3	GGLSDGEGPPGGR	68.8
					4	DREELAQQYETILR	44.97
					5	EELAQQYETILR	63.6
					6	HLQAVDYAAR	44.97
VDAC2_RAT	Voltage-dependent anion-selective channel protein 2	370.87	6	28.8	1	SCSGVEFSTSGSSNTDTGK	84.43
					2	WCEYGLTFTEK	53.4
					3	LTFDTTFSPNTGK	84.72
					4	YQLDPTASISAK	34.43
					5	VNNSSLIGVGYTQTLRPGVK	41.78
					6	LTLSALVDGK	72.11
VPP1_RAT	V-type proton ATPase 116 kDa subunit a isoform 1	305.23	6	8.9	1	ANIPIMDTGENPEVPFPR	35.01
					2	NFLELTELK	40.64
					3	LGFVAGVINR	63.91
					4	SVFIIFFQGDQLK	79.41

					5	ASLYPCPETPQER	31.41
					6	MQTNQTPPTYNK	54.85
AATM_RAT	Aspartate aminotransferase, mitochondrial	260.26	5	12.6	1	MNLGVGAYR	34.18
					2	FVTVQTISGTGALR	87.88
					3	DAGMQLQGYR	40.48
					4	VGAFTVVCK	42.51
					5	IAATILTSPDLR	55.21
AT2B2_RAT	Plasma membrane calcium-transporting ATPase 2	317.53	5	6.2	1	IDESSLTGESDQVR	107.94
					2	HLDACETMGNATAICSDK	31.95
					3	MVTGDNINTAR	47.02
					4	QVVAVTGDGTNDGPALK	95.34
					5	EASDIILTDDNFSSIVK	35.28
BASP1_RAT	Brain acid soluble protein 1	264.54	5	46.4	1	ESEPQAAADATEVK	51.15
					2	AEPEKSEGAAEEQPEPAPAPEQEAAAPGPAAGGEAPK	45.4
					3	AGEASAESTGAADGAPQEEGEAK	79.48
					4	APAPAAPAAEPQAEAPVASSEQSVAVK	53.05
					5	APAPAAPAAEPQAEAPVASSEQSVAVKE	35.46
CNTP1_RAT	Contactin-associated protein 1	197.25	5	5.0	1	SLGASSYYGLFTTAR	53.34
					2	AVATQGAFNSWDWVTR	39.13
					3	GCIENVIYNR	30.09
					4	VMETGVIDPEIQR	35.7
					5	VQGELSESNCGAMPR	38.99
DLDH_RAT	Dihydrolipoyl dehydrogenase, mitochondrial	294.43	5	14.5	1	NETLGGTCLNVGCIPSK	62.66
					2	NQVTATTADGSTQVIGTK	89.41
					3	IDVSVEAASGGK	58.64
					4	SEEQLKEEGVEFK	32.34
					5	EANLAASFGKPINF	51.38
GBB1_RAT	Guanine nucleotide-binding protein G(I)/G(S)/G(T) subunit beta-1	234.96	5	19.4	1	SELDQLRQEAEQLK	51.23
					2	ACADATLSQITNNIDPVGR	67.59
					3	LLVSASQDGK	31.82
					4	LIIWDSYTTNK	31.52
					5	LFVSGACDASAK	52.8
HSP7C_RAT	Heat shock cognate 71 kDa protein	261.58	5	10.1	1	VEIIANDQGNR	49.53
					2	TTPSYVAFTDTER	54.78
					3	NQVAMNPTNTVFDAK	45.18
					4	IINEPTAAAIAYGLDK	61.15
					5	FEELNADLFR	50.94
IDHP_RAT	Isocitrate dehydrogenase [NADP], mitochondrial	382.46	5	14.8	1	DQTNDQVTIDSALATQK	87.09
					2	LIDDMVAQVLK	85.67
					3	TIEAEAAHGTVTR	82.67
					4	VCVQTVESGAMTK	90.41
					5	DLAGCIHGLSNVK	36.62
LGI1_RAT	Leucine-rich glioma-inactivated protein 1	270.2	5	9.0	1	GLDSLTNVDLR	70.83
					2	DFDCIITEFAK	70.61

					3	GDVYICLTR	31.31
					4	FQELNVQAPR	60.74
					5	NFLFASSFK	36.71
NDUS4_RAT	NADH dehydrogenase [ubiquinone] iron-sulfur protein 4, mitochondrial	254.78	5	30.9	1	DTQLITVDEK	62.01
					2	LDVTPLTGVPEEHIK	48.9
					3	EDAVAFAEK	50.53
					4	HGWSYDVEGR	46.79
					5	SYGANFSWNK	46.55
S12A5_RAT	Solute carrier family 12 member 5	216.35	5	5.1	1	ESSPFINSTDTEK	34.8
					2	LWGLFCSSR	30.4
					3	ENLWSSYLTK	40.27
					4	IFTVAQMDDNSIQMK	48.8
					5	LVLLNMPGPPR	62.08
SEPT7_RAT	Septin-7	209.86	5	14.2	1	NLEGYVGFANLPNQVYR	44.53
					2	FEDYLNAESR	54.47
					3	ADTLTPEECQQFK	35.06
					4	DVTNNVHYENYR	33.41
					5	SPLAQMEEER	42.39
SNP25_RAT	Synaptosomal-associated protein 25	247.72	5	34.0	1	RADQLADESLESTR	30.81
					2	TLVMLDEQGEQLER	74.77
					3	AWGNNQDGVVASQPAR	60.53
					4	EQMAISGGFIR	43.25
					5	HMALDMGNEIDTQNR	38.36
VDAC1_RAT	Voltage-dependent anion-selective channel protein 1	272.34	5	20.1	1	WTEYGLTFTEK	56.16
					2	LTFDSSFSPNTGK	69.09
					3	VTQSNFAVGYK	39.54
					4	YQVDPDACFSAK	46.8
					5	LTLSALLDGK	60.75
1433Z_RAT	14-3-3 protein zeta/delta	197.3	4	22.0	1	SVTEQGAELSNEER	72.77
					2	YLAEVAAGDDKK	31.29
					3	GIVDQSQQAYQEAFEISK	33.41
					4	DSTLIMQLLR	59.83
ACSF2_RAT	Acyl-CoA synthetase family member 2, mitochondrial	213.79	4	8.5	1	TVGECLDATAQR	64.29
					2	AASGLLSIGLR	69.33
					3	GGVIAGSLAPPELIR	34.12
					4	TGDIASMDEQGFCR	46.05
AT1B1_RAT	Sodium/potassium-transporting ATPase subunit beta-1	191.27	4	16.8	1	SYEAYVLNIIR	77.39
					2	DDMIFEDCGSMPSEPK	32.75
					3	YNPNVLPVQCTGK	33.68
					4	AYGENIGYSEK	47.45
AT2A2_RAT	Sarcoplasmic/endoplasmic reticulum calcium ATPase 2	275.76	4	5.4	1	VDQSILTGESVSVIK	60.63
					2	TGTLTTNQMSVCR	75.08
					3	VGEATETALTCLVEK	84.39
					4	IGIFGQDEDVTSK	55.66

AT5F1_RAT	ATP synthase subunit b, mitochondrial	186.95	4	15.6	1	IAQLEEIK	48.01
					2	HYLFDVQR	32.57
					3	LDYHISVQDMMR	41.52
					4	HVIQSISAQQEK	64.85
ATAD3_RAT	ATPase family AAA domain-containing protein 3	194.32	4	7.4	1	LKEYEAAVEQLK	56.26
					2	TAGTLFGEGFR	40.44
					3	NVLMYGPPGTGK	36.06
					4	VFDWASTSR	61.56
ATP5I_RAT	ATP synthase subunit e, mitochondrial	303.49	4	50.7	1	VPPVQVSPLIK	61.02
					2	YSALILGMAYGAK	84.61
					3	YSALILGMAYGAK	63.27
					4	ELAEAEDVSIFK	94.59
C1QBP_RAT	Complement component 1 Q subcomponent-binding protein, mitochondrial	241.11	4	16.8	1	AFVEFLTDEIK	44.52
					2	AFVEFLTDEIKEEK	69.28
					3	AEEQEPELTSTPNFVVEVTK	53.39
					4	EVSFQTTGDSEWR	73.92
DHSB_RAT	Succinate dehydrogenase [ubiquinone] iron-sulfur subunit, mitochondrial	133.15	4	16.0	1	DLVPDLSNFYAQYK	35.35
					2	QQYLQSIEDR	30.47
					3	YLGPAVLMQAYR	35.32
					4	LQDPFSLYR	32.01
EAA2_RAT	Excitatory amino acid transporter 2	197.29	4	6.3	1	MHDSHLSSEEPK	48.78
					2	SELDTIDSQHR	67.37
					3	SADCSVEEEPWK	50.75
					4	SADCSVEEEPWKR	30.39
EF1A1_RAT	Elongation factor 1-alpha 1	228.28	4	10.0	1	YYVTIIDAPGHR	59.47
					2	EHALLAYTLGVK	49.22
					3	MDSTEPPYSQK	48.99
					4	IGGIGTVPVGR	70.6
GBB2_RAT	Guanine nucleotide-binding protein G(I)/G(S)/G(T) subunit beta-2	194.64	4	15.3	1	ACGDSTLTQITAGLDPVGR	82.35
					2	LLVSASQDGK	31.82
					3	LIIWDSYTTNK	31.52
					4	TFVSGACDASIK	48.95
GNAI2_RAT	Guanine nucleotide-binding protein G(i) subunit alpha-2	201.11	4	14.1	1	AMGNLQIDFADPQR	46.87
					2	IAQSDYIPTQQDVLR	49.63
					3	TTGIVETHFTFK	45.53
					4	LFDSICNNK	59.08
H4_RAT	Histone H4	188.9	4	40.8	1	DNIQGITKPAIR	45.96
					2	ISGLIYEETR	39.85
					3	VFLENVIR	45.64
					4	TVTAMDVVYALK	57.45
HS90A_RAT	Heat shock protein HSP 90-alpha	205.52	4	6.5	1	ADLINNLGTIAK	52.69
					2	EDQTEYLEER	34.04
					3	NPDDITNEEYGEFYK	74.21
					4	DQVANSAFVER	44.58

HS90B_RAT	Heat shock protein HSP 90-beta	191.23	4	6.8	1	ELISNASDALDK	39.76
					2	ADLINNLGTIAK	52.69
					3	EDQTEYLEER	34.04
					4	NPDDITQEEYGEFYK	64.74
K2C1_RAT	Keratin, type II cytoskeletal 1	233.07	4	5.8	1	FLEQQNQVLQTK	76.66
					2	WELLQQVDTSTR	70.26
					3	TNAENEFVTIK	34.9
					4	TNAENEFVTIKK	51.25
K6PL_RAT	6-phosphofructokinase, liver type	228.9	4	6.9	1	AIGVLTSGGDAQGMNAAVR	112.22
					2	TFVLEVMGR	42.1
					3	LPLMECVQVTK	34.46
					4	VFANAPDSACVIGLR	40.12
KAD4_RAT	Adenylate kinase isoenzyme 4, mitochondrial	175.5	4	19.7	1	LMMSELETR	54.69
					2	SAQHWLLDGFPR	38.52
					3	TLVQAEALDR	48.71
					4	GVLHQFSGTETNR	33.58
MCCA_RAT	Methylcrotonoyl-CoA carboxylase subunit alpha, mitochondrial	176.13	4	7.3	1	QEGIIFIGPPSTAIR	39.48
					2	EFQEQLESAR	30.08
					3	IIEEAPAPGIDPEVR	48.85
					4	HAPLVEFEEEEV	57.72
NLRX1_RAT	NLR family member X1	207.71	4	4.3	1	DNLIQMLSR	55.28
					2	AVLAQLGCPIK	56.09
					3	NLDALENAQAIK	50.85
					4	FSAEVLGSLR	45.49
PCCB_RAT	Propionyl-CoA carboxylase beta chain, mitochondrial	215.98	4	10.2	1	SVTNEDVTQEQLGGAK	67.07
					2	AFDNDVDALCNLR	64.95
					3	LVPELDTVVPLESSK	46.31
					4	ICCDLEVLASK	37.65
PLCB1_RAT	1-phosphatidylinositol-4,5-bisphosphate phosphodiesterase beta-1	186.37	4	4.6	1	ETELLDLSLVK	43.56
					2	EVIEAIAECAFK	63.18
					3	TSQGNAVNPVWEEEPIVFK	38.09
					4	LTDVAEECQNNQLK	41.54
RAB18_RAT	Ras-related protein Rab-18	169.34	4	22.8	1	MDEDVLTTLK	42.81
					2	ILIIGESGVGK	35.26
					3	LAIWDTAGQER	30.41
					4	IIQTPGLWESENQNK	60.86
RAP1A_RAT	Ras-related protein Rap-1A	179.09	4	27.2	1	YDPTIEDSYR	34.99
					2	VKDTEDVPMILVGNK	31.23
					3	QWCNCAFLESSAK	49.66
					4	INVNEIFYDLVR	63.21
S27A1_RAT	Long-chain fatty acid transport protein 1	212.05	4	8.2	1	LFYIYTSGTTGLPK	45.35
					2	GENVSTTEVEAVLSR	57.91
					3	VLASYAQPIFLR	67.79
					4	LLPQVDTTGTFK	41

SYPH_RAT	Synaptophysin	238.72	4	12.1	1	MDVVNQLVAGGQFR	73.84
					2	MDVVNQLVAGGQFR	69.47
					3	LHQVYFDAPSCVK	60.91
					4	MATDPENIIK	34.5
TENR_RAT	Tenascin-R	199.82	4	3.6	1	YEVSISAVR	42.13
					2	ITFTPSSGISSEVTVPR	47.09
					3	AAIENYVLTYK	51.9
					4	ELIVDAEDTWIR	58.7
THTR_RAT	Thiosulfate sulfurtransferase	218.67	4	18.9	1	VLDASWYSPGTR	35.86
					2	TYEQVLENLQSK	80.12
					3	YLGTQPEPDAVGLDSGHIR	43.42
					4	KVDLSQPLIATCR	59.27
1433B_RAT	14-3-3 protein beta/alpha	172.93	3	17.5	1	AVTEQGHELSNEER	46.58
					2	QTTVSNSQQAYQEAFEISK	66.52
					3	DSTLIMQLLR	59.83
AL1B1_RAT	Aldehyde dehydrogenase X, mitochondrial	179.5	3	6.9	1	LAPALATGNTVVMK	58.22
					2	EEIFGPVQPLFK	40.23
					3	YGLAAAVFTR	81.05
ALDH2_RAT	Aldehyde dehydrogenase, mitochondrial	135.76	3	7.3	1	TEQGPQVDETQFK	47.75
					2	GYFIQPTVFGDVK	33.94
					3	EEIFGPVMQILK	54.07
ANS1B_RAT	Ankyrin repeat and sterile alpha motif domain-containing protein 1B	149.34	3	3.7	1	ILQAIQLLPK	56.54
					2	NISCAAQDPEDLSTFAYITK	36.5
					3	TLANLPWIVEPGQEAK	56.3
ANXA6_RAT	Annexin A6	140.8	3	4.3	1	SELDMLDIR	42.27
					2	DAFVAIVQSVK	60.45
					3	SEIDLLNIR	38.08
AP2A2_RAT	AP-2 complex subunit alpha-2	148.52	3	3.2	1	GLAVFISDIR	66.47
					2	QSAALCLLR	30.8
					3	LTECLETILNK	51.25
AP2M1_RAT	AP-2 complex subunit mu	134.02	3	9.4	1	QSIAIDDCTFHQCVR	48.64
					2	IPTPLNTSGVQVICMK	54.07
					3	LNYSDHDVIK	31.31
ARL8B_RAT	ADP-ribosylation factor-like protein 8B	153.33	3	17.2	1	IWDIGGQPR	34.9
					2	GVNAIVYMIDAADR	68.77
					3	MNLSAIQDR	49.66
CALM_RAT	Calmodulin	187.24	3	30.9	1	ADQLTEEQIAEFK	74.84
					2	EAFSLFDKDGDGTITTK	64.39
					3	VFDKDGNGYISAAELR	48.01
COX2_RAT	Cytochrome c oxidase subunit 2	141.44	3	11.5	1	ILYMMDEINNPVLTVK	51.17
					2	YFENWSASMI	41.99
					3	YFENWSASMI	48.28
CX6C2_RAT	Cytochrome c oxidase subunit 6C-2	118.93	3	31.6	1	SSGALLPKPQMR	46.15
					2	NYDSMKDFEEMR	35.9

					3	NYDSMKDFEEMR	36.88
CXA1_RAT	Gap junction alpha-1 protein	112.07	3	11.8	1	VAQTDGVNVEMHLK	37.2
					2	SDPYHATTGPLSPSK	30.43
					3	QASEQNWANYSAEQNR	44.44
DPYL1_RAT	Dihydropyrimidinase-related protein 1	128.63	3	4.0	1	QIGENLIVPGGVK	32.77
					2	QIGENLIVPGGVK	32.4
					3	SAADIIALAR	63.46
E41L1_RAT	Band 4.1-like protein 1	195.28	3	5.2	1	VTLLDASEYECEVEK	85.42
					2	DYFGLTFCDADSQK	37.63
					3	VSTADSTQVDGGAPAAK	72.23
ETFB_RAT	Electron transfer flavoprotein subunit beta	119.64	3	14.9	1	EIIAVSCGPPQCQETIR	38.58
					2	AGDLGVDLTSK	45.75
					3	VETTEDLVAK	35.31
GABT_RAT	4-aminobutyrate aminotransferase, mitochondrial	155.56	3	7.2	1	GNYLVDVDGNR	34.39
					2	CLEEVEDLIVK	41.13
					3	GTFCSFDTPDEAIR	80.04
GLNA_RAT	Glutamine synthetase	124.15	3	14.2	1	LTGFHETSNINDFSAGVANR	32.62
					2	RPSANCDPYAVTEAIVR	38.44
					3	TCLLNETGDEPFQYKN	53.09
GNAI1_RAT	Guanine nucleotide-binding protein G(i) subunit alpha-1	157.24	3	10.2	1	IAQPNYIPTQQDVLR	52.63
					2	TTGIVETHFTFK	45.53
					3	LFDSICNNK	59.08
GNAZ_RAT	Guanine nucleotide-binding protein G(z) subunit alpha	107.8	3	11.0	1	GEITPELLGVMR	32.33
					2	LWADPGAQACFGR	35.82
					3	GQNTYEEAAVYIQR	39.65
KCAB2_RAT	Voltage-gated potassium channel subunit beta-2	146.19	3	11.2	1	QTGSPGMIYSTR	35.31
					2	AEVVLGNIIK	58.21
					3	IGVGAMTWSPLACGIVSGK	52.67
KIF2A_RAT	Kinesin-like protein KIF2A	188.99	3	5.0	1	FDYAFDDSAPNEMVYR	64.04
					2	FSLIDLAGNER	67.79
					3	IDILTELR	57.16
MICU1_RAT	Calcium uptake protein 1, mitochondrial	137.16	3	10.3	1	EVSSHEGSAADTAAEPYPEEK	35.6
					2	QPEHLGLDQYIIK	60.39
					3	QFGGMLLAYSGVQSK	41.17
MYL6_RAT	Myosin light polypeptide 6	119.36	3	20.5	1	CDFTEDQTAEFK	37.76
					2	EAFQLFDR	40.6
					3	ILYSQCGDVMR	41
NDUA5_RAT	NADH dehydrogenase [ubiquinone] 1 alpha subcomplex subunit 5	160.74	3	25.9	1	TTGLVGLAVCDTPHER	71.16
					2	YTEQITSEK	38.88
					3	YTEQITSEKLELVK	50.7
NFS1_RAT	Cysteine desulfurase, mitochondrial	134.03	3	8.6	1	THAYGWESEAAMER	34.88
					2	QQVASLIGADPR	56.92
					3	QPIAEIGQICSSR	42.23
ODO2_RAT	Dihydrolipoyllysine-	163.53	3	7.0	1	VEGGTPLFTLR	44.81

	residue succinyltransferase component of 2-oxoglutarate dehydrogenase complex, mitochondrial				2	LGFMSAFVK	60.22
					3	NVETMNYADIER	58.5
PI42A_RAT	Phosphatidylinositol-5-phosphate 4-kinase type-2 alpha	149.21	3	9.9	1	FGIDDQDFQNSLTR	69.81
					2	DVEFLAQLK	46.66
					3	HGAGAEISTVNPEQYSK	32.74
PI42B_RAT	Phosphatidylinositol-5-phosphate 4-kinase type-2 beta	149.45	3	9.6	1	FGIDDQDYQNSVTR	70.05
					2	DVEFLAQLK	46.66
					3	HGAGAEISTVNPEQYSK	32.74
RAB14_RAT	Ras-related protein Rab-14	152.03	3	19.5	1	GAAGALMVYDITR	46.62
					2	NLTNPNTVIILIGNK	46.1
					3	TGENVEDAFLEAAK	59.31
RAB2A_RAT	Ras-related protein Rab-2A	191.3	3	18.9	1	LQIWDTAGQESFR	64.92
					2	GAAGALLVYDITR	45.43
					3	TASNVEEAFINTAK	80.95
RAB3C_RAT	Ras-related protein Rab-3C	163.33	3	16.7	1	TYSWDNAQVILAGNK	64.54
					2	LVDIICDK	34.54
					3	MSESLETDPAITAAK	64.25
RAC1_RAT	Ras-related C3 botulinum toxin substrate 1	160.15	3	13.0	1	KLTPITYPQGLAMAK	38.57
					2	LTPITYPQGLAMAK	58.34
					3	YLECSALTQR	63.24
RB11A_RAT	Ras-related protein Rab-11A	110.19	3	15.3	1	GTRDDEYDYLFK	37.16
					2	STIGVEFATR	32.49
					3	AQIWDTAGQER	40.54
RHOA_RAT	Transforming protein RhoA	143.52	3	19.7	1	TCLLIVFSK	42.8
					2	QVELALWDTAGQEDYDR	56.3
					3	IGAFGYMECSAK	44.42
SCN3A_RAT	Sodium channel protein type 3 subunit alpha	132.86	3	1.8	1	FGGQDIFMTEEQK	61.61
					2	VLGESGEMDALR	36.86
					3	VSYEPITTTLK	34.39
SEPT5_RAT	Septin-5	102.7	3	8.4	1	VNIVPLIAK	31.04
					2	ADCLVPSEIR	34.28
					3	DVTCDVHYENYR	37.38
SIRT2_RAT	NAD-dependent deacetylase sirtuin-2	154.04	3	10.6	1	NLFTQTLGLGSQK	56.39
					2	LLDELTLEGVTR	59.46
					3	SPSTGLYANLEK	38.19
SNPH_RAT	Syntaphilin	116.72	3	8.1	1	YFVDINIQNK	33.52
					2	QGQPIYNISSLLR	30.09
					3	ISCSLSQPSAGSSGGSQL	53.11
SUCA_RAT	Succinyl-CoA ligase [GDP-forming] subunit alpha, mitochondrial	122.7	3	9.0	1	QGTFHSQQALEYGTK	44.93
					2	QGTFHSQQALEYGTK	32.01
					3	LIGPNCPGIINPGECK	45.76
TIM44_RAT	Mitochondrial import inner membrane translocase subunit TIM44	185.12	3	7.9	1	VTDLLGGLFSK	55.15
					2	TEMSEVLTEILR	38.54

					3	ILDISNVDLAMGK	91.43
TOM22_RAT	Mitochondrial import receptor subunit TOM22 homolog	148.42	3	16.2	1	LWGLTEMFPER	45.19
					2	LQMEQQQQLQQR	61.76
					3	LQMEQQQQLQQR	41.47
TXTP_RAT	Tricarboxylate transport protein, mitochondrial	147.86	3	11.3	1	GLSSLLYGSIPK	54.73
					2	GTYQGLTATVLK	41.19
					3	NTLDCGVQILK	51.94
VIME_RAT	Vimentin	125.17	3	7.5	1	SLYSSSPGGAYVTR	31.35
					2	ILLAELEQLK	54.43
					3	EEAESTLQSFR	39.39
1433E_RAT	14-3-3 protein epsilon	90.48	2	8.6	1	MDDREDLVYQAK	30.65
					2	DSTLIMQLLR	59.83
1433G_RAT	14-3-3 protein gamma	128.07	2	9.7	1	NVTELNEPLSNEER	68.24
					2	DSTLIMQLLR	59.83
1433T_RAT	14-3-3 protein theta	126.25	2	9.8	1	AVTEQGAELSNEER	66.42
					2	DSTLIMQLLR	59.83
ABCB7_RAT	ATP-binding cassette sub-family B member 7, mitochondrial	114.33	2	3.3	1	VAISLGFLGGAK	40.92
					2	VLSGVSFEVPAGK	73.41
ACADM_RAT	Medium-chain specific acyl-CoA dehydrogenase, mitochondrial	83.44	2	5.9	1	ENVLIGEGAGFK	30.99
					2	IYQIYEGTAQIQR	52.45
ADDA_RAT	Alpha-adducin	74.59	2	3.8	1	VNLQGDIVDR	33.1
					2	TLASAGGPDNLVLLDPGK	41.49
AMPL_RAT	Cytosol aminopeptidase	88.17	2	5.0	1	GVLFASGQNLAR	53.82
					2	QLMESPANEMTPTR	34.35
AOFB_RAT	Amine oxidase [flavin-containing] B	118.04	2	5.4	1	YVDLGGSYVGPTQNR	80.4
					2	YVISAIPPVLGMK	37.64
ARF1_RAT	ADP-ribosylation factor 1	150.54	2	13.8	1	DAVLLVFANK	74.23
					2	QDLPNAMNAAEITDK	76.31
ARF6_RAT	ADP-ribosylation factor 6	88.24	2	12.0	1	FNVWDVGGQDK	45.4
					2	DAIILIFANK	42.84
BCAS1_RAT	Breast carcinoma-amplified sequence 1 homolog (Fragment)	106.39	2	6.5	1	GSSQPGQAPSAGTSDTAR	56.69
					2	MLDAQVQTDPVSIGPVGK	49.7
BR44_RAT	Brain protein 44	76.48	2	14.2	1	TVFFWAPIMK	44.27
					2	YSLVIIPK	32.21
BRSK1_RAT	no description	103.04	2	N/A	1	SVSGASTGLSSSPLSSPR	50.04
					2	FQVDISSSEGPEPSPR	53
CAZA2_RAT	F-actin-capping protein subunit alpha-2	89.22	2	8.7	1	LLLNNDNLLR	58.24
					2	FTVTPSTTQVVGILK	30.98
CISD1_RAT	CDGSH iron-sulfur domain-containing protein 1	107.99	2	25.9	1	VVHAFDMEDLGDK	33.45
					2	HNEETGDNVGPLIIK	74.54
CNTN1_RAT	Contactin-1	96.86	2	2.5	1	YSMVGGNLVINNPDK	52.93
					2	ELTITWAPLSR	43.93
COF1_RAT	Cofilin-1	122.59	2	13.9	1	ASGVAVSDGVIK	68.77
					2	YALYDATYETK	53.82

COX41_RAT	Cytochrome c oxidase subunit 4 isoform 1, mitochondrial	85.92	2	14.2	1	SEDYALPSYVDR	30.22
					2	IQFNESFAEMNK	55.7
COX5B_RAT	Cytochrome c oxidase subunit 5B, mitochondrial	87.17	2	15.5	1	EIMIAAQR	51.67
					2	EDPNLVPSVSNK	35.5
CPNE9_RAT	Copine-9	76.27	2	3.3	1	SDPFLVFYR	31.9
					2	DIVQFVPFR	44.37
CTBP1_RAT	C-terminal-binding protein 1	77.86	2	7.2	1	GETLGIIGLGR	47.82
					2	GAALDVHESEPFSFSQGPLK	30.04
CX6A1_RAT	Cytochrome c oxidase subunit 6A1, mitochondrial	106.12	2	21.6	1	IWKALTYFVALPGVGVSMLNVFLK	40.49
					2	ALTYFVALPGVGVSMLNVFLK	65.63
DHB8_RAT	Estradiol 17-beta-dehydrogenase 8	90.41	2	10.4	1	SALALVTGAGSGIGR	54.62
					2	AGVIGLTQTAAR	35.79
DNM1L_RAT	Dynamin-1-like protein	97.09	2	2.6	1	MEALIPVINK	41.91
					2	SSVLESLVGR	55.18
EAA1_RAT	Excitatory amino acid transporter 1	129.88	2	5.5	1	IVQVTAADAFLDLIR	51.94
					2	DVEMGNSVIEENEMK	77.94
FA54B_RAT	Protein FAM54B	84.95	2	10.7	1	ASFETLPNISDLCLK	39.18
					2	TTCSSSEEDDCISLSK	45.77
FAHD2_RAT	Fumarylacetoacetate hydrolase domain-containing protein 2	102.16	2	7.3	1	TMVQFLER	42.89
					2	TFDTFCPLGPALVTK	59.27
FKBP8_RAT	Peptidyl-prolyl cis-trans isomerase FKBP8	146.85	2	7.9	1	TAEDGPDLEMLSGQER	103.84
					2	VLAQQGEYSEAIPILR	43.01
FUMH_RAT	Fumarate hydratase, mitochondrial	98.81	2	5.9	1	AIEMLGGELGSK	38.33
					2	IYELAAGGTAVGTGLNTR	60.48
GDN_RAT	Glia-derived nexin	67.27	2	5.5	1	DIVTVANAVFVR	33.43
					2	LVLVNAVYFK	33.84
GTR1_RAT	Solute carrier family 2, facilitated glucose transporter member 1	103.02	2	3.7	1	VTILELFR	51.51
					2	TFDEIASGFR	51.51
HOME1_RAT	Homer protein homolog 1	89.53	2	6.0	1	LTAALLESTANVK	45.75
					2	TLLEILDGK	43.78
HSDL1_RAT	Inactive hydroxysteroid dehydrogenase-like protein 1	64.3	2	7.3	1	AAVDSFYLLYR	33.7
					2	WAVISGATDGIGK	30.6
IVD_RAT	Isovaleryl-CoA dehydrogenase, mitochondrial	110.71	2	5.7	1	VPAANILSQESK	51.76
					2	LYEIGGGTSEVR	58.95
K1C14_RAT	Keratin, type I cytoskeletal 14	94.73	2	4.5	1	VTMQNLNDR	53.11
					2	EVATNSELVQSGK	41.62
K2C6A_RAT	Keratin, type II cytoskeletal 6A	157.16	2	4.0	1	SLDLDSIIAEVK	94.58
					2	YEELQITAGR	62.58
K2C73_RAT	Keratin, type II cytoskeletal 73	115.79	2	4.2	1	FLEQQNQVLQTK	76.66
					2	LALDIEIATYR	39.13
KCNA2_RAT	Potassium voltage-gated channel subfamily A member 2	87.98	2	4.6	1	VVINISGLR	50.4
					2	TLAQFPETLLGDPK	37.58
KCRU_RAT	Creatine kinase U-type, mitochondrial	125.09	2	6.2	1	VVVDALSGLK	57.21
					2	LGYILTCPSNLGTGLR	67.88

KPCA_RAT	Protein kinase C alpha type	118.86	2	3.9	1	LSVEIWDWDR	39.03
					2	DVVIQDDDVECTMVEK	79.83
MIRO2_RAT	Mitochondrial Rho GTPase 2	116.02	2	3.2	1	LPIILVGNK	46.75
					2	NISELFYYAQK	69.27
ML12B_RAT	Myosin regulatory light chain 12B	120.95	2	12.2	1	FTDEEVDELYR	76.09
					2	GNFNYIEFTR	44.86
MMSA_RAT	Methylmalonate-semialdehyde dehydrogenase [acylating], mitochondrial	106.36	2	5.2	1	TLADAEGDVFR	45.43
					2	AISFVGSNQAGEYIFER	60.93
MOG_RAT	Myelin-oligodendrocyte glycoprotein	127.33	2	9.0	1	ALVGDEAELPCR	66.03
					2	LAGQFLEELR	61.3
MYH11_RAT	Myosin-11 (Fragments)	96.79	2	1.9	1	EDQSILCTGESGAGK	56.37
					2	ALELDPNLYR	40.42
MYO1D_RAT	Myosin-Id	106.19	2	2.5	1	SNCVLEAFGNAK	46.08
					2	NSMIALVDNLASK	60.11
NDUAB_RAT	NADH dehydrogenase [ubiquinone] 1 alpha subcomplex subunit 11	83.86	2	19.1	1	FFEAYNETPDGTQCHR	36.74
					2	LEGWELFATPK	47.12
NDUS6_RAT	NADH dehydrogenase [ubiquinone] iron-sulfur protein 6, mitochondrial	114.13	2	21.6	1	IIACDGGGGALGHPK	80.28
					2	VYINLDKETK	33.85
NFH_RAT	Neurofilament heavy polypeptide	98.03	2	2.1	1	AQALQEECGYLR	48.35
					2	SAQEEITEYR	49.68
NMDE2_RAT	Glutamate [NMDA] receptor subunit epsilon-2	71.63	2	1.2	1	GVDDALLSLK	41.56
					2	DFYLDQFR	30.07
OXR1_RAT	Oxidation resistance protein 1	121.8	2	3.8	1	VVSSTSEEEEAFTEK	69.97
					2	MAESGPDEAPAGEAAAR	51.83
PDK1_RAT	[Pyruvate dehydrogenase [lipoamide]] kinase isozyme 1, mitochondrial	120.49	2	6.0	1	AVPLAGFGYGLPISR	65.08
					2	LYAQYFQGDLK	55.41
PHB2_RAT	Prohibitin-2	102.31	2	7.4	1	DLQMVNISLR	53.34
					2	IVQAEGEAEAAK	48.97
PHB_RAT	Prohibitin	90.64	2	8.1	1	IYTSIGEDYDER	44.23
					2	FDAGELITQR	46.41
PLEC_RAT	Plectin	65.68	2	0.6	1	YSELTTLTSQYIK	32.69
					2	DPYSGQSVSLFQALK	32.99
RAB3B_RAT	Ras-related protein Rab-3B	121.87	2	14.2	1	TYSWDNAQVILVGNK	61.35
					2	MSDSMDTDPSVLGASK	60.52
RAB3D_RAT	GTP-binding protein Rab-3D	95.89	2	10.5	1	TYSWDNAQVILVGNK	61.35
					2	LVDIICDK	34.54
RAB6A_RAT	Ras-related protein Rab-6A	113.87	2	11.5	1	GSDVIIMLVGNK	82.11
					2	ELNVMFIETSAK	31.76
RALA_RAT	Ras-related protein Ral-A	122.53	2	14.1	1	VKEDENVPFLLVGNK	61.79
					2	ADQWNVNYVETSAK	60.74
RAP2B_RAT	Ras-related protein Rap-2b	118.67	2	15.3	1	ALAEEWSCPFMETSAK	60.46
					2	ASVDELFAEIVR	58.21
RASH_RAT	GTPase HRas	91.46	2	13.8	1	LVVVGAGGVGK	40.96

					2	TGEGFLCVFAINNTK	50.5
RLA2_RAT	60S acidic ribosomal protein P2	109.33	2	40.0	1	ILDSVGIEADDER	70.81
					2	LASVPAGGAVAVSAAPGSAAPAAGSAPAAAEEK	38.52
ROGDI_RAT	Protein rogdi homolog	132.87	2	7.7	1	ATAMAASAAER	82.96
					2	LMDAVMLQLTR	49.91
RS4X_RAT	40S ribosomal protein S4, X isoform	100.49	2	9.9	1	FDTGNLCMVTGGANLGR	56.07
					2	LSNIFVIGK	44.42
RSSA_RAT	40S ribosomal protein SA	121.93	2	10.2	1	AIVAIENPADVSVISSR	73.05
					2	FAAATGATPIAGR	48.88
SCMC2_RAT	Calcium-binding mitochondrial carrier protein SCaMC-2	116.74	2	4.9	1	IDAQEIMQSLR	82.13
					2	TGQYSGMLDCAK	34.61
SCPDH_RAT	Probable saccharopine dehydrogenase	90.49	2	6.1	1	ATLVLNCVGPYR	45.93
					2	SVSNLKPVPVIGSK	44.56
SEP11_RAT	Septin-11	72.67	2	4.6	1	STLMDTLFNTK	38.31
					2	VNIIPIIAK	34.36
SERA_RAT	D-3-phosphoglycerate dehydrogenase	105.22	2	5.1	1	ILQDGGLQVVEK	47.9
					2	AGTGVDNVDLEAATR	57.32
SPTN2_RAT	Spectrin beta chain, brain 2	78.07	2	0.8	1	DALLLWCQMK	47.11
					2	ETWLSENQR	30.96
STML2_RAT	Stomatin-like protein 2	131.33	2	8.8	1	AEQINQAAGEASAVLAK	70.88
					2	DVQTTDTSIEELGR	60.45
STX1B_RAT	Syntaxin-1B	125.29	2	10.1	1	AIEQSIEQEEGLNR	73.43
					2	TTTNEELEDMLESGK	51.86
SYN3_RAT	Synapsin-3	87.12	2	4.3	1	ANTGSAMLEQVAMTER	49.56
					2	KSFASLFSD	37.56
UCRI_RAT	Cytochrome b-c1 complex subunit Rieske, mitochondrial	141.29	2	9.9	1	SGPFAPVLSATSR	53.61
					2	EIDQEAAVEVSQLR	87.68
VAMP2_RAT	Vesicle-associated membrane protein 2	169.88	2	28.4	1	LQQTQAQVDEVVDIMR	76.48
					2	ADALQAGASQFETSAAK	93.4
VATB2_RAT	V-type proton ATPase subunit B, brain isoform	104.42	2	4.9	1	AVVQVFEGTSGIDAK	54.74
					2	TPVSEDMLGR	49.68
VGLU1_RAT	Vesicular glutamate transporter 1	99.91	2	4.5	1	DPPVVDCTCFGLPR	48.87
					2	YIEDAIGESAK	51.04

Annexe 6. Etude du mélange standard MALDI-TOF/TOF versus ESI-LIT-FTICR. Peptides communs aux deux modes d'ionisations.

ESI FTICR	pI	Masse	MALDI TOF TOF	pI	Masse
APLDNDIGVSEATR	4.03	1457.56	APLDNDIGVSEATR	4.03	1457.56
CACSNHEPYFGYSGAFK	6.73	1881.07	CACSNHEPYFGYSGAFK	6.73	1881.07
CCSDVFNQVVK	5.82	1241.44	CCSDVFNQVVK	5.82	1241.44
CCTESLVNR	5.99	1024.17	CCTESLVNR	5.99	1024.17
CGLVPVLAENYK	5.99	1305.55	CGLVPVLAENYK	5.99	1305.55
CLMEGAGDVAFVK	4.37	1339.59	CLMEGAGDVAFVK	4.37	1339.59
DDPHACYSTVFDK	4.41	1497.60	DDPHACYSTVFDK	4.41	1497.60
DKPDNFQLFQSPHGK	6.75	1757.92	DKPDNFQLFQSPHGK	6.75	1757.92
DLGEEHFK	4.65	974.04	DLGEEHFK	4.65	974.04
DNPQTHYYAVAVVK	6.74	1604.78	DNPQTHYYAVAVVK	6.74	1604.78
DVSLLHKPTTQISDFHVATR	6.92	2265.55	DVSLLHKPTTQISDFHVATR	6.92	2265.55
EALDFFAR	4.37	968.08	EALDFFAR	4.37	968.08
EKDIVGAVLK	6.17	1071.28	EKDIVGAVLK	6.17	1071.28
ELPDPQESIQR	4.14	1311.41	ELPDPQESIQR	4.14	1311.41
FDEFFSAGCAPGSPR	4.37	1587.73	FDEFFSAGCAPGSPR	4.37	1587.73
FESNFNTQATNR	6.00	1428.48	FESNFNTQATNR	6.00	1428.48
FKDLGEEHFK	5.45	1249.39	FKDLGEEHFK	5.45	1249.39
GDFQFNISR	5.84	1083.17	GDFQFNISR	5.84	1083.17
GVIFYESHGK	6.75	1136.27	GVIFYESHGK	6.75	1136.27
HLVDEPQNLIK	5.32	1305.50	HLVDEPQNLIK	5.32	1305.50
HPEYAVSVLLR	6.75	1283.49	HPEYAVSVLLR	6.75	1283.49
HQQQFFQFR	9.76	1265.40	HQQQFFQFR	9.76	1265.40
HSTVFDNLPNPEDR	4.54	1640.73	HSTVFDNLPNPEDR	4.54	1640.73
HSTVFDNLPNPEDRK	5.38	1768.90	HSTVFDNLPNPEDRK	5.38	1768.90
IGLNCQLAQVAER	5.99	1414.64	IGLNCQLAQVAER	5.99	1414.64
ILESGPFVSCVK	5.99	1278.53	ILESGPFVSCVK	5.99	1278.53
KGEREDLIAYLK	6.18	1434.66	KGEREDLIAYLK	6.18	1434.66
KNYELLCGDNTR	6.06	1425.58	KNYELLCGDNTR	6.06	1425.58
KPVTDAENCHLAR	6.74	1453.64	KPVTDAENCHLAR	6.74	1453.64
KQTALVELLK	8.59	1142.40	KQTALVELLK	8.59	1142.40
KTGQAPGFSYTDANK	8.50	1584.71	KTGQAPGFSYTDANK	8.50	1584.71
KTYDSYLGDDYVR	4.43	1594.70	KTYDSYLGDDYVR	4.43	1594.70
KVPQVSTPTLVEVSR	8.75	1639.91	KVPQVSTPTLVEVSR	8.75	1639.91
LCQLCAGK	8.06	835.05	LCQLCAGK	8.06	835.05
LKECCDKPLLEK	6.17	1418.73	LKECCDKPLLEK	6.17	1418.73
LLEACTFHKP	6.74	1158.38	LLEACTFHKP	6.74	1158.38
LVNELTEFAK	4.53	1163.34	LVNELTEFAK	4.53	1163.34

NECFLSHKDDSPDLPK	4.66	1845.01	NECFLSHKDDSPDLPK	4.66	1845.01
NTDGSTDYGILQINSR	4.21	1753.84	NTDGSTDYGILQINSR	4.21	1753.84
NYELLCGDNTR	4.37	1297.41	NYELLCGDNTR	4.37	1297.41
QTALVELLK	6.00	1014.23	QTALVELLK	6.00	1014.23
RHPEYAVSVLLR	8.75	1439.68	RHPEYAVSVLLR	8.75	1439.68
SIGGEVFIDFTK	4.37	1312.49	SIGGEVFIDFTK	4.37	1312.49
SISIVGSYVGNR	8.46	1251.40	SISIVGSYVGNR	8.46	1251.40
SLHTLFGDELCK	5.30	1362.56	SLHTLFGDELCK	5.30	1362.56
TGQAPGFSYTDANK	5.50	1456.53	TGQAPGFSYTDANK	5.50	1456.53
TYDSYLGDDYVR	3.93	1466.52	TYDSYLGDDYVR	3.93	1466.52
VDEDQPFPAVPK	4.03	1341.48	VDEDQPFPAVPK	4.03	1341.48
VLGIDGGEGKEELFR	4.41	1618.81	VLGIDGGEGKEELFR	4.41	1618.81
VVGLSTLPEIYEK	4.53	1447.69	VVGLSTLPEIYEK	4.53	1447.69
WCTISTHEANK	6.74	1289.43	WCTISTHEANK	6.74	1289.43
YICDNQDTISSK	4.21	1386.50	YICDNQDTISSK	4.21	1386.50
YSQQQLMETSHR	6.75	1507.64	YSQQQLMETSHR	6.75	1507.64
YYGYTGAFR	8.50	1097.20	YYGYTGAFR	8.50	1097.20

Annexe 7. Etude du mélange standard LC-MALDI-TOF/TOF versus LC-ESI-LIT-FTICR. Peptides uniques ESI et peptides uniques MALDI

PEPTIDE UNIQUE LC-ESI LIT-FTICR	pI	Masse	PEPTIDE UNIQUE LC-MALDI TOF TOF	pI	Masse
ANGTTVLVGMPAGAK	8.8	1386.63	AEFVEVTK	4.53	922.05
CCAADDKEACFAVEGPK	4.32	1756.98	ATDGGAHGVINVSVSEAAIEASTR	4.65	2312.48
CKGTDVQAWIR	8.22	1276.48	CCTKPESER	6.13	1052.19
DQTVIQNTDGNNNEAWAK	4.03	2018.08	DSADGFLK	4.21	851.91
DWENPGVTQLNR	4.37	1428.52	DTHKSEIAHR	6.92	1193.28
EACFAVEGPK	4.53	1050.19	ECVPNSNER	4.53	1047.11
ECCHGDLLECADDR	4.1	1578.71	ENFEVLCK	4.53	981.13
EDLIAYLK	4.37	964.13	ESKPPDSSKDECMVK	4.78	1679.88
ETYGDMADCCEK	3.92	1364.48	FNDDFSR	4.21	899.92
ETYGDMADCCEKQEPER	4.08	2004.15	GPNHAVVSR	9.76	936.04
EYEATLEECCAK	4.09	1388.53	GTGKECVPNSNER	6.14	1390.49
GTDVQAWIR	5.84	1045.16	GYLAVAVVK	8.59	919.13
GYSLGNWVCAAK	8.2	1268.45	HGLDNYR	6.74	873.92
KENFEVLCK	6.14	1109.31	IGDYAGIK	5.83	835.96
LKPDPNTLCDEFK	4.56	1519.73	KSCHTAVDR	8.23	1016.14
LPLVGGHEGAGVVVGMGENVK	5.4	2019.35	KSCHTGLGR	9.51	958.1
LTAACFDR	5.83	896.03	LCVLHEK	6.74	841.04
LVVSTQTALA	5.52	1002.18	LGEYGFQNALIVR	6	1479.7
RDWENPGVTQLNR	6.07	1584.71	LKPDPNTLCDEFKADEK	4.44	1963.19
RPCFSALTPDETYVPK	6.06	1824.08	MIFAGIK	8.5	779.01
SANLMAGHWVAISGAAGGLGSLAVQYAK	8.33	2701.1	NECFLSHK	6.74	977.1
SVTDCTSNFCLFQSNSK	5.55	1881.06	SCHTAVDR	6.46	887.97
TSDANINWNNLK	5.5	1389.49	SCHTGLGR	7.99	829.93
TVMENFVAFVDK	4.37	1399.62	SHCIAEVEK	5.38	1015.15
VHKECCHGDLLECADDR	4.8	1943.15	TCVADESHAGCEK	4.65	1349.45
VHKECCHGDLLECADDRADLAK	4.86	2441.73	TDRPSQQLR	9.26	1100.2
VLGIDGGEGK	4.37	944.05	TGPNLHGLFGR	9.44	1168.32
VPQVSTPTLVEVSR	5.97	1511.74	TPHPALTEAK	6.41	1064.21
WCAIGHQER	6.74	1099.23	TSHMDCIK	6.4	934.09
YNGVFQECCQAEDK	4.14	1633.77	YLYEIAR	6	927.07

Annexe 8. Etude d'un extrait d'Escherichia Coli. Protéines identifiées pour chaque mode d'ionisation.

Protéines uniques MALDI	Protéines uniques ESI	Proteine communes
AGAL_ECOLI	ACP1_SHIFL	AHPC_SHIFL
AROK_ECO57	DBHB_ECO57	CH10_ECO57
CH60_ENTAE	EFG_ECO57	CH60_ACTPL
CH60_ENTAM	ENO_AERHH	CH60_ECO57
CH60_ERWCT	ENO_KLEP7	CSPA_ECO57
CH602_CHRVO	FKBA_ECO57	CSPC_ECO57
CYSK_ECO57	FUR_ECO57	DBHA_ECO57
DAPD_ERWCT	FUR_KLEPN	DNAK_ECO57
DNAK_ACTSZ	GLNH_ECO57	EFTS_ECO57
DNAK_AERHH	HINT_ECO57	EFTU_ECO57
DNAK_ERWCT	HISJ_ECO57	FKBB_ECOLI
DNAK_PASMU	IDH_ECOLI	GPMA_ECO57
EFTU_MARAV	IF3_ECO57	HNS_ECO57
EFTU1_YERPE	MDH_ECO57	KAD_ECO57
ENO_ECO57	NDK_ECO57	MALE_ECO57
G3P1_ECO57	PGK_SHIFL	ODP2_ECOLI
GNTY_ECOLI	RL1_ECO57	OMPA_SHIDY
GREA_SHIFL	RL17_ERWCT	PTGA_ECOL6
K2C6A_RAT	RL4_SALPA	RBSB_ECOLI
NIFU_SHIFL	RS2_ECO57	RL10_ECO57
ODP1_ECOLI	RS3_ECO57	RL2_ECO57
PT1_SALTY	SLYD_ECO57	RL2_PSYIN
RL15_SHISS	SODF_SALTY	RL24_ECO57
RL17_SODGM	SODF_SHIFL	RL25_ECO57
RL18_NITMU	THIO_ECO57	RL7_ECO57
RL2_ACIAD	TPX_ECO57	RL9_ECO57
RL2_BAUCH	TRY1_BOVIN	RPOA_ECOK1
RL2_IDILO		RPOA_VIBF1
RL20_SHISS		RS1_ECO57
RL3_ECO57		RS13_ECO57
RL9_SALTY		RS4_SHIBS
RNE_ECOLI		TIG_ECO57
RRF_SHIFL		TNAA_ECO57
RS6_ECOLI		
RS9_ECO57		
YEBR_ECOLI		
YIIU_ECOLI		
YJGD_SHIFL		
YJGF_ECOL6		

Annexe 9..Etude d'un extrait d'Escherichia Coli. Protéines identifiées pour chaque mode d'ionisation.

Protéines uniques MALDI	Protéines uniques ESI	Proteine communes
AGAL_ECOLI	ACP1_SHIFL	AHPC_SHIFL
AROK_ECO57	DBHB_ECO57	CH10_ECO57
CH60_ENTAE	EFG_ECO57	CH60_ACTPL
CH60_ENTAM	ENO_AERHH	CH60_ECO57
CH60_ERWCT	ENO_KLEP7	CSPA_ECO57
CH602_CHRVO	FKBA_ECO57	CSPC_ECO57
CYSK_ECO57	FUR_ECO57	DBHA_ECO57
DAPD_ERWCT	FUR_KLEPN	DNAK_ECO57
DNAK_ACTSZ	GLNH_ECO57	EFTS_ECO57
DNAK_AERHH	HINT_ECO57	EFTU_ECO57
DNAK_ERWCT	HISJ_ECO57	FKBB_ECOLI
DNAK_PASMU	IDH_ECOLI	GPMA_ECO57
EFTU_MARAV	IF3_ECO57	HNS_ECO57
EFTU1_YERPE	MDH_ECO57	KAD_ECO57
ENO_ECO57	NDK_ECO57	MALE_ECO57
G3P1_ECO57	PGK_SHIFL	ODP2_ECOLI
GNTY_ECOLI	RL1_ECO57	OMPA_SHIDY
GREA_SHIFL	RL17_ERWCT	PTGA_ECOL6
K2C6A_RAT	RL4_SALPA	RBSB_ECOLI
NIFU_SHIFL	RS2_ECO57	RL10_ECO57
ODP1_ECOLI	RS3_ECO57	RL2_ECO57
PT1_SALTY	SLYD_ECO57	RL2_PSYIN
RL15_SHISS	SODF_SALTY	RL24_ECO57
RL17_SODGM	SODF_SHIFL	RL25_ECO57
RL18_NITMU	THIO_ECO57	RL7_ECO57
RL2_ACIAD	TPX_ECO57	RL9_ECO57
RL2_BAUCH	TRY1_BOVIN	RPOA_ECOK1
RL2_IDILO		RPOA_VIBF1
RL20_SHISS		RS1_ECO57
RL3_ECO57		RS13_ECO57
RL9_SALTY		RS4_SHIBS
RNE_ECOLI		TIG_ECO57
RRF_SHIFL		TNAA_ECO57
RS6_ECOLI		
RS9_ECO57		
YEBR_ECOLI		
YIIU_ECOLI		
YJGD_SHIFL		
YJGF_ECOL6		

Annexe 10. Etude d'un extrait d'Escherichia Coli. Analyse différentielle des peptides en fonction du mode d'ionisation.

MALDI SEQUENCE PEPTIDIQUE	pI	Masse	ESI SEQUENCE PEPTIDIQUE	pI	Masse
FAINLK	8.75	704.87	ITDVEVLK	4.37	916.08
FGFTSR	9.75	713.79	AALELAEQR	4.53	1000.12
HTPFFK	8.76	775.91	AEITASLVK	6.05	931.10
WFNESK	6.00	809.88	AQFTDAAIK	5.88	964.09
AISLSVR	9.79	744.89	FNVEVVAIR	6.00	1046.23
APGFGDR	5.88	718.77	GIPTLLLFK	8.75	1001.28
EHILLGR	6.85	836.99	IIGEQLGVK	6.00	956.15
FNDAVIR	5.84	833.94	SFGAPTITK	8.47	921.06
GLSLGMR	9.75	732.90	VPMNIVAQR	9.72	1027.25
HLPEPFR	6.75	895.03	AGENVGVLLR	6.05	1027.19
IEYDPNR	4.37	905.96	ATLEDLGQAK	4.37	1045.16
IYGVLER	6.00	849.00	AVTAAVEELK	4.53	1030.19
LEYDPNR	4.37	905.96	DSDTVVVNYK	4.21	1139.23
LPNGVLR	9.75	767.93	FESEVYILSK	4.53	1214.38
LQALLGR	9.75	769.94	GNFDLEGLER	4.14	1149.23
NNVVVSR	9.75	786.89	GPAAVNVTAI	5.52	912.05
QALELPR	6.00	825.96	GYNGLAEVGK	6.00	1007.11
VAEFFGK	5.97	796.92	NGEFIEITEK	4.25	1179.29
YPGHDPR	6.74	840.89	YYQGTPSPVK	8.50	1139.27
DGAYVTLR	5.84	894.00	ALEGDAEWEAK	4.00	1218.29
DLANDGYR	4.21	922.95	DDVTGEELTTR	3.92	1235.27
EAFDTGVR	4.37	893.95	DIALGEEFVNK	4.14	1234.37
EVIEFYSK	4.53	1014.14	ELPELTAEFIK	4.25	1289.49
FADYDEAR	4.03	986.01	ENLEALLVALK	4.53	1212.45
FKDEEVQR	4.68	1050.14	IMIDLDGTENK	4.03	1248.41
GYVPASTR	8.75	849.94	LFGVTTLDIIR	5.84	1247.50
LFGSIGTR	9.75	849.99	MVAPVDGTIGK	5.59	1087.30
LQHIDFVR	6.74	1027.19	SFELPALPYAK	5.72	1235.45
NFLVPKGK	10.00	902.10	SSGTSYPDVLK	5.55	1153.25
NIEFFEAR	4.53	1025.13	AVAAGMNPMDLK	5.88	1217.46
SGFKYHGR	9.99	951.05	DDSFFDVYTECR	3.84	1496.57
SLEQYFGR	5.72	999.09	ETTFNELMNQQA	3.80	1425.53
TEFDVILK	4.37	964.13	IQNAGTEVVEAK	4.53	1258.39
VVNPELHK	6.72	935.09	LENWPPASIADE	3.57	1341.44
AQYEEIAKR	6.19	1107.23	LNIDQNPGTAPK	5.84	1267.40
AYREEAIIK	6.19	1092.26	LVADSITSQLER	4.37	1331.49
DGIPAVVER	4.37	955.08	LVTDELVIALVK	4.37	1312.61
ENAEYHAAR	5.40	1060.09	MAPPQISAEVLK	5.75	1283.55
EQQGFCEGR	4.53	1053.11	NSDIQPTVESLK	4.37	1330.46

EQQNGWQER	4.53	1174.19	QAIVAEVSEVAK	4.53	1243.42
ETGEIHYGR	5.40	1061.12	QLGEDPWVAIAK	4.37	1326.51
IEIEAIAVR	4.53	1013.20	QYDINEAIALLK	4.37	1390.60
LAGGVAVIK	8.75	827.03	SDLFNVNAGIVK	5.55	1276.46
LEESHIVVR	5.40	1081.24	SLYEADLVDEAK	3.92	1352.46
MFTINAEVR	5.75	1080.27	VIEFSDDSIEAR	3.92	1380.47
NILGDVFHR	6.74	1070.22	VNYGVTVLPTFK	8.56	1337.58
RFKDEEVQR	6.18	1206.32	VVGQLGQVLGPR	9.72	1222.45
TEFYADLNR	4.37	1128.21	DLSDVTLGQFAGK	4.21	1350.49
TRDNEIVAK	5.74	1045.16	ECTLETLEEMLEK	3.98	1567.79
VAFTALVEK	5.97	977.17	EEESAAAAEVEER	3.90	1419.42
VEDALHATR	5.32	1011.10	FRPGTDEGDYQVK	4.56	1511.61
VIDHYENPR	5.32	1142.24	IAEQEGIAEDGYR	4.00	1450.52
VIENAEGDR	4.14	1002.05	IGTDPTYAPFESK	4.37	1425.56
VKALADAAR	8.72	914.07	LATLPTYEEAIAR	4.53	1447.65
VLENAEGDR	4.14	1002.05	TESFAQLFEESLK	4.25	1528.68
YVLAGEGNK	6.00	950.06	TTLTAAITTVLAK	8.41	1303.56
AENQYYGTGR	6.05	1158.19	VLNQFDDAGIVTR	4.21	1447.61
ANPEQLEEQR	4.25	1213.27	YGIPQISTGDMLR	5.84	1450.67
DAEANAEADR	3.92	1061.03	ALDAIIASVTESLK	4.37	1430.66
DLNIDPATLR	4.21	1127.26	DQLLENLQEGMEVK	4.00	1645.84
EVLEALANER	4.25	1143.26	DVFMGVDELQVGMR	4.03	1595.85
FTDEDEQGLR	3.92	1209.23	EGDAVQLVGFGTFK	4.37	1467.64
GEVLAVGNGR	6.00	971.08	EIAYFFGEGEVCPR	4.25	1616.81
GKPFAPLLEK	8.59	1099.34	GNTGENLLALLEGR	4.53	1456.62
GTQAQFIMEK	6.00	1152.33	IATDPFVGNLTFFR	5.84	1597.83
HYGALQGLNK	8.60	1100.24	IQIVGDDLFVTNTK	4.21	1562.78
ILADIAVFDK	4.21	1104.31	MTESFAQLFEESLK	4.25	1659.87
LTQEQLDNFR	4.37	1263.37	QAVTNPQNTLFAIK	8.75	1544.77
MIPGFEDGIK	4.37	1106.30	QQIEEATSDYDREK	4.18	1711.76
SYYALAESVK	5.72	1130.26	SAGGIVLTGSAAAK	8.47	1202.37
TAVINAASGR	9.41	959.07	VATEFSETAPATLK	4.53	1464.64
VLDLIAHISK	6.71	1108.35	VAVFTQGANAEAAK	5.97	1376.53
VPLPPLTEER	4.53	1150.34	AALESTLAAITESLK	4.53	1517.74
VTVQSLDVVR	5.81	1115.30	AGDNAPMAYIELVDR	4.03	1634.82
VVEPLITLAK	5.97	1082.35	AYEDAETVTGVINGK	4.14	1566.68
YEELQITAGR	4.53	1179.30	DAQSALTVSETTFGR	4.37	1582.69
ARVEDALHATR	6.80	1238.37	DATGIDPVSLIAFDK	3.93	1561.75
AVEGTPFECLK	4.53	1193.38	DITLAMDCAASEFYK	4.03	1677.90
AVIESENSAER	4.25	1204.26	EEFGGELIDGGPWLK	4.00	1646.82
AWHSSSETIAK	6.79	1216.32	FNQIGSLTETLAAIK	6.00	1605.85
DKEISEDDDRR	4.23	1377.39	HPSEIVNVGDEITVK	4.65	1636.82
EKDGAVEAEDR	4.18	1218.24	HYAHVDCPGHADYVK	6.25	1711.87
FGEIEEVELGR	4.09	1277.40	INPAGAPTYVPGEYK	6.00	1576.77

FNIDADKVNPR	5.96	1288.43	LIDMGEEIGLATVYR	4.14	1679.95
GQNEDQNVGIK	4.37	1201.26	LKDLETQSQDGTFDK	4.23	1724.84
HAVTEASPMVK	6.75	1169.36	LTGLEGEQLGIVSLR	4.53	1584.83
HPAVPVDVVHR	6.92	1225.42	LVVATDTAFVPFEFK	4.37	1683.96
HPVTPWGVQTK	8.76	1249.44	NVALEEQAVEAVLAK	4.25	1583.80
IEQAPGQHGAR	6.75	1163.26	QLAEDPFNNWVALNK	4.37	1758.95
IILLGAPGAGK	8.75	1009.26	SLGQFNLDGINPAPR	5.55	1598.78
ISDAAQAHFAK	6.74	1158.28	STLTPVVISNMDEIK	4.37	1646.92
MGSEVFHHLAK	6.69	1255.46	TSSTGLVYQVVEAGK	5.66	1538.72
NQGDHLLHSTR	6.92	1277.36	AKDEADEKDAIATVNK	4.44	1717.85
RPLLHVETPPR	9.61	1314.55	AVAAVNGPIAQAILGK	8.80	1492.78
SYEEELAKDPR	4.41	1336.42	EGDDVALVGFGTFAVK	4.03	1624.81
VDGTKPVAEVR	6.04	1170.33	ITTVQAAIDYINGHQA	5.08	1714.90
VLGFITDAGGR	5.81	1105.26	MIAPILDEIADEYQGK	3.92	1806.06
VNDEGIIEDAR	3.92	1230.30	MVVTLIHPIAMDDGLR	5.19	1781.16
VTAERDPANLK	6.04	1213.36	QEAAPAAAPAPAAGVK	6.00	1419.60
APAPEYVPEAPR	4.53	1296.45	QEDANFSNNAMAEAFK	4.14	1786.89
GGGISGQAGAIR	9.75	1043.15	SQDLASQAEESFVEAE	3.45	1739.77
IHSEEDERPIGR	4.83	1437.53	VGDTVIEFDLPLLEEK	3.83	1817.07
ISADKVDQEVER	4.32	1388.50	YDEAPSNVAQAVIEAR	4.14	1732.87
LLANQEEGTQIR	4.53	1371.51	AAGAELVGMEDLADQIK	3.92	1730.95
NIVVILPSSGER	6.00	1283.49	AVGDSLEAQQYGIAFPK	4.37	1793.99
RPEIIAAIAEAR	6.14	1309.53	DLLGATNPANALAGTLR	5.84	1667.88
VTVEHPDKLEEK	4.83	1423.59	EIPSDIVYQDDLVTAFR	3.84	1981.19
EGVSKDDAEALKK	4.78	1389.53	ELLSQYDFPGDDTPIVR	3.84	1965.15
ILENGEVKPLDVK	4.68	1453.70	FCGAEGLNNVITLSTFR	5.99	1842.10
ISELSEGQIDTLR	4.14	1460.60	FGGYAQSGLLAEITPDK	4.37	1766.97
TGEVPADVAAQAR	4.37	1284.39	GMGESNPVTGNTCDNVK	4.37	1722.86
TQDATHGNSLSHR	6.61	1423.46	IDAAFQDEVAASEGFLK	3.92	1810.98
VQGKDEVILTLNK	6.04	1456.70	DALAPHISAETIEYHYGK	5.27	2015.21
AFDQIDNAPEERAR	4.32	1631.72	DTTTIIDGVGEEAAIQGR	3.92	1845.98
ANPEQLEEQREETR	4.33	1728.79	EFLENYLLTDEGLEAVNK	3.91	2097.31
ATLGEVGNAEHMLR	5.40	1497.69	FTGEVSLTGQPFVMEPSK	4.53	1954.23
AVAEACGSQAVIVR	6.04	1373.59	LVIEMETNGTIDPEEAIR	3.91	2030.28
KQIEEATSDYDREK	4.51	1711.80	NAEFLQAYGVAIADGPLK	4.37	1877.13
NFDNMREDEGLADR	4.11	1681.75	VLNIFPSIDTGVCAASVR	5.80	1862.17
VANLGSLGDQVNVK	5.81	1413.59	VVADIAGVPAQINIAEVR	4.37	1835.13
VIGITNEEAISTAR	4.53	1473.65	DVTTGDTLCDPDAPIILER	3.71	2044.26
VILAGEVTTPVTVR	5.97	1454.73	LGEDNINVVEGNEQFISASK	4.00	2163.33
NNSLSQEVQNAQHQR	6.75	1752.82	SIVHPSYNSNTLNNDIMLIK	6.46	2273.59
AATILAEQLEAFVDLR	4.14	1760.02	GEILGGMAAVEQPEKPAAQPK	4.79	2121.44
KGDEIAAVVLQVDAER	4.32	1712.92	TFEVLATNGDTHLGGEDFDSR	4.10	2281.38
GTAMNPVDHPHGGGEGR	5.99	1688.79	TTPSIIAYTQDGETLVGQPAK	4.37	2190.44
NIPVGSTVHNVEMKPGK	8.60	1807.10	AGDQIQSGVDAAIKPGNTLPMR	6.00	2239.53

TKPHVNVGTIGHVDHGK	8.34	1796.02	SGETEDATIADLAVGTAAGQIK	3.92	2118.28
GAAGGHTATHHASAAPARPQPVE	7.03	2191.35	ANDAAGDGTTTATVLAQAIITEGLK	4.03	2402.64
			AVIESENSAERDQLLENLQEGMEVK	4.06	2832.09

Annexe 11. Etude de polygônes de souris. Protéines identifiées en fonction du mode d'ionisation. (LC-MALDI-TOF/TOF versus LC-ESI-FTICR)

Protéine Souris MALDI	Protéine ESI Souris	Protéine Communes
K1C15_MOUSE	ACTA_MOUSE	CO1A1_MOUSE
K2C1B_MOUSE	ACTB_MOUSE	CO1A2_MOUSE
K2C5_MOUSE	CO4A1_MOUSE	CO3A1_MOUSE
	EMIL1_MOUSE	CO4A2_MOUSE
	FIBB_MOUSE	CO6A1_MOUSE
	K22E_MOUSE	CO6A2_MOUSE
	K2C1_MOUSE	COCA1_MOUSE
	K2C73_MOUSE	FBN1_MOUSE
	POSTN_MOUSE	FIBG_MOUSE
		FINC_MOUSE
		K1C10_MOUSE
		LAMA4_MOUSE
		LAMA5_MOUSE
		LAMB2_MOUSE
		LAMC1_MOUSE
		NID1_MOUSE
		PGBM_MOUSE

Annexe 12. Etude de polygônes de souris. Analyse différentielles des peptides identifiés en fonction du mode d'ionisation.

MALDI Sequence souris	pI	Masse	ESI Sequence souris	pI	Masse
FIDNLR	5.84	776.89	DLTDYLMK	4.21	998.16
ICLDIR	5.83	731.91	AMDYDLLLR	4.21	1109.31
RLTLAR	12.00	728.89	DLLQAAQDK	4.21	1001.10
GFIPNIR	9.75	815.97	IVEVFEIGPK	4.53	1130.35
LAADDFR	4.21	806.87	LAALSIEESK	4.53	1060.21
RFDQELR	6.07	963.06	QLEEAENELK	4.09	1202.28
YFIAPVK	8.59	837.03	VNEILSALER	4.53	1143.31
CPVGYVLR	8.22	906.11	AMDFNGILTIR	5.88	1250.48
EYEELCPR	4.25	1038.14	DASSSVSTLEK	4.37	1123.18
LGEQNFHK	6.75	972.07	FDAGSGMATIR	5.84	1125.26
NLNEQGLR	6.00	943.03	LALDIEIATYR	4.37	1277.48
RFVEDVSR	6.07	1007.11	LEPTVPEDSGR	4.14	1199.28
VFAVHQGR	9.73	913.05	LGMVQAIMSAR	9.75	1176.46
AEQLRDEAR	4.68	1087.16	QSVEADINGLR	4.37	1201.30
AGYQSTLTR	8.79	996.09	TNAENEFVTIK	4.53	1265.39
FASFIDKVR	8.75	1082.27	VVLEVASEAGR	4.53	1129.28
GFVYKPDLK	8.50	1066.27	CECPVGFFYNDK	4.37	1421.61
GIDKPQCHR	8.23	1053.20	DGFFGLSASDPR	4.21	1268.35
GPAGPQGPR	9.75	835.92	ETPSWTGPGFVR	6.10	1333.47
GPSGPQGIR	9.75	867.96	GQAGVMGFPGPK	8.75	1145.34
GSTGPAGIR	9.75	814.90	LDILAQEVNFLR	4.37	1430.67
GVVGPQGAR	9.75	839.95	QATGDYMGVSLR	5.84	1297.45
HEAYGECYK	5.40	1099.18	SQECYFDPELYR	4.14	1549.67
HQTHGSLLR	9.76	1048.17	TSPDGPYQVSLR	5.50	1319.44
LASYLDKVR	8.59	1064.25	VGTFSLDAANPK	5.81	1219.36
LLPPTQNNR	9.75	1052.20	VPSGLYLGTCER	5.97	1294.49
RDDDPLNAR	4.43	1071.11	DFDSLAQPSFFDR	3.93	1544.64
VGPESDKYR	6.04	1050.14	ENYAELLDDGFLK	3.92	1526.66
AHLPLDINFR	6.79	1195.39	IPGDQIVSVVFIK	5.84	1414.71
DYTGGEHCER	4.65	1166.19	QSLEASLAETEGR	4.25	1390.47
FMNQEVETQR	4.53	1281.41	AAAITSDLLESLGR	4.37	1416.59
LGIPVKLEPR	8.75	1121.39	AHGQDLGTAGSCLR	6.78	1385.52
LSFDQPNDFK	4.21	1210.31	DQLAQYESGLMDLR	4.03	1638.81

NKYEDEINKR	6.18	1308.41	EGQEVEFLVTSLPR	4.25	1603.79
ALALGALQNIR	9.79	1139.36	FGFNPLEFENFSWR	4.53	1789.97
ALSSAGQHVAR	9.80	1096.21	GFSSGSAVVSGGSR	9.75	1254.32
ATPFIECNGGR	6.04	1164.30	ISFFDGFEGGFNFR	4.37	1639.79
EQVGDQYQTVR	4.37	1322.40	ITASATCGEEAPTR	4.53	1406.53
ESLEVQIHPSR	5.40	1294.43	LSAEDLVLEGAGLR	4.14	1442.63
GCQPCACHPSR	7.98	1158.33	SIEYSPQLEDASAK	4.14	1537.64
GPAGPSGPVGK	8.75	923.04	STLQEANDILNNLK	4.37	1572.74
GPVGPHGPPGK	8.76	999.14	SYTITGLQPGTDYK	5.55	1543.69
GQVEQANQELR	4.53	1271.35	SYYYAISDFAVGGR	5.55	1568.71
GTQDNNLLYYR	5.83	1356.46	TLPGGNQCIVPICR	7.75	1470.77
HDPRDDDLNLR	4.56	1365.43	YSFCTDHAVLVQTR	6.73	1639.85
HHAEHSVGRPR	9.62	1282.39	DGFFGLDYADYFGCR	3.93	1745.88
IHLYTLNDNAR	6.74	1329.48	EAQEVKDVDQNLMDR	4.11	1789.93
LSERENQYTLR	6.14	1408.53	EGFFGNPLAPNPADK	4.37	1573.73
QHLANQQALGR	9.76	1235.37	EVSEAVVEKLEPEYR	4.33	1776.96
AMLQVHGGSGPR	9.80	1209.39	GVTYNIIVEALQNQR	6.00	1717.94
DLLQAAQDKLQR	5.96	1398.58	HSQTTDDPLCPPGTK	5.21	1596.73
GDEGPPGPEGLR	4.14	1180.24	LPAIEPSDQGQYLCR	4.37	1689.90
GVQGPPGPAGPR	9.75	1089.22	TLPTGCFNTPSIEKP	5.66	1604.84
LHTLGDNLLDPR	5.21	1363.54	VFLTVPSLSSTAEEK	4.53	1607.82
NGFSITGGEFTR	6.00	1285.38	VLDISIPASPEQIQR	4.37	1665.91
RVLFDTGLVNPR	9.60	1386.62	YSEIEPSTEGEVIYR	4.09	1771.90
RVVLEVASEAGR	6.14	1285.47	DIIYIGGAPDVATLTR	4.21	1674.91
SLDLDSIIAEVK	4.03	1302.49	EELMMVLAGLEQLQIR	4.25	1873.26
SLLPDVEGLHEK	4.65	1336.51	EHLLMALADLDELLVR	4.31	1851.19
SVVPQGGPHSLR	9.49	1233.39	ILYHGYSLLYVQGNER	6.75	1925.17
YLQEIYNSNNQK	6.00	1513.63	LREGQEVEFLVTSLPR	4.79	1873.14
AETVQAALEEAQR	4.25	1415.52	LSDLQESINQALDHVR	4.54	1838.01
AHPVSNAIDGTER	5.32	1366.45	LYIDETVNDNIPLNLR	4.03	1902.13
ASLHGGEPTTIIR	6.79	1351.53	NLEWIAGGTWTPSALK	6.00	1743.98
EDGRPLPSSAQQR	6.17	1440.54	QDLGSPEGIALDHLGR	4.54	1677.83
GHTPTHPGTLNQR	9.76	1415.53	SLFPVVLEQLDDYNAK	4.03	1851.09
IAHVELADAGQYR	5.32	1442.59	SYELPDGQVITIGNER	4.14	1790.95
LGVRPSQGGEAPR	9.60	1323.47	VGVVQYSHEGTFEAIR	5.40	1791.98
LKEAEREVTDLLR	4.87	1571.79	DIAEIIKDIHNLEDIKK	4.83	2007.31
TLQFGHMSVTVEK	6.41	1476.71	FLTTTPNSLLVSWQAPR	9.75	1931.22

VESTEQLIEIASR	4.25	1474.63	GDGGPPGMTGFPGAAGR	5.84	1501.64
VSCLEIPGPHGPK	6.71	1333.57	GMVFGIPDGVLELVPQR	4.37	1827.17
YDDEECTLPIAGR	3.92	1481.60	HPQGTVVFTTQVPTLGR	9.76	1838.10
GDPGEAGPQGDQGR	4.03	1340.33	HPTPLALGQFHTVTLLR	9.76	1901.24
GGSLPTHHQTHGSR	9.77	1471.56	SLADVDTILAHTMGDVR	4.41	1814.04
KGLEELLIGGSHLK	6.76	1493.77	SQSVRPGADVTFICTAK	7.94	1780.03
SGLLSVSSGAAAHR	9.49	1312.45	TFGEVTDLDNEVNGMLR	3.92	1910.09
AHNQDLGLAGSCLAR	6.78	1525.70	DAEEVISQTIDTIVDMIK	3.77	2020.28
DYRPQVGVIADPSSK	5.96	1631.81	ITFRPDSADGMLLYNGQK	5.96	2026.29
GEAGAAGPSGPAGPR	6.00	1251.32	NTFAEITGLSPGVTYLFK	6.00	1958.24
GYRGDEGPPGPEGLR	4.68	1556.65	STDFGHTYQPWQFFASSK	6.46	2134.29
ITQDDDVICTTEYSR	3.84	1758.87	STLQEANDILNNLKDFDR	4.23	2106.28
VEVLPVSLPGEHGQR	5.40	1616.84	VAPEEHPTLLTEAPLNPK	4.75	1956.23
YQCACNPGYHPTHDR	6.90	1761.91	VAPEEHPVLLTEAPLNPK	4.75	1954.25
NIGASVEFHCAVPNER	5.40	1742.93	WQSQLGGLQGQDLSQVER	4.37	2029.20
EGGQLPPGHSVQDGVLR	5.32	1745.91	DFLSQEGADPDSIEMVATR	3.77	2081.24
GAAGPPGATGFPGAAGR	9.75	1411.54	GMLEPVQKPDVILVGAGYR	6.07	2042.42
HALQSASAGSGSFTDVR	6.74	1690.79	LNQLAINLSGIILGINQDR	5.84	2065.40
GEPGPAGSVGPVGAVGPR	6.00	1560.73	NLVWNAGALHYSDEVEIIR	4.65	2199.45
MGQGSPGDALVPSGEQLR	4.37	1798.99	SDNVPPPTDLQFVELTDVK	3.84	2114.34
GSPGADGPAGSPGTPGPQGIAGQR	5.84	2089.21	SSPVIIDASTAIDAPSNLR	4.21	1927.14
			STLQEANDILNNLKDFDRR	4.68	2262.46
			VSVPLIAQGNSYPSETTVK	5.97	1990.24
			YFSYDCGADFPGIPLAPPR	4.21	2086.35
			AGIEIFVVVVGPQVNEPHIR	5.40	2173.54
			AGNSLAASTAEETAGSAQSR	4.53	1878.93
			ATGDPWLTDGSYLDGSGFAR	3.93	2086.20
			KIPFTDIYIGGAPQEVLQSR	6.07	2232.56
			LDVEFKPLEPNGILLFSGGK	4.68	2173.54
			LETCFLKYDDEECTLPIAGR	4.18	2316.63
			MVEEIVKYEALLLTHETSIR	4.90	2374.78
			NNYATMRPDSTEIDQDTINR	4.23	2354.49
			SGPVEDFVSLAMVGGHLEFR	4.65	2147.43
			VQEQLTSFWEENQSLATHIR	4.75	2416.63
			YGGLHFSDQVEVFSPPGSDR	4.54	2194.34
			DTTPLSVLCGADIQVVSVGIK	4.21	2115.47
			GEKGEPGGAGADGVPGKDGPR	4.78	1908.01

GLTPGVIYEGQLISIQQYGHR	6.75	2329.64
GQTVTFTCVATGVPTPIINWR	8.25	2261.62
KFSTMPFLFCNINNVCNFASR	8.96	2453.88
NLDLDSIIAEVQNQYEMIAHK	4.31	2444.74
QNVVPTVVAVGGDVDMDVLTK	3.93	2156.48
VGVVQYSHEGTFEAIRLDDER	4.50	2420.62
AEMLQALASLEAVLLQTVYNTK	4.53	2406.82
AVAAEALSTATHVQSQLQGMQK	6.79	2269.56
ELVDEEADEAQELLSQAENWQR	3.67	2602.71
IVYSPVAGTRPSESIVVPGNTR	8.75	2299.61
KDLYANTVLSGGTTMYPGIADR	5.96	2343.64
KQNVVPTVVAVGGDVDMDVLTK	4.43	2284.65
QLISTHFAPGDFQGFALVNPQR	6.74	2443.75
AGPTTLSIDENIGEQFAAVSIDR	3.92	2404.62
ATYLNSFSHVGTGIVHAINNVVR	8.80	2469.79
FQGLDLNEELYLGGYPDYGAIPK	3.92	2572.85
GVVNFAVVITDGHVTGSPCGGIK	6.73	2227.56
VLTQIGTSIQDFLEAEDDLSSFR	3.77	2584.82
YQAAQQLQTLEQQSISLQQDTER	4.14	2706.91
AIAFQDCPVDLFFVLDTSESVALR	3.84	2657.03
AVEIYASVAQLTPVDSEALENEANK	3.91	2661.90
IASVKPSDAGTYVCQAQNALGTAQK	8.18	2521.83
KNQLAAQIQEAQAMLAMDTSETSEK	4.41	2737.05
LGSQATGVQGQAGQLLDTTESTLGR	4.37	2488.69
DGSEASLEWSSDRQDIAVISDSYFPR	3.96	2931.08
ELIQNVKDFLSQEGADPDSIEMVATR	4.02	2906.21
LFYAPTSGGPEELVPIPGNTNYAILR	4.53	2790.17
LQELESLIANLGTGDDMVTDQAFEDR	3.62	2881.12
SDTQRDTTPLSVLCGADIQVVSVGIK	4.43	2703.06
AVEASNAYSSILQAVQAAEDAAGQALR	4.14	2704.93
AVEIYASVAQLTPVDSEALENEANKIK	4.25	2903.24
EHLLMALAGIDALLIQASYTQQPAESR	4.65	2940.36
LTQLEAELTAVQDENFNANHALSGLER	4.25	2984.23
GPEGPQGPPGHVGPPGPDECEILDIIMK	4.17	2837.21
LQELESLIANLGTGDDMVTDQAFEDRLK	3.90	3122.45
RLEQWAQELQQTGVLGAFESSFLNMQGK	4.79	3196.58
SSIAELNNNIQSVSDTSSVTFQYLTLLK	4.37	3073.40

VKLQELESLIANLGTGDDMVTDQAFEDR	3.90	3108.42
GDRGETGPAGPPGAPGAPGAPGPVGPAGK	6.07	2449.67
LTAEQAHFFLHSVTLVPVEEFSTEFVEPR	4.62	3360.77
TASPDQTEMTIEGLQPTVEYVVSVYAQNR	4.00	3227.55
YLIVVTDGHPLEGYKEPCGGLEDAVNEAK	4.35	3117.48
GFSGLQGPPGSPGSPGEQGPSGASGPAGPR	6.00	2647.80
GYSGLQGLPGLAGLHGDQGAPGPVGPAGPR	6.74	2754.06
KGEFAGDDSLLDLTPEDTVFYVGGVPANFK	3.96	3202.52
CAATNAAGTTQSHVLLLVQALPQISTPPEIR	6.74	3201.69
DVFGFVAGSDQLNVISCQGLSQGRPGISLVK	5.95	3192.64
LQLVGSGLHEAEAAGEAQQAVLEGLQGLLSR	4.48	3145.52
TMTFHGHGFLPLALPDVAPITEVVYSGFGFR	5.92	3377.91
VPQIPYGASVHIEPYTELYHYSSSVITSSSTR	6.00	3569.93
GLPGPPGAPGPQGFQGPPGEPGEPGGSGPMGPR	4.53	2991.29
CPDYTCPITFSSPADITILLDSSASVGSHNFETTK	4.22	3719.11
ILCPGGEGFRPNPITVILEDIDECQELPGLCQGGK	4.08	3712.27
VGSAEAFAQVLVQGSSSNLPDTSIPGGSTPTVQVTPQLETR	4.14	4127.53

Annexe 13. Etude du stratum corneum plantaire en LC2D. Protéines identifiés en fonction du mode d'ionisation.

PROTEINE STRATUM CORNEUM MALDI	PROTEINE STRATUM CORNEUM ESI	PROTEINE STRATUM CORNEUM COMMUN
DAB2P_HUMAN	ACTG_HUMAN	ALBU_HUMAN
EVPL_HUMAN	AHNK_HUMAN	ANXA2_HUMAN
GNAI2_HUMAN	AT8B2_HUMAN	ARGI1_HUMAN
JPH4_HUMAN	CASPE_HUMAN	CALL5_HUMAN
K0753_HUMAN	CC017_HUMAN	CATA_HUMAN
K1C15_HUMAN	CCD46_HUMAN	CDSN_HUMAN
K1C20_HUMAN	CENPF_HUMAN	DESP_HUMAN
K1C28_HUMAN	CTND1_HUMAN	DSC1_HUMAN
K2C79_HUMAN	DCD_HUMAN	DSG1_HUMAN
KI20A_HUMAN	EEA1_HUMAN	ECM1_HUMAN
KRT36_HUMAN	ELP1_HUMAN	EF2_HUMAN
LCE1B_HUMAN	ENOA_HUMAN	FABP5_HUMAN
LCE1C_HUMAN	ENOB_HUMAN	FILA_HUMAN
LMO7_HUMAN	ESCO1_HUMAN	G3P_HUMAN
MRCKB_HUMAN	GLRX1_HUMAN	GRDN_HUMAN
NEST_HUMAN	GOGB1_HUMAN	HORN_HUMAN
NFH_HUMAN	GRP78_HUMAN	HSPB1_HUMAN
PA24B_HUMAN	ICA1L_HUMAN	K1C10_HUMAN
PRDX1_HUMAN	K0552_HUMAN	K1C13_HUMAN
SBSN_HUMAN	K1C12_HUMAN	K1C14_HUMAN
SPTCS_HUMAN	K2C71_HUMAN	K1C16_HUMAN
STAR9_HUMAN	K2C73_HUMAN	K1C17_HUMAN
SYNE2_HUMAN	K2C74_HUMAN	K1C18_HUMAN
TLK2_HUMAN	K2C75_HUMAN	K1C19_HUMAN
	KAPCA_HUMAN	K1C9_HUMAN
	KI18A_HUMAN	K22E_HUMAN
	KIF2A_HUMAN	K22O_HUMAN
	KRT38_HUMAN	K2C1_HUMAN
	KRT85_HUMAN	K2C1B_HUMAN
	LCE2B_HUMAN	K2C3_HUMAN
	LCE3D_HUMAN	K2C4_HUMAN
	LMNA_HUMAN	K2C5_HUMAN
	MACF4_HUMAN	K2C6A_HUMAN
	MYH9_HUMAN	K2C6B_HUMAN
	NEBL_HUMAN	K2C6C_HUMAN
	OLM2A_HUMAN	K2C72_HUMAN
	PCNT_HUMAN	K2C78_HUMAN
	PLAK_HUMAN	K2C8_HUMAN
	PNPH_HUMAN	K2C80_HUMAN

	RAD_HUMAN	KPRP_HUMAN
	RNAS7_HUMAN	KPYM_HUMAN
	SODC_HUMAN	LCE3E_HUMAN
	SPB12_HUMAN	LEG7_HUMAN
	SPR2G_HUMAN	PLEC1_HUMAN
	SYNC1_HUMAN	PRDX2_HUMAN
	TRIO_HUMAN	SPR1A_HUMAN
	ZN750_HUMAN	SPR1B_HUMAN
		SPR2E_HUMAN
		TGM3_HUMAN
		THIO_HUMAN
		TPIS_HUMAN
		ZA2G_HUMAN

Annexe 14. Etude du stratum corneum plantaire en LC2D. Analyse différentielles des peptides identifiés en fonction du mode d'ionisation.

UNIQUE PEAU MALDI	pI	Masse	UNIQUE PEAU ESI	pI	Masse
EVTQLR	6.10	744.85	LASYLDK	5.83	808.93
FFDQYR	5.84	874.95	LEYDDLR	4.03	922.99
ILLDVK	5.84	699.89	CPQKTTRR	10.86	989.16
ILNEMR	6.00	774.93	DLKDEIVR	4.56	987.12
RVDQLK	8.75	757.89	ENLELQAR	4.53	972.07
TIEDLR	4.37	745.83	KEQQLQER	6.14	1058.16
DYSPYFK	5.83	919.00	QQLERQNK	8.75	1043.15
FDILPSR	5.84	846.98	RLQQQELR	9.60	1070.22
GFDEYMK	4.37	888.99	DQYEQMAEK	4.14	1141.22
GYSPTHR	8.75	816.87	DVDAAYMNK	4.21	1026.13
IDVEILR	4.37	857.02	DYQELMNVK	4.37	1139.29
IDVHWTR	6.74	926.04	EYQELMNTK	4.53	1155.29
IKEWYEK	6.14	995.14	GLIDYETFK	4.37	1085.22

LTGMAFR	9.75	794.97	KQQLEVELR	6.14	1142.32
LVFDGLR	5.84	818.97	LEGGEVDLK	4.14	959.06
QRKMLAK	11.17	874.11	LENEIQTYR	4.53	1165.27
QRLECEK	6.14	905.04	LSSEVEALR	4.53	1003.12
QRPAEIK	8.75	840.98	LTYEIEDEK	4.00	1139.22
QRPSEIK	8.75	856.98	NILNELFQR	6.00	1146.31
QSPSYGR	8.75	793.83	QKVEEELNR	4.79	1144.25
QSSVSFR	9.75	809.88	QLDSIVGER	4.37	1016.12
QTRPILK	11.00	855.05	QLLEGEESR	4.25	1060.13
RRVDQLK	10.84	914.08	VDELEAALR	4.14	1015.13
SEIDNVK	4.37	803.87	VDPEIQNVK	4.37	1041.17
SEVTELR	4.53	832.91	VLDELTLTK	4.37	1031.21
SRQFSSR	12.00	866.93	VLLQEEGTR	4.53	1044.17
VIEGINR	5.97	799.93	YQAECSQFK	5.99	1103.21
AEISELNR	4.53	931.01	DALNIETAIK	4.37	1087.24
ASTSTTIR	9.79	835.91	ERFIEQEKAK	6.33	1277.44
DIVYIGLR	5.84	948.13	FKDLGEENFK	4.68	1226.35
DLIDFDDR	3.77	1008.05	GMQDLVEDFK	4.03	1181.33
EDDSKNLR	4.56	976.01	IGAEVYHNLK	6.75	1143.31
ENKELVKR	8.69	1015.18	KQTALVELVK	8.59	1128.38
FFVGGNWK	8.75	954.10	LAELEEALQK	4.25	1143.30
FQNALLVR	9.75	960.14	LEGLEDALQK	4.14	1115.25
GFSANSAR	9.75	808.85	LTYEIEDEKR	4.41	1295.41
GLVGIEFK	6.00	862.04	MDSLVTANTK	5.59	1079.23
GNLEEENR	4.25	959.9	NMQDLVEDFK	4.03	1238.

		7			38
GRLDSELR	6.07	945.04	NMQDLVEDLK	4.03	1204.36
HEISEMNR	5.40	1015.11	QLIDKETNDR	4.56	1231.33
IENHEGVR	5.40	953.02	QLLQEQESVK	4.53	1201.34
KGYSPTHR	9.99	945.05	RLSSEVEALR	6.14	1159.31
KRPSSLER	10.84	972.11	RVLDELTLTK	6.07	1187.40
KVSFQLER	8.75	1006.17	RWEYENELSK	4.79	1353.45
LLEGEECR	4.25	948.06	SLEEAEAYSR	4.25	1154.20
MSAGGSAR	9.50	735.81	STSSFSCLSR	7.96	1074.17
NATILELR	6.00	929.08	TLEGELHDLR	4.65	1182.30
NLSEAQLR	6.00	930.03	TNQELQEINR	4.53	1244.33
NQEKEEMK	4.79	1035.14	ANLSRENEVVK	6.19	1258.40
QEIAEINR	4.53	972.07	AQEILSQLPIK	6.05	1239.48
QELAERAR	6.14	972.07	ARLELEIETYR	4.79	1392.57
QIEHCEGR	5.40	971.06	DAVEDLESVGK	3.92	1161.23
QRPYGSHR	10.84	1000.08	DAYQKQKEQLR	8.50	1406.56
RQELLEAR	6.14	1014.15	DIISDTSGDFR	3.93	1225.28
SEIDHVKK	6.47	955.08	DVDPGEHYILK	4.54	1285.42
SEISELRR	5.86	989.10	EIKIEISELNR	4.79	1343.54
SLLLSGLR	9.47	858.05	EKVLEDCQLPK	4.68	1301.52
SNKPIILR	11.00	940.15	FPLSNQNMLLR	9.75	1332.58
SQGGWGHR	9.49	883.92	KEMSSIISLNK	8.59	1249.49
TSFTSVSR	9.41	883.96	LDIDSPPITAR	4.21	1197.35
VLEQDKAR	6.04	958.08	LDTSEVVFNSK	4.37	1238.36
VPEPCHPK	6.71	906.07	LENLFEALNNK	4.53	1304.47

VSELQRQR	9.57	1015.14	LKDLEALLNSK	6.07	1243.47
WISIMTER	6.00	1035.23	LKQEVATFSQR	8.75	1306.48
AELELELGR	4.25	1029.16	NKYETEINITK	6.14	1352.51
AFIGFEGVK	6.05	967.13	NSKIEISELNR	6.14	1302.45
AKEIDSMQK	6.11	1049.21	NTAEWLLSHTK	6.75	1299.45
ATMQNLNDR	5.88	1062.17	NTLTQTTENLR	6.00	1290.40
CDQQQIQCR	5.82	1121.25	QGSHYEQSVDR	5.32	1305.33
CPPPAPRPR	10.35	990.19	SYVVACKPPQK	9.19	1219.46
DQYEKMAEK	4.68	1141.26	TPAQYDASELK	4.37	1222.32
EKVQINVVK	8.69	1056.27	TTAENEFVMLK	4.53	1282.47
FVSTTSSSR	9.75	971.03	TTAQYDQASTK	5.50	1213.27
GGSGGSYGR	8.75	796.79	VELEAALQQAK	4.53	1199.37
GLVPPNASR	9.75	910.04	ALQDIQKEKSLK	8.54	1400.64
IGHPAPNFK	8.76	980.13	ATTLSVTPEMER	4.53	1334.51
IGKPAPDFK	8.59	972.15	DLDLDSIIAEVR	3.84	1358.51
ISITEGIER	4.53	1017.15	EEAIQVAIAELR	4.25	1341.53
KLLEGEECR	4.79	1076.23	GHILELLTEVTR	5.40	1380.61
KQHLEIELK	6.76	1137.34	HVGDLGNVTADK	5.21	1225.32
LEGEIATYR	4.53	1051.16	IEISELNRVIQR	6.14	1469.70
LFAYPDTHR	6.74	1119.25	ITSPNDPCLTGK	5.83	1245.41
LNVITVGPR	9.75	968.16	LDELEGALQQAK	4.14	1314.46
LPVEEAYKR	6.14	1104.27	LEGLEDALQKAK	4.68	1314.50
LRAEIDNVK	6.07	1057.21	LLKEYQELMNVK	6.14	1507.81
LRSEIDHVK	6.75	1096.25	QSVEADINGLRR	6.07	1357.49
LRSEIDNVK	6.07	1073.	RAQEILSQLPIK	8.75	1395.

		21			67
NKYEDEINK	4.68	1152.23	RHPDYSVVLLLR	8.75	1467.73
QDIAFAYQR	5.84	1111.22	TAAENEFVTLKK	5.81	1350.53
QFTSSSSMK	8.75	1002.11	TFCQLILDPIFK	5.50	1437.76
QLVQEELRK	6.14	1142.32	TLNNKFASFIDK	8.26	1397.59
QRLLEAQKR	10.84	1141.34	TRLEQEIATYRR	8.41	1535.72
RGFSANSAR	12.00	965.04	TTNQNVIKKQNK	10.30	1415.61
RSEPIYNSR	8.75	1121.22	VDLLNQEIEFLK	4.14	1460.69
SGSGWSSSR	9.47	909.91	VQISQLHQEIQR	6.72	1478.67
SKMIDKNLR	9.99	1104.33	YICENQDSISSK	4.37	1386.50
SSIFEEISK	4.53	1039.15	YLDFSSIITEVR	4.37	1442.63
STMQELNSR	5.72	1065.17	ASLENSLEETKGR	4.79	1433.54
TLLEAENSR	4.53	1032.12	CPPVQPYPPCQQK	8.05	1484.75
VGEFSGANK	5.97	907.98	DELADEIANSSGK	3.92	1348.39
VILEIDNAR	4.37	1042.20	DPILFPSFIHSQK	6.74	1528.77
YGQHGSGSR	8.75	947.96	EEQQLQGNINELK	4.25	1542.67
YTTTSSSSR	8.75	989.01	ETQGIEKLVLINK	6.24	1484.76
AGEVQEPELR	4.25	1127.22	FDQQKNDYDQLQK	4.43	1669.77
DLAVLQDKLR	5.96	1170.37	FNTANDDNVTQVR	4.21	1493.55
DLENRLASAK	6.07	1116.24	HENTSQVPLQESR	5.40	1524.61
EDLYLKPIQR	6.17	1274.48	NYSPYYNTIDDLK	4.21	1605.72
EHLMLEEELR	4.48	1298.48	QEYDESGPSIVHR	4.65	1516.59
EITQEMQTLK	4.53	1220.40	RFGNLKNGVNDIK	9.99	1474.68
ETQSQLETER	4.25	1220.26	SVVLQLADGQIFK	5.55	1417.67
FQLVACPQER	5.99	1190.38	TGSQYDIQDAIDK	3.93	1453.53

GRGGGGGGFR	12.00	876.93	TLELQGLINDLQR	4.37	1512.73
GTEVQLTELR	4.53	1145.28	VQDQDLPNTPHSK	5.21	1478.58
ILQQIPDHPK	6.74	1188.39	AKLDELEGALQQAK	4.68	1513.71
KDVDGAYMTK	5.96	1127.28	AKLVDLEEALQKAK	6.22	1555.84
KLEEGQKNIR	8.59	1214.39	CKLAELEGALQKAK	8.18	1501.80
KREYENELAK	6.23	1279.42	DEETGLCLLPLKEK	4.41	1587.85
KVHQIELAPR	8.75	1190.41	DSQQFHLVPVHLDR	5.98	1690.88
LELQQLQAER	4.53	1227.38	ETQTECEWTVDTSK	4.00	1656.74
LFDQAFGLPR	5.84	1163.34	ETVSEESNVLCLSK	4.25	1537.70
LRSEIDNVKK	8.59	1201.39	GDGPVQGIINFEQK	4.37	1501.66
QLSALAEQQR	6.00	1143.26	LGKDAVEDLESVGK	4.32	1459.62
QRLDDEARQR	6.12	1286.37	LVINGNPITIFQER	6.00	1613.88
RVEEDIQQQK	4.68	1272.38	NKLEGLEDALQKAK	6.18	1556.78
SKYEDEINKR	5.90	1281.39	QSLGELIGTLNAAK	6.00	1414.62
SLYGLGGSKR	9.99	1037.18	RLLEGEDAHLTQYK	5.45	1672.86
SLYNLGGSKR	9.99	1094.24	SFSTASAITPSVSR	9.47	1410.55
VDRAVEGARR	9.48	1128.26	SGAQASSTPLSPTR	9.47	1359.46
WEAEPVYVQR	4.53	1276.41	SVEEVASEIQPFLR	4.25	1603.79
YEELQVTAGK	4.53	1137.25	TAEEQGELAFQDAK	4.00	1536.62
YQELQITAGR	6.00	1178.31	TTCSRQFTSSSSMK	9.50	1550.72
AAAERSKMIDK	8.63	1219.42	VTVNPGLLVPLDVK	5.81	1463.78
AEYEALAEQNR	4.25	1293.36	CIKDEETGLCLLPLK	4.68	1675.03
AGLEDLQVAFR	4.37	1218.38	DAEDWFFSKTEELNR	4.18	1886.99
ATLENDFVVLK	4.37	1248.44	DAEEWFFTKTEELNR	4.25	1915.05
EQYGQYALAVR	6.10	1297.	EHEIVVNKLKAESEK	5.57	1752.

		43			99
GGVEEGPTVLR	4.53	1113.24	GKGMELNSEVLDIQR	4.68	1688.92
GRPAVCQPQGR	10.35	1168.34	ILNEMRDQYEQMAEK	4.41	1898.14
GVQGLNHGMDK	6.74	1155.29	KVPQVSTPTLVEVSR	8.75	1639.91
KEDLYLKPIQR	8.50	1402.66	LGPNYLHIPVNCPYR	8.21	1756.06
LDWLDAETSRR	4.56	1361.48	LLEAQIATGGIIDPK	4.37	1538.80
LEKPAKYDDIK	6.12	1319.52	QLLADFSCNKFPAIK	8.20	1695.01
NNIKEASELLK	6.14	1258.44	QNANLQTAIAEAEQR	4.53	1656.77
QEELQQLEQQR	4.25	1428.52	QNLEPLFEQYINNLR	4.53	1891.11
QGSHHEQSVNR	6.92	1278.31	QRASLETAIADAEQR	4.68	1658.79
QITVNDLPVGR	5.84	1211.38	QVVDGGIIHHISGMR	6.92	1618.87
QLQNIIQATSR	9.75	1271.44	RGFSANSARLPGVSR	12.30	1574.76
SFSIFLSDGQR	5.55	1256.38	SEADSDKNATILELR	4.32	1661.79
SLYYYIQQDTK	5.55	1421.57	TLNDMRQEYEQLIAK	4.68	1852.09
VCDCSTPSECR	4.37	1199.33	VNQIGSVTESIQACK	5.97	1576.79
YKYPEGSDQER	4.68	1371.43	VTATDLDEPDTLHTR	4.22	1683.79
AEFHHSIMSQYK	6.96	1477.66	ADLTGISPSPNLYLSK	5.88	1675.90
AITGFDDPFSGK	4.21	1254.36	AGDKDDITEPAVCALR	4.23	1673.86
ALNNKFASFIDK	8.64	1367.57	ALNSMGQDLERPLELR	4.68	1842.10
AVVGDAQYHHFR	6.96	1399.53	DGGADGMSAECECNIK	3.92	1599.72
EQDRLLQEKYQR	6.28	1605.77	EIPAWVPFDPAAQITK	4.37	1783.06
HHEASSHADISR	6.26	1346.38	FASFIDKVQFLEQQNK	6.07	1942.20
HHEASTHADISR	6.26	1360.41	GEATATDAEAREAALR	4.41	1631.72
KEQVPSGAELER	4.79	1342.47	GLGTDEDSLIEIICSR	3.92	1720.91
LEKPAKYDDIKK	8.38	1447.69	IIRQEPSDSPMFIINR	6.07	1916.23

LKECCEKPLLEK	6.21	1432.76	KQASNLETAIADAEQR	4.68	1744.88
LLNNKFASFIDK	8.59	1409.65	KQRASLETAIADAEQR	6.18	1786.96
LQDLQTALQKAK	8.59	1356.59	LDSELKNMQDMVEDYR	4.11	1986.20
QSSVSFRSGGSR	12.00	1254.32	LNFSHGTHEYHAETIK	6.27	1884.04
RLDQCPESPLQR	6.06	1441.62	SLLAPLNVELDPEIQK	4.14	1779.06
QSSSYGQHESASR	6.75	1423.42	SQGVFQCGPASVIGVR	7.96	1604.84
TATPQQAQEVHEK	5.37	1466.57	THNLEPYFESFINNLR	5.37	1994.19
VPSHLQAETLVGK	6.72	1378.59	VAFEDYISNATHMLSR	5.32	1854.07
ALDGINSGITHAGR	6.79	1381.51	VDIETPNLEGTLTGPR	4.14	1711.89
ASTSTTIRSHSSSR	12.00	1477.55	VLQGLEIELQSQLSMK	4.53	1816.14
AVQGFHTGVHQAGK	8.81	1436.59	VSLDVNHFAPDELTVK	4.54	1784.00
ELQNAHNGVNQASK	6.85	1509.60	AEDGSVIDYELIDQDAR	3.66	1908.99
HGSGSGQSSGFGHK	8.76	1329.35	CEMEQQSQEYQILLDVK	4.00	2084.34
HSGIGHGQASSAVR	9.76	1363.46	CIKDEETGLCLLPLKEK	4.87	1932.32
KGYSPTHREEEYGK	6.76	1680.79	CITDPQTGLCLLPLKEK	6.05	1872.27
LGHGVNNAAGQAGK	8.76	1293.40	EGGLGPLNIPLLADVTR	4.37	1735.01
LGQGAHHAAGQAGK	8.76	1302.42	ELTTEIDNNIEQISSYK	4.00	1997.14
LGQGVNHAADQAGK	6.74	1365.47	GFFDPNTEENLTYLQLK	4.14	2029.23
SCQQNQKQCQPPPK	8.89	1613.83	GLGVGFGSGGGSSSSVK	8.75	1439.54
SCQQSQQQCQPPPK	7.79	1586.76	GVNLPGAAVDLPAVSEK	4.37	1636.87
VAHEINHGIGQAGK	6.89	1430.59	HGVQELEIELQSQLSKK	5.50	1966.22
YGQQGSGSGQSPSR	8.75	1395.41	HSQHGSVSYNSNPVVFK	8.61	1887.04
YQELQVSAQLHGDR	5.32	1643.78	MNLLNQQIQEELSRVTK	5.90	2044.35
YQGTILSIDDNLQR	4.21	1635.79	NIRVGDGDAAAPEPACR	4.56	1711.87
GLPSPYNMSSAPGSR	8.75	1520.	NNATLQAEKQALKTQLK	9.70	1899.

		68			18
HGSGSGQSSSYGPYR	8.60	1526.54	QDPPSVVVTSHQAPGEK	5.32	1775.94
NLPLADQGSSHHITVK	6.92	1716.91	QEIECQNQEYSLLLSIK	4.25	2038.30
SGHSGYHHSHTTPQGR	8.55	1745.79	QTRLEGAEINKSLLALK	8.59	1884.21
SSSGSSSSYGQHGSGSR	8.49	1614.56	RTMQALEIELQSQLSMK	6.14	2006.36
HAETSSGGQAASSHEQAR	6.00	1810.81	RTMQNLEIELQSQLSMK	6.14	2049.39
HAETSSGGQAASSQEQAR	5.40	1801.80	TDLEKDIISDTSGDFRK	4.36	1940.09
HTQTSSGGQAASSHEQAR	6.92	1839.86	THNLEPYFESFINNLRR	6.42	2150.38
HGSSSGSSSHYGQHGSGSR	8.77	1858.82	VPEPCPSTVTPAPAQQK	5.97	1750.00
HGSSSGSSSRYGQHGSGSR	10.84	1877.86	AAVPSGASTGIYEALELR	4.53	1805.02
QGSSAGSSSSYGQHGSGSR	8.75	1783.75	CPEPCPPPKCPEPCPPPK	6.12	1916.32
HGSGLGHSSSHGQHGSGSGR	9.78	1885.89	GADFLVTEVENGGSLGSK	4.14	1779.92
QSLGHSRHGSGSGQSPSPSR	12.00	2006.08	KEGGLGPLNIPLLADVTR	6.07	1863.19
GEQHGSSSGSSSSYGQHGSGSR	6.92	2123.05	LVINGNPITIFQERDPSK	6.07	2041.33
GERHGSSSGSSSSYGQHGSGSR	8.76	2151.11	QLEQENAELEATLLERSK	4.33	2101.30
SEQHGSSSGSSSSYGQHGSGSR	6.66	2153.08	RISIGGGSCAISGGYGSR	9.50	1697.89
SGSGQSSGYSQHGSGSSHSSGYR	8.36	2244.19	SCQQNQQQCQPPPKCPPK	8.65	2039.33
GGSGGGGGGSSGGRGSGGGSSGGSIGGR	12.00	2080.03	SDLEMQYETLQEELMALK	3.91	2171.46
			SVEDRFDQQKNDYDQLQK	4.36	2256.37
			VAPEEHPVLLTEAPLNPK	4.75	1954.25
			VIAPSSSLPTSLTIHHPR	9.73	1913.21
			HRPQVAIICGSGLGGLTDK	8.23	1922.23
			ISGVGIDQPPYGIFVINQK	5.83	2045.37
			LLEAQACTGGIIHPTTGQK	6.74	1938.23
			NFTEVHPDYGSHIQALLDK	5.21	2184.39

			NKLNDLEDALQQAKEDLAR	4.44	2184.39
			NKLNDLEEALQQAKEDLAR	4.51	2198.42
			QMKINVQNNVDLGQPVKNK	9.70	2167.51
			SKELTTEIDNNIEQISSYK	4.41	2212.40
			VGDFVATDLDTGRPSTTVR	4.43	2007.19
			ARPFPDGLAEDIDKGEVSAR	4.44	2143.34
			EVATNSELVQSGKSEISELR	4.49	2176.37
			HFSIHPDTGVITTTTPFLDR	5.98	2255.52
			ISEDNKDEQIGGFLTEQLNK	4.18	2278.46
			LNNQCELLSQLKGNLEEENR	4.49	2344.58
			NLALCPANHAPLQEAAVIPR	6.74	2098.45
			QGSSVSQDRDSEGHSEDSER	4.29	2192.11
			QLSSEKLMDKEQQVADLQLK	4.78	2331.67
			SSSDHHFNQTIGSASPSTAR	6.66	2087.15
			TTQFSCTLGEKFEETTADGR	4.41	2221.38
			VVGPISGADLHGMLEMPDLR	4.54	2107.47
			AQQIHSQTSQQYPLYDLDLGK	5.21	2433.66
			EVATNSELVQSGKSEISELRR	4.95	2332.55
			ISLVLGGDHSLAIGSISGHAR	6.92	2060.34
			LASYLDKVQALEEANNDLENK	4.18	2377.59
			NKIIAATIENAQPILQIDNAR	6.07	2306.65
			TLNGGGSGAGGSRGGGQERER	9.17	1960.01
			TQTVCNFTDGALVQHQEWDGK	4.53	2377.57
			HFSIHPDTGVITTTTPFLDREK	6.00	2512.80
			KTQTVCNFTDGALVQHQEWDGK	5.38	2505.

					74
			LDGFPPGRPSPDNLNQICLPNR	5.95	2420.73
			LLEGEDAHLSSSQFSSGSQSSR	4.65	2309.39
			NILDRQDPPSVVVTSHQAPGEK	5.38	2387.63
			QSLGHGQHGSGSGQSPSPSRGR	12.00	2161.24
			SKAEAESLYQSKYEELQITAGR	4.94	2501.73
			SRAEAESWYQTKYEELQVTAGR	4.94	2602.80
			SRTEAESWYQTKYEELQQTAGR	4.94	2661.82
			AFSAVDTDGNGTINAQELGAALK	4.03	2263.45
			CPEPYLPPPCPPEHCPPPPCQDK	4.65	2541.96
			EIETYHNLLEGGQEDFESSGAGK	4.14	2510.61
			QSGTPHAETSSGGQAASSHEQAR	6.00	2281.30
			RLLEGEDAHLSSSQFSSGSQSSR	5.45	2465.58
			HGSGSGQSSSYGPYGSGSGWSSSR	8.60	2319.30
			HGSGSGQSSSYSPYGSGSGWSSSR	8.60	2349.33
			ITITNDQNRLTPEEIERMVNDAEK	4.36	2830.12
			VIHDNFGIVEGLMTTVHAITATQK	5.99	2596.00
			HQSPDCCESEPSGGSGCCHSSGGCC	4.63	2414.54
			LSVQSAISTQPEAVKQQLEETSEIR	4.49	2772.06
			VPEPCHPKVPEPCPSIVTPAPAQQK	6.71	2650.11
			GSDHTDVCGNVVGSSGGSSSSGGSDK	4.41	2340.33
			HGSGSGHSSSYGQHGSGSGWSSSSGR	8.77	2477.42
			MSGECAPNVSVSVSTSHTTISGGGSR	6.50	2508.72
			RFEPCSSSYLPLRPSEGFPNYCTPPR	8.05	3001.38
			GSSGGGCFGGSSGGYGGLGGFGGGSFR	8.22	2286.38

			LENSPVENVTAASTLLSQAKIDTGENK	4.41	2830.10
			NHKEEMSQLTGQNSGDVNVEINVAPGK	4.83	2896.14
			TQTVCNFTDGALVQHQEWDGKESTITR	4.75	3065.32
			GHYESGSGQTSGFGQHESGSGQSSGYSK	6.00	2790.77
			KTQTVCNFTDGALVQHQEWDGKESTITR	5.48	3193.50
			SSSGQSSGYTQHGSGSGHSSSYEQHGSR	6.78	2826.76
			DIENQYETQITQIEHEVSSSGQEVQSSAK	4.14	3265.41
			GGGGGGYGSGGSSYGSGGGSYGSGGGGGGGR	8.50	2384.29
			GGGGSFGYSYGGGSGGGFSASSLGGGFGGGSR	8.59	2705.75
			NPVQCLPPASSGCAPSSGGCGPSSEGGCFLNHHR	6.88	3311.64
			SPVQCLPPASSGCAPSSGGCGPSSEGGCFLNHHR	6.65	3284.62
			CPPKNPVQCLPPASSGCAPSSGGCGPSSEGGCFLNHHR	7.85	3737.19
			GSYGSGGSSYGSGGGSYGSGGGGGGHGSYGSGSSSGGYR	8.39	3313.20
			GGSGGSHGGGSGFGGESGGSYGGGEEASGSGGGYGGGSGK	4.75	3224.10
			GQCGSGSGQSPNYGQHGSGSGQSSSNDTHGSGSGQSSGFSQHK	7.01	4098.05
			GGSGGSYGGGSGSGGGSGGGYGGGSGGGHSGGSGGGHSGGSGG NYGGGSGSGGGSGGGYGGGSGSR	8.45	4974.70